國立臺灣師範大學化學系博士論文

指導教授：謝明惠 博士

Bimetallic Carbonyl Chalcogenide Clusters: Synthesis, Electrochemistry, Optical Properties, and Computational Studies

研究生：繆佳曄

中華民國一百零一年三月

謝 誌

取得化學領域之最高學位“哲學博士”曾是我遙不可及的夢想，所謂「堅其志，苦其心，勤其力，事無大小，必有所成」，秉持此信念一步一腳印地求學問，而今日終能美夢成真。回憶研究所的日子中，在此我要特別感謝我的指導教授 謝明惠博士，在專業領域之悉心指導、獨立思考之邏輯推演以及待人處事之應對進退，您的諄諄教誨以及嚴謹態度著實鞭策我不斷地努力精確求學、時時檢討自我以及勇於開創的胸襟，在此，獻上我最由衷的敬意與謝忱。

本論文亦承蒙口試委員李國安博士、許文賢博士、張一知博士及陳輝龍博士給予寶貴意見與指正，使之更臻完備，僅在此致上誠摯的謝意。

感謝師大貴儀中心郭頂審助教、何秋慧助教、郭依婷助教、林懿雯助教在 X-ray、NMR 及 Mass 的技術支援。而 EA、SQUID 及 ICP-AES 的測定則分別感謝台大貴儀中心陸靖蔚小姐與清大貴儀中心鄭武漢先生以及李采芸小姐的幫助。另外，感謝系上泰莉助教、彥慧助教、美玲助教、怡旬助教、玉珍助教、雅純助教、碧秀助教、靜芬助教以及姜大鵬先生和戴興堂先生在行政事務上的協助。

回首 D405b 實驗室的生活，首先感謝緯廷學長在實驗上的啟蒙以及妙行、佳樺學姊們在我初期進到這間實驗室時，給予我許多指導與幫助，使我奠定良好的研究基礎。此外，感謝陳輝龍教授在理論計算方面的啟蒙與

大力指導。另外，謝謝同窗佩琪、欣慧、宛珍在學業與研究上的互相切磋，晏頤、建男、宗毅、凱捷、立慈在實驗室事務上的協助，以及沛凡、柏綱、偉成、俊鋒、宇薪、超民、奕文、昌鴻、威名、彥銘、育緯、旻憲、思緯、蓉怡、佩瑄、韋綸、俞君、綺翰、詹昂、翔竣、志龍、舜柏的陪伴與幫助，也因為有你們這群可愛學弟妹的加入，讓我的研究生涯更增添了許多歡樂。

最後非常感謝我的家人，由於你們無時無刻的支持和鼓勵，給予我無限的精神後盾，當面對排山倒海的困難及挫折，總是能排除萬難並勇往直前地攻讀我人生最高學歷的博士學位，此外也非常幸運能認識涵榮並感謝你以及你的家人給予我最美好的回憶。將此博士論文誠心地分享於我的家人以及關心我的摯友們，總而言之，此刻心情百感交集，無法一語道盡，即獻上我百分百的心以及最誠摯的祝福給予你們大家。

繆佳曄 謹致

2012 年 3 月 于師大化學

§ 中文摘要 §

1. E/Mn/Cr/CO (E = S, Se) 系統之研究

當[PPN][$E_2Mn_3(CO)_9$] (E = S, Se)、$Cr(CO)_6$和 PPNCl 以莫耳比 1：1：2 或 1：2：2 於混合乙腈及甲醇之鹼性溶液(4M)中反應，可得到含 hydride 之混合錳鉻化合物 [PPN]$_2$[$HE_2Mn_3Cr(CO)_{14}$] (E = S, [PPN]$_2$[**1a**]; Se, [PPN]$_2$[**1b**])。然而，起始物之陽離子來源為 TMBA 時，進而加入 $Cr(CO)_6$ 以莫耳比 1：1 於鹼性甲醇溶液(4M)中加熱迴流反應，可獲得八面體結構之混合錳鉻團簇物[TMBA]$_3$[$E_2Mn_3Cr(CO)_{12}$] (E = S, [TMBA]$_3$[**2a**]; Se, [TMBA]$_3$[**2b**])。化合物 **1a** 和 **1b** 亦可於鹼性甲醇溶液中加熱迴流並進行合環反應而轉變成化合物 **2a** 和 **2b**。此外，若化合物 **1a** 和 **1b** 加入一或兩當量 $Cr(CO)_6$ 於二氯甲烷溶液中加熱迴流反應，則可進行擴核反應而得到含 hydride 之混合錳鉻化合物 [$HE_2Mn_3Cr_2(CO)_{19}$]$^{2-}$ (E = S, **3a**; Se, **3b**)。其化合物生成及相關性質、結構轉換以及電化學性質藉由理論計算進一步驗證。

2. E/Mn/Ru/CO (E = S, Se) 系統之研究

當[PPN][$E_2Mn_3(CO)_9$] (E = S, Se)與 $Ru_3(CO)_{12}$ 以莫耳比 1：1 於混合乙腈及甲醇溶液中加熱迴流反應，可得到八面體結構之同核含釕團簇物[$HE_2Ru_4(CO)_{10}$]$^-$ (E = S, **3a**; Se, **3b**)和異核含混合錳釕團簇物[$E_2Mn_2Ru_2(CO)_{11}$]$^{2-}$ (E = S, **4a**; Se, **4b**)。此外，化合物 **4a** 和 **4b** 相較於等電子的八面體結構之同核含錳團簇物[$E_2Mn_4(CO)_{12}$]$^{2-}$ (E = S, **1a**; Se, **1b**)和異核含混合錳鉻團簇物[$E_2Mn_3Cr(CO)_{12}$]$^{3-}$ (E = S, **2a**; Se, **2b**)具有良好電子傳遞行為，其氧化位置發生在雙錳金屬羰基片段。紫外可見光吸收光譜顯示此系列同核及異核化合物之電子躍遷為 MLCT (Mn→E or COs)或混合 MLCT 及 MMCT (Mn→Cr or Ru)特性，並藉由反射光譜得知此系列化合物其能隙介於 1.25 至 1.80 eV。其化合物生成及相關性質、電子吸收以及電化學性質藉由理論計算進一步驗證。

3. Te/Ru/Cu/CO 系統之研究

當$[PPh_4]_2[TeRu_5(CO)_{14}]$加入一當量$[Cu(MeCN)_4][BF_4]$於二氯甲烷溶液及低溫下反應，可得到三銅橋接之雙八面體結構的團簇物$[PPh_4]_2[\{TeRu_5(CO)_{14}\}_2Cu_3Cl]$ ($[PPh_4]_2$[**1**])。若將上述反應之$[Cu(MeCN)_4][BF_4]$提高至兩當量，可獲得四銅橋接之雙八面體結構團簇物$[PPh_4]_2[\{TeRu_5(CO)_{14}\}_2Cu_4Cl_2]\cdot CH_2Cl_2$ ($[PPh_4]_2$[**2**]$\cdot CH_2Cl_2$)和雙銅蓋接之八面體結構團簇物$[TeRu_5(\mu\text{-}CO)_2(CO)_{12}Cu_2(MeCN)_2]$ (**3a**)；然而，此反應若於室溫下進行，則可獲得化合物 **2** 以及化合物 **3a** 之結構異構物$[TeRu_5(\mu\text{-}CO)_3(CO)_{11}Cu_2(MeCN)_2]$ (**3b**)。此外，化合物 **1** 和 **2** 的生成反應涉及二氯甲烷之碳氯鍵活化，而化合物 **3a** 和 **3b** 的生成是藉由反應溫度控制。化合物 **1─3** 的生成及相關性質、結構轉換、電子吸收以及電化學性質藉由理論計算進一步驗證。

4. Te/Fe/Cu/dipyridyl 系統之研究

當$[TeFe_3(CO)_9\{Cu(MeCN)\}_2]$與不同有機含氮配子依劑量莫耳比於四氫呋喃溶液中反應，可獲得一維或二維含有機配子之混合鐵銅羰基的有機金屬-有機混合之配位聚合物 **1─4**。此外，利用一鍋化方式將$[TeFe_3(CO)_9]^{2-}$、$[Cu(MeCN)_4][BF_4]$與有機配子 H_2bpe or tmdpy 於四氫呋喃溶液中反應，可得到聚合物 **3** 和 **4** 其結構中的陰離子之混合鐵銅團簇物$[\{TeFe_3(CO)_9Cu\}_2L]^{2-}$ (L = H_2bpe, **5**; tmdpy, **6**)。化合物 **1─6** 之生成及相關性質、電子吸收以及導電性藉由理論計算進一步驗證。

關鍵字：第十六族元素、異核金屬、團簇物、電化學、電子吸收光譜、理論計算

§ Abstract §

1. E/Mn/Cr/CO (E = S, Se) System

When trigonal-bipyramidal clusters, $[PPN][E_2Mn_3(CO)_9]$ (E = S, Se), were treated with $Cr(CO)_6$ and PPNCl in a molar ratio of 1: 1: 2 or 1: 2: 2 in 4 M KOH/MeCN/MeOH solutions, mono-$Cr(CO)_5$-incorporated HE_2Mn_3-complexes $[PPN]_2[HE_2Mn_3Cr(CO)_{14}]$ (E = S, $[PPN]_2$[**1a**]; Se, $[PPN]_2$[**1b**]), respectively, were formed. However, when the $TMBA^+$ salts for $[E_2Mn_3(CO)_9]^-$ were mixed with $Cr(CO)_6$ in a molar ratio of 1: 1 in 4 M KOH/MeOH solutions and refluxed at 60 ^oC, mono-$Cr(CO)_3$-incorporated E_2Mn_3Cr octahedral clusters $[TMBA]_3[E_2Mn_3Cr(CO)_{12}]$ (E = S, $[TMBA]_3$[**2a**]; Se, $[TMBA]_3$[**2b**]), respectively, were obtained. Clusters **1a** and **1b** (with [TMBA] salts) underwent metal core closure to form octahedral clusters **2a** and **2b** upon treatment with KOH/MeOH at 60 ^oC. In addition, **1a** and **1b** were found to undergo cluster expansion to form di-$Cr(CO)_5$-incorporated HE_2Mn_3-clusters $[HE_2Mn_3Cr_2(CO)_{19}]^{2-}$ (E = S, **3a**; Se, **3b**), respectively, upon the addition of 1 or 2 equiv of $Cr(CO)_6$ heated in refluxing CH_2Cl_2. The nature, cluster transformation, and electrochemical properties of the mixed manganese─chromium carbonyl sulfides and selenides were systematically discussed in terms of the chalcogen elements, the introduced chromium carbonyl group, and the metal skeleton, with the aid of molecular calculations at the BP86 level of the density functional theory.

2. E/Mn/Ru/CO (E = S, Se) System

Heating trinuclear E_2Mn_3-trigonal-bipyramidal clusters, $[E_2Mn_3(CO)_9]^-$ (E = S, Se) with $Ru_3(CO)_{12}$ in a molar ratio of 1: 1 in MeCN/MeOH solutions afforded two tetranuclear products, E_2Ru_4-octahedral clusters $[HE_2Ru_4(CO)_{10}]^-$ (E = S, **3a**; Se, **3b**) and mixed-metal $E_2Mn_2Ru_2$-octahedral clusters $[E_2Mn_2Ru_2(CO)_{11}]^{2-}$ (E = S, **4a**; Se, **4b**). In addition, **4a** and **4b** exhibited intense electronic communication through the M_4 square during oxidation of $Mn_2(CO)_6$ fragment, which were compared to the analogous homonuclear group 7 clusters,

$[E_2Mn_4(CO)_{12}]^{2-}$ (E = S, **1a**; Se, **1b**) and the heteronuclear mixed-group 6/7 clusters, $[E_2Mn_3Cr(CO)_{12}]^{3-}$ (E = S, **2a**; Se, **2b**). The electronic absorptions of $[E_2Mn_3(CO)_9]^-$ and **1** were assigned as the MLCT (Mn→E or COs) transitions while those of **2** and **4** were attributed to the MLCT (Mn→E or COs) and MMCT (Mn→Cr or Ru) transitions. Moreover, these clusters also showed optical transitions with band gaps of 1.25 to 1.80 eV. Furthermore, the formation and electronic properties as well as electrochemical and optical properties of these E_2M_4-octahedral carbonyl sulfides and selenides were studied and elucidated with the aid of molecular calculations at the BP86 level of the density functional theory.

3. Te/Ru/Cu/CO System

When $[PPh_4]_2[TeRu_5(CO)_{14}]$ was treated with 1 equiv. of $[Cu(MeCN)_4][BF_4]$ in dichloromethane (CH_2Cl_2) at low temperature, the Cu_3Cl-incorporated di-$TeRu_5$ carbonyl cluster $[PPh_4]_2[\{TeRu_5(CO)_{14}\}_2Cu_3Cl]$ ($[PPh_4]_2$[**1**]) was formed. When $[PPh_4]_2[TeRu_5(CO)_{14}]$ reacted with 2 equiv. of $[Cu(MeCN)_4][BF_4]$ in CH_2Cl_2 at low temperature, both Cu_4Cl_2-incorporated di-$TeRu_5$ carbonyl clusters $[PPh_4]_2[\{TeRu_5(CO)_{14}\}_2Cu_4Cl_2]\cdot CH_2Cl_2$ ($[PPh_4]_2$[**2**]$\cdot CH_2Cl_2$) and $[TeRu_5(\mu\text{-}CO)_2(CO)_{12}Cu_2(MeCN)_2]$ (**3a**) were obtained. However, similar reaction of $[PPh_4]_2[TeRu_5(CO)_{14}]$ with 2 equiv. of $[Cu(MeCN)_4][BF_4]$ in CH_2Cl_2 at room temperature produced complexes **2** and $[TeRu_5(\mu\text{-}CO)_3(CO)_{11}Cu_2(MeCN)_2]$ (**3b**). The formation of **1** and **2** involved the abstraction of chloride from dichloromethane while the formation of isomers **3a** and **3b** was governed by the reaction temperature. The nature, transformation, electrochemical, and optical properties of these CuX (X = MeCN or Cl)-incorporated mono- or di-$TeRu_5$-based clusters were discussed in terms of the effects of copper, tellurium, temperature, and the size of the metal skeleton, which was elucidated in detail by DFT calculations at the MPW1PW91 level of the density function theory.

4. Te/Fe/Cu/dipyridyl System

Four new mixed-metal cluster-based 1D or 2D organometallic-organic hybrid polymers

1─4 were synthesized from the reactions of the neutral heterometallic cluster $[TeFe_3(CO)_9\{Cu(MeCN)\}_2]$ with various ditopic organic linkers such as 1,2-bis(4-pyridine)ethene (bpe), 1,2-bis(4-pyridine)ethane (H_2bpe), and 4,4′-trimethylene-dipyridine (tmdpy) in the stoichiometric molar ratios in THF. Besides, the corresponding anionic clusters in **3** and **4**, $[\{TeFe_3(CO)_9Cu\}_2L]^{2-}$ (L = H_2bpe, **5**; tmdpy, **6**), could be isolated from a one-pot reaction of $[TeFe_3(CO)_9]^{2-}$, $[Cu(MeCN)_4][BF_4]$, and H_2bpe or tmdpy. The ternary Te─Fe─Cu─dipyridyl complexes **1─6** were characterized spectroscopically and their nature, formation, and semiconducting properties were discussed systematically in terms of the nature of N-donor dipyridyl linkers, the dimensionalities, and the intermolecular hydrogen interactions with the aid of molecular calculations at the B3LYP level of the density functional theory.

Keywords: group 16 elements, heteronuclear metals, clusters, electrochemistry, UV-vis spectra, computational studies.

Contents

Chapter 1

Introduction

1.1 Background

In cluster chemistry, Cotton introduced the term ‘‘metal atom cluster’’ in 1964 to point out ‘‘a finite group of metal atoms that are held together mainly, or at least to a significant extent, by bonds directly between the metal atoms, even through some nonmetal atoms may also be intimately associated with the cluster’’.[1] After years of research in this area, several books have illustrated the developments of cluster chemistry, including new bonding modes, versatile reactivities, and diverse structures as well as the activation of small molecules and homo- and heterogeneous catalysis.[2] One of many aspects of cluster chemistry that attracted much attention from chemists was to discover chemically different metals through direct metal─metal bonding, however, up to date many combinations still remain unknown.

In metal carbonyl chemistry, carbonyls are the most common ligands for organometallic clusters and seem to stabilize the M─M bonds.[2a,2b] The reason is that the COs can effectively stabilize $M(CO)_n$ fragments which leads these fragments close to within the metal─metal bonding distance of each other. From 1930s through 1950s, Hieber first discovered a series of neutral and anionic carbonyl complexes containing more than one metal and/or main-group elements.[3] Most studies in this field were mainly aimed at the neutral complexes whereas the chemistry of anionic complexes remained scarce. Recently, anionic metal carbonyl clusters have been reported to be utilized as synthetic synthons for further cluster-growth reactions to construct homo- or hetero-nuclear metal carbonyl clusters.[4] In the group 7 (Mn) system, our group reported the stepwise growth from the smaller clusters, $[E_2Mn_3(CO)_9]^-$ (E = S, Se), into larger E-rich or Mn-rich clusters (Figure

1.1),[4] however, controlled-cluster expansion of $[E_2Mn_3(CO)_9]^-$ with group 6 (Cr) and group 8 (Ru) to form mixed-metal carbonyl chalcogenide clusters were not explored.

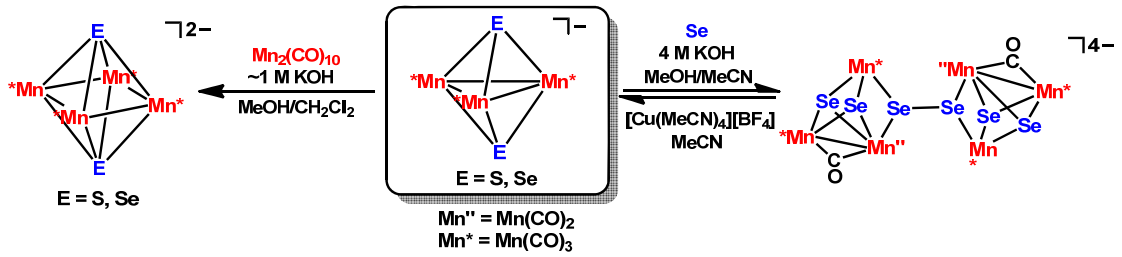

Figure 1.1. Stepwise cluster-growth reactions from the trigonal-bipyramidal clusters $[E_2Mn_3(CO)_9]^-$ (E = S, Se).

For group 7 system (Ru), if we treated the octahedral cluster $[TeRu_5(CO)_{14}]^{2-}$ with various amounts of CuX (X = Cl, Br, I), a series of CuX-, Cu_2X_2-, and Cu_4X_2-linked mono- or di-$TeRu_5$-based and Cu_2X_2-incorporated Te_2Ru_4-based carbonyl clusters were formed, respectively (Figure 1.2).[4]

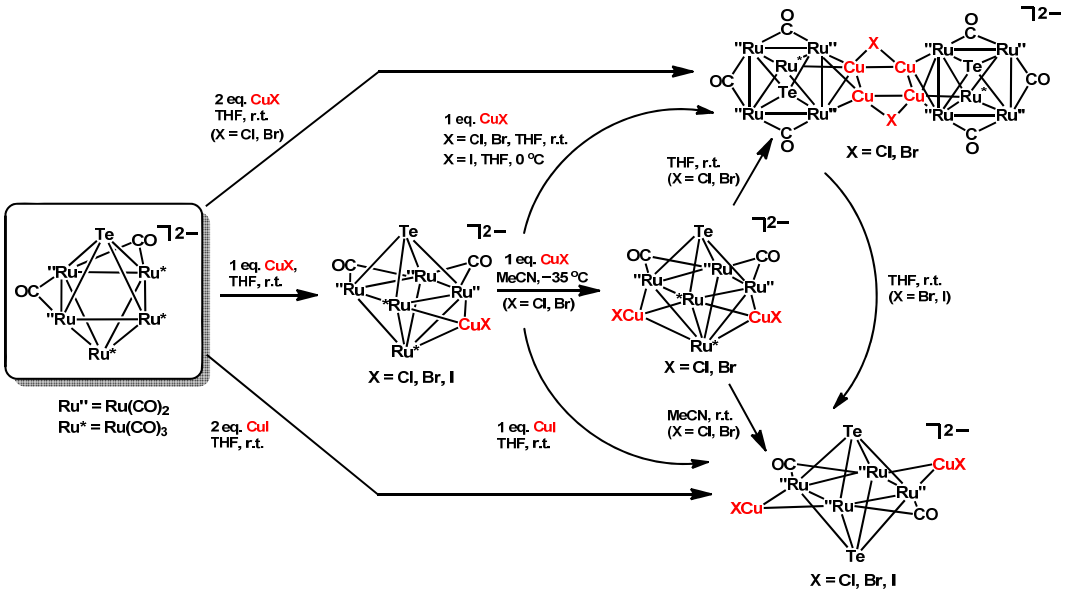

Figure 1.2. Stepwise cluster-growth reaction from the octahedral clusters $[TeRu_5(CO)_{14}]^{2-}$.

Apart from the development of fundamental chemistry among mixed-metal clusters, the exploration of the redox capacity of the high-nuclearity homo- or heterometal carbonyl clusters was even more important because of their potential uses as molecular capacitors.[4,5] Besides, recent studies reported by Nishihara et al. showed that homo-nuclear M_3 (M = Ru,

Co, Rh, Ir, Ni, and Pt) and hetero-nuclear Ir_3Co_6 and Co_3Fe_3 dithiolene carbonyl clusters exhibited interesting electron communication (Figure 1.3).[6]

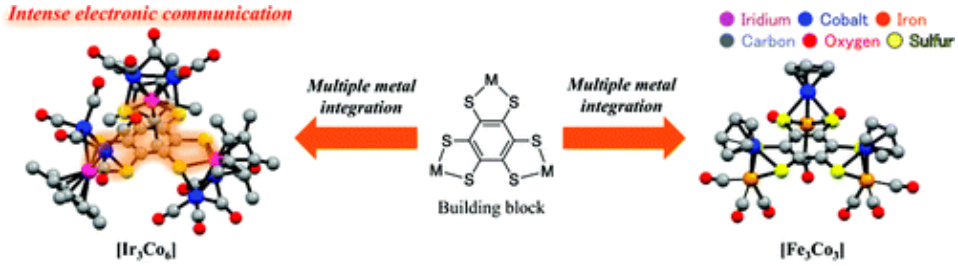

Figure 1.3. Mixed-metal Ir_3Co_6 and Co_3Fe_3 dithiolene carbonyl clusters.

On the other hand, coordination polymers (CPs) are currently one of the hottest topics in Inorganic and Supramolecular chemistry.[7] Recent development of crystalline conducting materials[8] has attracted much interest due to their applications on novel technologies such as porous electrodes for batteries, fuel cells, sensors, and nanomaterials.[9] Nevertheless, the formation of organometallic-organic hybrid CPs involving metal carbonyl clusters was relatively scarce and their dimensionalities were restricted to one-dimensional (1D) frameworks, which were mainly reported by our group and others.[4] Very recently, Scheer et al. first discovered a two-dimensional (2D) organometallic-organic hybrid material, $[\{\{Cp_2Mo_2(CO)_4P_2\}_2Cu_2(H_2bpe)\}\{BF_4\}_2]_n$, by using a phosphorus-containing complex as a precursor with 1,2-bis(4-pyridine)ethane (H_2bpe) (Figure 1.4).[10]

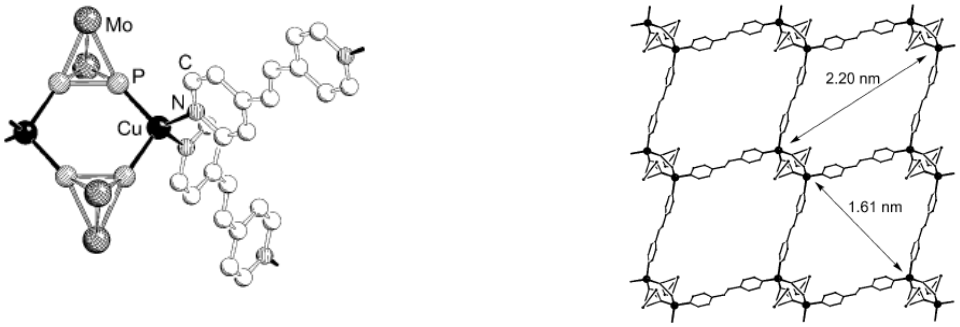

Figure 1.4. Structure of 2D CP $[\{\{Cp_2Mo_2(CO)_4P_2\}_2Cu_2(H_2bpe)\}\{BF_4\}_2]_n$ and its portion of the crystal packing diagram.

With these perspectives, we desired to explore the studies on new heterobimetallic Mn─Cr, Mn─Ru, and Ru─Cu carbonyl chalcogenide clusters as well as 2D

organometallic-organic Fe─Cu─dipyridyl CPs by the stepwise cluster-expansion reactions or self-assembly reactions. Furthermore, the nature, formation, and transformation as well as electrochemical and optical properties of these resultant mixed-metal carbonyl chalcogenide complexes will be systematically discussed and further rationalized by the density functional theory (DFT) calculations.

1.2 Objectives

Based on the unexplored and interesting issues above-mentioned, our objectives in this work are set as follows:

(1) In the E/Mn/Cr/CO (E = S, Se) system, the rational routes for the synthesis of different structures of mixed group 6 and group 7 carbonyl chalcogenide complexes will be studied by the introduction of $Cr(CO)_6$ into trigonal-bipyramidal clusters $[E_2Mn_3(CO)_9]^-$ (E = S, Se). The effect of the incoming $Cr(CO)_x$ fragment will be probed by the studies of the electrochemistry of the resultant complexes.

(2) In the E/Mn/Ru/CO (E = S, Se) system, the extension to the facile synthesis of mixed-metal Mn─Ru carbonyl chalcogenide octahedral clusters from $[E_2Mn_3(CO)_9]^-$ (E = S, Se) will be investigated. Besides, we will also systematically discuss the incorporation of manganese, chromium, and ruthenium carbonyl fragments into the E_2M_4 core in terms of their electrochemical and optical properties.

(3) In the Te/Ru/Cu/CO system, we will investigate the reactivity of $[TeRu_5(CO)_{14}]^{2-}$ with $[Cu(MeCN)_4][BF_4]$ and further explore electrochemical and optical properties of the resultant clusters.

(4) In the Te/Fe/Cu/dipyridyl system, we desire to construct low- or high-dimensional Te─Fe─Cu─dipyridyl organometallic-organic CPs from the reactions of $[TeFe_3(CO)_9\{Cu(MeCN)\}_2]$ with various N-donor ligands. Furthermore, their nature,

formation, and optical properties will be discussed systematically in terms of the nature of N-donor linkers, the dimensionalities, and structural features.

References:

(1) (a) Bertrand, J. A.; Cotton, F. A.; Dollase, W. A. *J. Am. Chem. Soc.* **1963**, *85*, 1349─1350. (b) Cotton, F. A. *Inorg. Chem.* **1964**, *3*, 1217─1220. (c) Cotton, F. A. *Q. Rev. Chem. Soc.* **1966**, *20*, 389─401.

(2) (a) Shriver, D. F., Kaesz, H. D., Adams, R. D. *The Chemistry of Metal Cluster Complexes*; Wiley-VCH, Weinheim, 1990. (b) Braunstein, P., Rosé, J. *Metal Clusters in Chemistry*; Braunstein, P., Oro, L. A., Raithby, P. R., Eds.; Wiley-VCH: Weinheim, 1999; Vol. *2*, Chapter 2.2, pp 616─677. (c) Braunstein, P., Rosé, J. In *Catalysis by Di- and Polynuclear Metal Cluster Complexes*; Adams, R. D., Cotton, F. A., Eds.; Wiley-VCH: New York, 1998; Chapter 13. pp 443─508. (d) Schmid, G. *Clusters and Colloids. From Theory to Applications*; Wiley-VCH, Weinheim, 1964. (e) *Comprehensive Organometallic Chemistry II*; Abel, E. W., Stone, F. G. A., Wilkinson, G., Eds.; *Heteronuclear Metal─Metal Bonds*, Vol. *10*; Adams, R. D., Ed.; Elsevier: Oxford, 1995. (f) *Metal Clusters in Catalysis*; Gates, B. C., Guczi, L., Knözinger, H., Eds.; *Studies in Surface Science and Catalysis Series*; Elsevier: Amsterdam, 1986; Vol. *29*. (g) Hermans, S., Khimyak, T., Raja, R., Sankar, G., Thomas, J. M., Johnson, B. F. G. in *Nanotechnology in Catalysis*; Zhou, B., Hermans, S., Somorjai, G. A., Eds.; Kluwer Academic, Plenum Publishers: New York, 2004.

(3) (a) Hieber, V. W.; Gruber, J. *Z. Anorg. Allg. Chem.* **1958**, *296*, 91─103. (b) Hieber, V. W.; Gruber, J.; Lux, F. *Z. Anorg. Allg. Chem.* **1959**, *300*, 275─287. (c) Hieber, V. W.; Beck, W. *Z. Anorg. Allg. Chem.* **1960**, *305*, 265─273. (d) Herrmann, W. A. *J. Organomet. Chem.* **1990**, *383*, 21─44.

(4) Shieh, M.; Miu, C.-Y.; Chu, Y.-Y.; Lin, C.-N. *Coord*. *Chem*. *Rev*. **2012**, *256*, 637─694.

(5) Femoni, C.; Iapalucci, M. C.; Kaswalder, F.; Longoni, G.; Zacchini, S. *Coord*. *Chem*. *Rev*. **2006**, *250*, 1580─1604.

(6) (a) Kambe, T.; Tsukada, S.; Sakamoto, R.; Nishihara, H. *Inorg*. *Chem*. **2011**, *50*, 6856─6858. (b) Tsukada, S.; Shibata, Y.; Sakamoto, R.; Kambe, T.; Ozeki, T.; Nishihara, H. *Inorg*. *Chem*. **2012**, *51*, 1228─1230.

(7) (a) Batten, S. R., Neville, S. M., Turner, D. R. *Coordination Polymer*: *Design*, *Analysis and Application*; RSC: Cambridge, U.K., 2009. (b) Steed, J. W., Atwood, J. L. *Supramolecular Chemistry*, 2nd ed.; Wiley: Chichester, U.K., 2009.

(8) Givaja, G.; Amo-Ochoa, P.; Gómez-García, C. J.; Zamora, F. *Chem*. *Soc*. *Rev*. **2012**, *41*, 115─147.

(9) (a) Carne, A.; Carbonell, C.; Imaz, I.; Maspoch, D. *Chem*. *Soc*. *Rev*. **2011**, *40*, 291─305. (b) Mas-Balleste, R.; Gomez-Herrero, J.; Zamora, F. *Chem*. *Soc*. *Rev*. **2010**, *39*, 4220─4233. (c) Mas-Balleste, R.; Gomez-Navarro, G.; Gomez-Herrero, J.; Zamora, F. *Nanoscale*, **2011**, *3*, 20─30.

(10) Attenberger, B.; Welsch, S.; Zabel, M.; Peresypkina, E.; Scheer, M. *Angew*. *Chem*. *Int*. *Ed*. *Engl*. **2011**, *50*, 11516─11519.

Chapter 2

Stepwise Construction of Manganese─Chromium Carbonyl Chalcogenide Complexes: Synthesis, Electrochemical Properties, and Computational Studies[a]

Abstract

When trigonal-bipyramidal clusters, $[PPN][E_2Mn_3(CO)_9]$ (E = S, Se), were treated with $Cr(CO)_6$ and PPNCl in a molar ratio of 1: 1: 2 or 1: 2: 2 in 4 M KOH/MeCN/MeOH solutions, mono-$Cr(CO)_5$-incorporated HE_2Mn_3-complexes $[PPN]_2[HE_2Mn_3Cr(CO)_{14}]$ (E = S, $[PPN]_2$[**1a**]; Se, $[PPN]_2$[**1b**]), respectively, were formed. X-ray crystallographic analysis showed that **1a** and **1b** were isostructural and each displayed an E_2Mn_3 square-pyramidal core with one of the two basal E atoms externally coordinated with one $Cr(CO)_5$ group and one Mn─Mn bond bridged by one hydrogen atom. However, when the $TMBA^+$ salts for $[E_2Mn_3(CO)_9]^-$ were mixed with $Cr(CO)_6$ in a molar ratio of 1: 1 in 4 M KOH/MeOH solutions and refluxed at 60 ^oC, mono-$Cr(CO)_3$-incorporated E_2Mn_3Cr octahedral clusters $[TMBA]_3[E_2Mn_3Cr(CO)_{12}]$ (E = S, $[TMBA]_3$[**2a**]; Se, $[TMBA]_3$[**2b**]), respectively, were obtained. Clusters **2a** and **2b** were isostructural and each consisted of an octahedral E_2Mn_3Cr core, in which each Mn─Mn or Mn─Cr bond of the Mn_3Cr plane was semi-bridged by one carbonyl ligand. Clusters **1a** and **1b** (with [TMBA] salts) underwent metal core closure to form octahedral clusters **2a** and **2b** upon treatment with KOH/MeOH at 60 ^oC. In addition, **1a** and **1b** were found to undergo cluster expansion to form di-$Cr(CO)_5$-incorporated HE_2Mn_3-clusters $[HE_2Mn_3Cr_2(CO)_{19}]^{2-}$ (E = S, **3a**; Se, **3b**), respectively, upon the addition of

[a]This **chapter** has been published on *Inorg. Chem.* **2011**, *50*, 7735─7748.

1 or 2 equiv of $Cr(CO)_6$ heated in refluxing CH_2Cl_2. Clusters **3a** and **3b** were structurally related to clusters **1a** and **1b**, but with the other bare E atom (E = S, **3a**; Se, **3b**) further externally coordinated with one $Cr(CO)_5$ group. The nature, cluster transformation, and electrochemical properties of the mixed manganese─chromium carbonyl sulfides and selenides were systematically discussed in terms of the chalcogen elements, the introduced chromium carbonyl group, and the metal skeleton, with the aid of molecular calculations at the BP86 level of the density functional theory.

2.1. Introduction

Heterometallic cluster complexes represent a challenging area of synthetic chemistry due to their numerous applications in catalysis,[1,2] magnetism,[3,4] nanoscience,[5] and nanotechnology.[6] Although systematic syntheses of heteronuclear cluster complexes have advanced significantly during the past few years,[1c,7] rational stepwise cluster-growth processes, based on coupling reactions of suitable transition-metal species or the conversion of existing structural geometries to new ones, were few due to the lack of practical methodologies. In addition to the development of the fundamental chemistry among mixed-metal clusters, the exploration of the redox capacity of the high-nuclear homo- or hetero-metal carbonyl clusters is even more important, due to their potential uses as molecular capacitors.[5b,8]

Whereas homonuclear iron[9–11] carbonyl chalcogenide clusters are well-developed, carbonylmanganese[9a–9c,12–14] and carbonylchromium[9a–9c,15–17] chalcogenide complexes have not been explored as much, and mixed manganese─chromium carbonyl chalcogenide complexes are even more rare.[18,19] Very recently, our group reported two mixed chromium─manganese selenide carbonyl complexes from the reaction of the paramagnetic species $[Se_2Cr_3(CO)_{10}]^{2-}$ with $Mn(CO)_5Br$ in acetone.[19c] However, the question of how to

search for suitable building blocks for step-by-step construction of mixed-metal ternary E─Mn─Cr complexes (E = chalcogen elements) is still a great challenge. Our previously reported trigonal-bipyramidal clusters, $[E_2Mn_3(CO)_9]^-$ (E = S, Se),[14a] were electron-precise anion clusters and could be viewed as potential candidates for incorporation with other nucleophilic or electrophilic transition metal fragments. To extend our studies of the chemistry of mixed Mn─Cr clusters, we have examined the interaction of $[E_2Mn_3(CO)_9]^-$ (E = S, Se) with group 6 chromium carbonyl species, $Cr(CO)_6$, under carefully controlled conditions. This paper describes the full details of the syntheses and characterization of a new family of heterometallic Mn─Cr chalcogenide carbonyl cluster complexes, which included three different types of structures, mono- and di-$Cr(CO)_5$-incorporated HE_2Mn_3 square-pyramidal complexes and mono-$Cr(CO)_3$-incorporated E_2Mn_3Cr octahedral complexes. In addition, the electrochemical properties of these mixed Mn─Cr clusters were systematically investigated to address and compare their redox capability in terms of the effect of the incoming chromium group that was either attached to the square-pyramidal E_2Mn_3 core or incorporated into the octahedral E_2M_4 core. Finally, the electronic properties, stepwise cluster-expansion reactions, and electrochemistry of these new Mn─Cr carbonyl sulfides and selenides were further elucidated and discussed on the basis of density functional theory (DFT) calculations.

2.2. Results and Discussion

2.2.1. Synthesis of Complexes $[HE_2Mn_3Cr(CO)_{14}]^{2-}$ (E = S, 1a; Se, 1b). On the basis of the electron-counting rule, trigonal-bipyramidal complexes $[E_2Mn_3(CO)_9]^-$[14a] (E = S and Se) are electron-precise species (48 electrons). Although stepwise growth from smaller clusters, $[E_2Mn_3(CO)_9]^-$ (E = S, Se), into larger E-rich or Mn-rich clusters was found, providing facile routes to a series of nanosized manganese carbonyl chalcogenide

clusters,[14a,14d,14e] until now, stepwise, controlled-cluster expansion of $[E_2Mn_3(CO)_9]^-$ (E = S, Se) with other transition metal fragments to form mixed-metal carbonyl chalcogenide clusters had not been explored.

In the present study, when $[PPN][E_2Mn_3(CO)_9]$ was treated with $Cr(CO)_6$ and PPNCl in a molar ratio of 1: 1: 2 or 1: 2: 2 in concentrated KOH/MeCN/MeOH solutions (4 M) in an ice-water bath, mono-$Cr(CO)_5$-incorporated HE_2Mn_3-based complexes, $[PPN]_2[HE_2Mn_3Cr(CO)_{14}]$ (E = S, $[PPN]_2$[**1a**]; Se, $[PPN]_2$[**1b**]), were formed in moderate yields of 41 and 44%, respectively (see Scheme 2.1). Clusters **1a** and **1b** also can be isolated as the $[TMBA]^+$ salts by similar procedures. They were both fully characterized by IR, NMR, ICP-AES, and elemental analysis, as well as single-crystal X-ray diffraction analysis. Oak Ridge thermal ellipsoid plot (ORTEP) diagrams of the structures of **1a** and **1b** were shown in Figures S2.1 and 2.1. Clusters **1a** and **1b** were isostructural species and each displayed an E_2Mn_3 square-pyramidal core (E = S, **1a**; Se, **1b**) with each Mn atom terminally coordinated with three COs, in which one Mn─Mn bond was bridged by one hydrogen atom and one of the two basal E atoms was externally coordinated with one $Cr(CO)_5$ group.

The ^{1}H NMR study further confirmed the existence of the hydrides of **1a** and **1b**. For the dianionic **1a**, ^{1}H NMR gave the hydride resonance at −8.94 ppm. This value is close to the previously reported values for the hydride bridging the Mn─Mn bond in the neutral S_2Mn_2-based species $[Mn_2(CO)_6(\mu\text{-H})\{\mu\text{-S}(SC_3H_5)C{=}C(PPr^i_3)S\}]$[20a] (−7.99 ppm) and $[Mn_2(CO)_6(\mu\text{-H})\{\mu\text{-S}(SR)C{=}C(PCy_3)S\}]$ (R = $SnBu_3$, $SnPh_3$, and $CH_2CH{=}CH_2$)[20b] (−8.59, −8.72, −8.42, respectively). However, it had a greater down-field shift than those in $[Mn_2(CO)_6(\mu\text{-H})(\mu\text{-}S_2CPCy_3)]^-$[20c] (−12.01 ppm) and $[Mn_2(CO)_6(\mu\text{-H})(\mu\text{-R}'SC(S)PR_3)]$[20c] (ranging from −13.43 to −13.77 ppm). On the other hand, the ^{1}H NMR signal for the hydride of **1b** (−7.78 ppm) was close to that of **1a** (−8.94 ppm). There were no previous examples of hydride-bridged Mn─Mn bonds reported in the Se─Mn system, according to a search of the

Cambridge Crystallographic Data Centre.

The formation of the anions **1** was proposed to occur via the $[HCr(CO)_5]^-$[21] attack on the starting clusters $[E_2Mn_3(CO)_9]^-$ (E = S, Se),[14a] followed by the hydride transfer and CO_2 loss, giving rise to complexes **1a** and **1b**. This hypothesis was supported by the independent experiments that $[E_2Mn_3(CO)_9]^-$ (E = S, Se) readily reacted with the isolated $[HCr(CO)_5]^-$ anion to give clusters **1a** and **1b** with the comparable yields, respectively. In addition, the formation of $[HCr(CO)_5]^-$ anion was detected by IR spectroscopy in the course of the reaction of $[E_2Mn_3(CO)_9]^-$ with $Cr(CO)_6$ in KOH/MeOH/MeCN. Furthermore, the reaction of $[E_2Mn_3(CO)_9]^-$ with reductants such as KOH/MeOH or Na-Ketyl produced the known square-pyramidal clusters $[E_2Mn_3(CO)_9]^{2-}$.[13a,14e] Therefore, the source of the hydride in **1** was most likely from the hydride of $[HCr(CO)_5]^-$ which was produced from the nucleophilic attack of OH^- on CO of $Cr(CO)_6$, followed by the beta-elimination and loss of CO_2.

Scheme 2.1

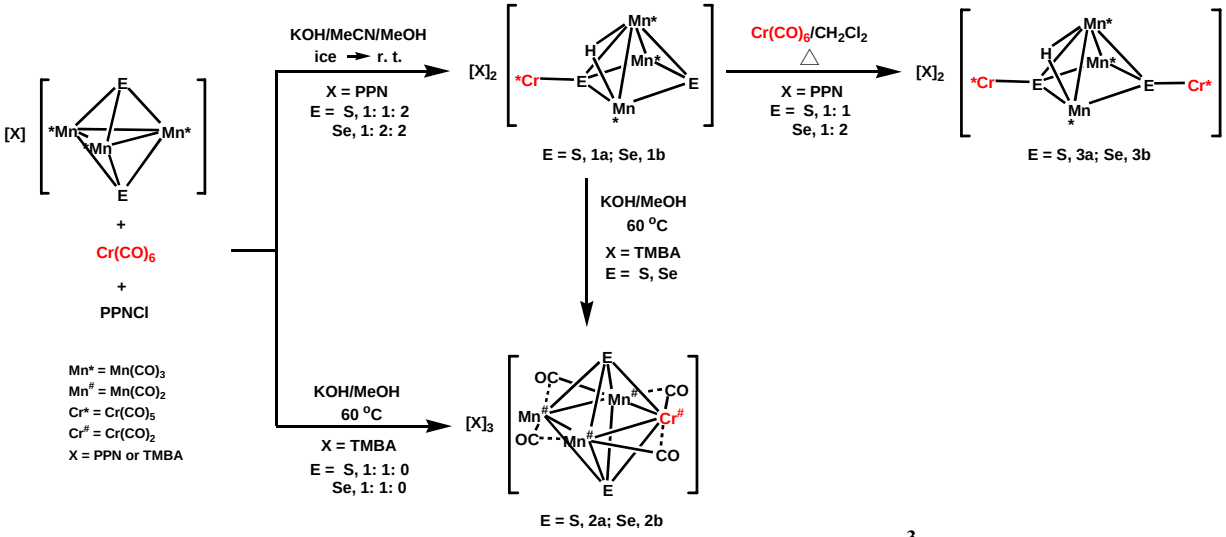

2.2.2. Synthesis of Octahedral Complexes $[E_2Mn_3Cr(CO)_{12}]^{3-}$ (E = S, 2a; Se, 2b).

With careful control of the reaction conditions (the source of the cations and the temperature), the reaction of $[TMBA][E_2Mn_3(CO)_9]$ with $Cr(CO)_6$ in a molar ratio of 1: 1 in 4 M KOH/MeOH at 60 °C led to the formation of mono-$Cr(CO)_3$-incorporated octahedral complexes $[TMBA]_3[E_2Mn_3Cr(CO)_{12}]$ (E = S, $[TMBA]_3$[**2a**]; Se, $[TMBA]_3$[**2b**]),

respectively (see Scheme 1.1.). The anionic **2a** and **2b** were extremely air- and moisture-sensitive and could only be isolated as the $[TMBA]^+$ salt, but this was not feasible for other cationic salts such as $[PPN]^+$ and $[Et_4N]^+$. The formation of octahedral clusters **2a** and **2b** from trigonal bipyramidal clusters $[E_2Mn_3(CO)_9]^{-}$[14a] (E = S and Se) was complicated by the Mn─Mn bond cleavage, E─Cr and Mn─Cr bond formation, and CO migration from the terminal to the bridging mode. Complexes **2a** and **2b** were also fully characterized using spectroscopic methods. As shown in Figures S2.2 and 2.2, **2a** and **2b** each displayed a bimetallic Mn_3Cr square bicapped above and below by two quadruple-bridging chalcogenide atoms.

2.2.3. Synthesis of Complexes $[HE_2Mn_3Cr_2(CO)_{19}]^{2-}$ (E = S, 3a; Se, 3b). To further investigate the nucleophilicity of the triply bridging μ_3-E ligand of complexes **1a** and **1b**, the reaction of **1a** or **1b** with 1 or 2 equiv of $Cr(CO)_6$ heated in refluxing CH_2Cl_2, respectively, were carried out. These reactions led to the formation of novel cluster-expansion products, di-$Cr(CO)_5$-incorporated HE_2Mn_3-based complexes $[HE_2Mn_3Cr_2(CO)_{19}]^{2-}$ (E = S, **3a**; Se, **3b**), with moderate yields (see Scheme 2.1). Clusters **3a** and **3b** are isomorphous and each was shown by X-ray analysis to have two asymmetric $Cr(CO)_5$ groups connected by the square-pyramidal $E_2Mn_3(CO)_9$ core with each Mn atom terminally coordinated with three COs, in which two basal E atoms were both externally coordinated with the $Cr(CO)_5$ groups, with one of the two Mn─Mn bonds bridged by one hydrogen atom (Figures S2.3 and 2.3).

The existence of the hydrides of complexes **3a** and **3b** was confirmed by an ^1H NMR experiment, showing the ^1H NMR singlet at −8.97 and −7.80 ppm, respectively. These values were close to the values of complexes **1a** and **1b** (−8.94, −7.78 ppm), indicative of the minimal effect of an additional $Cr(CO)_5$ fragment. The infrared spectra of **3a** and **3b** showed the absorptions characteristic of terminal carbonyls, with a pattern similar to that of clusters **1a** and **1b**, but with the frequencies shifted to higher energies due to the electron-withdrawing

effect of the $Cr(CO)_5$ fragment. This result seems to suggest, as might be expected, that **3a** and **3b** each consisted of an $[H(\mu_3\text{-}E)(\mu_4\text{-}E)Mn_3Cr(CO)_{14}]$ core in which the bare μ_3-E atom was further linked to the introduced $Cr(CO)_5$ unit via the donor-acceptor bond.

2.2.4. Electron Counts of 1a, 1b, 2a, **2b, 3a, and 3b.** As shown in Scheme 2.1, the dianionic clusters **1** (**1a** and **1b**) and **3** (**3a** and **3b**) were all electron-deficient E_2Mn_3-based square-pyramidal complexes with 70 and 86 electrons, respectively. Because the externally bound $Cr(CO)_5$ moiety is thought to donate zero electrons to the metal skeleton, the dianionic clusters **1a**, **1b**, **3a**, and **3b** were found to possess seven skeletal electron pairs each, according to the Wade's rule, in accord with the 7 skeletal electron pairs required for a square pyramidal structure. The octahedral complexes of **2** (**2a** and **2b**) were electron-deficient 66 electron-species, and each possessed a *closo*-geometry with 7 skeletal electron pairs in terms of Wade's rule. The *nido*-clusters **1** and **3** and *closo*-clusters **2** were all found to be diamagnetic species according to SQUID analysis.

2.2.5. Transformation of Complexes 1a and 1b to Octahedral Complexes 2a and 2b. As described above, the reaction of $[E_2Mn_3(CO)_9]^-$ with $Cr(CO)_6$ in 4M KOH/MeCN/MeOH basic solutions in an ice-water bath produced mono-$Cr(CO)_5$-incroporated HE_2Mn_3-complexes $[HE_2Mn_3Cr(CO)_{14}]^{2-}$ (E = S, **1a**; Se, **1b**), while a similar reaction refluxed at 60 ^oC led to the formation of mono-$Cr(CO)_3$-incorporated octahedral clusters $[E_2Mn_3Cr(CO)_{12}]^{3-}$ (E = S, **2a**; Se, **2b**). Therefore, clusters **1a** and **1b** were thought to act as the intermediate complexes for the formation of clusters **2a** and **2b**. This was indeed the case. By careful treatment with potassium hydroxide at 60 ^oC, cluster **1a** or **1b** could be successfully converted into the octahedral cluster **2a** or **2b**, which was accompanied by a remarkable color change from reddish-brown (complexes **1a** and **1b**) to purplish-black (complex **2a**) or greenish-black (complex **2b**). Simultaneously, the ^1H NMR spectra showed that the hydride signals of **1a** and **1b** disappeared as they transformed into

complexes **2a** and **2b**. In addition, the CO frequencies for *closo*-**2a** and **2b** were quite similar, but shifted to low energies compared to those for *nido*-**1a** and **1b**, due to the pronounced effect of the charge. In a previous study, it was postulated that the square pyramidal complex with a pendant metal fragment could be the key intermediate for the formation of an octahedral complex.[22] However, there were no experimental examples to directly verify this assumption. The present study demonstrated a novel example of a facile conversion from a metal fragment-attached square pyramidal structure to the octahedral geometry. Moreover, the metal-core closure of clusters **1a** and **1b** to give octahedral clusters **2a** and **2b** upon treatment with KOH will be discussed later with the theoretical calculations.

2.2.6. X-ray Structural Comparison of $[Et_4N]_2$[1a], $[PPh_4]_2$[1b], $[TMBA]_3$[2a]·CH_2Cl_2, $[TMBA]_3$[2b]·0.5 CH_2Cl_2, $[PPN]_2$[3a], and $[PPN]_2$[3b]. As shown in Figures S2.1 and 2.1, complexes **1a** and **1b** each displayed a square-pyramidal E_2Mn_3 core with one E atom bonded to an additional $Cr(CO)_5$ fragment, in which each cluster contained a nearly planar E_2Mn_2 base, with average distances of 0.090 and 0.073 Å, respectively, to the least-squares plane. The three Mn atoms of clusters **1a** and **1b** were six-, seven-, and eight-coordinated, respectively. The hydride of **1a** or **1b** across one Mn─Mn bond was refined with an isotropic temperature factor, in which the H─Mn distances in **1a** or **1b** were not equal (1.5929(9)/1.8362(8) Å, **1a**; 1.69(4)/1.66(4) Å, **1b**).

Clusters **1a** and **1b** possessed four metal atoms: one chromium and three manganese. These four metal atoms were assembled in a cluster bridged by the chalcogen atoms with two different bonding modes: E(2) is a triply bridging atom that bridges three manganese atoms, but E(1) is a quadruple-bridging atom that bridges three manganese atoms and a pendant $Cr(CO)_5$ group. To the best of our knowledge, the related mixed-metal carbonyl chalcogenide clusters containing both μ_3- and μ_4-E bonding modes are limited to the neutral complexes: $[CpRe_2Mo(CO)_8(\mu_3\text{-}S)(\mu_4\text{-}S)CpMo(CO)_3]$,[23a] $[Fe_2Mn(CO)_9(\mu_3\text{-}S)(\mu_4\text{-}S)Mn(CO)_5]$,[23b]

$[CpMoMn_2(CO)_9(\mu_3\text{-}S)(\mu_4\text{-}S)Mn(CO)_4]$,[23c] $[Os_3(CO)_9(\mu_3\text{-}S)(\mu_4\text{-}S)W(CO)_5]$,[23d] $[Fe_3(CO)_9(\mu_3\text{-}S)(\mu_4\text{-}S)W(CO)_4PMe_2Ph]$,[23e] $[\{P(CH_2Ph)Ph_2\}_2Ru_3(CO)_7(\mu_3\text{-}Se)(\mu_4\text{-}Se)W(CO)_5]$,[22] and $[Co_3(CO)_7(\mu_3\text{-}Te)(\mu_4\text{-}Te)Nb(C_5Me_4Et)_2]$,[23f] and no examples of anionic mixed-metal carbonyl chalcogenides were ever reported prior to the present study. A search of the Cambridge Crystallographic Data failed to identify any structurally characterized E─Mn─Cr compound that contained both μ_3- and μ_4-E bonding modes. Clusters **1a** and **1b** represent the first examples of E─Mn─Cr clusters possessing both μ_3- and μ_4-E bonding modes.

Clusters **2a** and **2b** were isostructural and each contained two structurally independent entities in the unit cell. As shown in Figures S2.2 and 2.2, clusters **2a** and **2b** each had a crystallographic center of symmetry at the center of the disordered E_2M_4 octahedral core (E = S, **2a**; Se, **2b**). The square heterometallic M_4 unit in **2a** or **2b**, was supported by two Mn─Mn and two Mn─Cr bonds, with two μ_4-E atoms capping above and below the M_4 plane. In **2a**, each M atom of the M_4 square in the two independent forms was coordinated with two terminal COs and one semi-bridging CO, where Mn(1), Mn(2), Mn(3), and Mn(4) atoms and Cr(1), Cr(2), Cr(3), and Cr(4) atoms of the squares were disordered with 75 and 25% occupancy, respectively. In **2b**, one independent square M_4 plane showed the disordered M(1) and M(2) atoms where Mn and Cr are with 75 and 25% occupancy, and the other one showed the disordered M(3) atom with Mn and Cr present in a 50:50 ratio. According to a literature search, clusters **2a** and **2b** were structurally similar to the other neutral mixed-metal E_2M_4 octahedral complexes: $[(\mu_4\text{-}S)_2Ru_3W(CO)_{11}(PMe_2Ph)]$,[24a] $[(\mu_4\text{-}Se)_2Fe_3Ru(CO)_{10}(\mu\text{-}CO)]$,[24b] $[(\mu_4\text{-}Se)_2WRu_3(\mu\text{-}CO)_4(CO)_6(L)_2]$ (L = phosphane),[22] $[(\mu_4\text{-}S)_2PtRu_3(CO)_6(\mu\text{-}CO)_2(\eta^2\text{-}P\text{─}P)]$ (P─P = dppf or dppr),[24c] and $[(\mu_4\text{-}Se)_2WRu_3(\mu\text{-}CO)_4(CO)_7(L)]$ (L = phosphine ligand).[24d] Clusters **2a** and **2b** represent the first examples of mixed group 7 and 6 carbonyl chalcogenide complexes in this octahedral E_2M_4 arrangement.

As shown in Figures S2.3 and 2.3, clusters **3a** and **3b** were isomorphous, and each contained five metal atoms: two chromium and three manganese. These five metal atoms are assembled in a cluster that is bridged by two quadruple μ_4-E atoms (E = S, **3a**; Se, **3b**) with one hydride across one Mn─Mn bond. They could also be regarded as di-$Cr(CO)_5$ groups sandwiching a HE_2Mn_3 metal core, or the μ_3-E atom of complexes **1a** and **1b** further bonded to a secondary $Cr(CO)_5$ group. X-ray analysis of complex **3a** revealed that C(3), O(3); C(4), O(4); C(5), O(5); and C(17), O(17) atoms in the four terminal COs of the di-$Cr(CO)_5$ fragments were disordered with 50, 55, 55, and 60% occupancy, respectively (See Figure S2.3). Similar to **1a** and **1b**, complexes **3a** and **3b** each contained a very slightly distorted E_2Mn_2 base of the E_2Mn_3 metal core, with average distances of 0.082 and 0.040 Å, respectively, to the least-squares planes, regardless of the effect of the two attached $Cr(CO)_5$ groups. This novel type of structural feature containing both the H-bridged Mn─Mn bond and two μ_4-E quadruple-bridging atoms is the only example reported in main group-containing manganese complexes.

For further comparison, the distances of the E─Mn, Mn─Mn, E─Cr, H─Mn, and Mn─Cr bonds of $[PPN]_2$[**1a**], $[PPh_4]_2$[**1b**], $[TMBA]_3$[**2a**]·CH_2Cl_2, $[TMBA]_3$[**2b**]·0.5 CH_2Cl_2, $[PPN]_2$[**3a**], $[PPN]_2$[**3b**], and related complexes are listed in Table 2.1. In general, the corresponding E─Mn, Mn─Mn, and E─Cr averaged bond distances in these new E─Mn─Cr clusters were similar to those reported for related complexes.[12g,13a,14a,18b,19a,19c,25] The average Mn─Cr distances in **2a** and **2b** were 2.6(3) and 2.73(3) Å, which are comparatively shorter than those found in $[Cp_2Cr_2(\mu\text{-}SCMe_3)(\mu_3\text{-}S)_2Mn(CO)_3]$ (2.77(8) Å)[18b] and $[CrMn_2(CO)_8(\mu\text{-}CO)_2(\mu_3\text{-}SN_2C_4H_5)_2]$ (2.849(1) Å)[25], suggesting stronger Mn─Cr bonding due to the *closo*-octahedral skeleton. The corresponding average E─Mn, Mn─Mn, E─Cr, and H─Mn distances of **1a**, **1b**, **3a**, and **3b** were similar, due to the small effect of the secondary $Cr(CO)_5$ group. In addition, the Mn─Mn and E─Cr bond lengths of **2a** and **2b** were slightly

shorter than those of **1a** and **1b**, while the E─Mn bond lengths of **2a** and **2b** were longer than those of **1a** and **1b**, probably due to the increased bonding character associated with the Cr atom. Moreover, in general, the distances of E─Mn, Mn─Mn, E─Cr, H─Mn, and Mn─Cr in the Se_2-based Mn─Cr complexes were slightly longer than the S_2-based Mn─Cr complexes, due to the larger atomic radius of the Se atom compared with the S atom. It is also interesting to note that the size of $[E_2Mn_3(CO)_9]^-$ (E = S, Se), **1**, **2**, and **3** including COs were approximately 0.774(0.884), 0.976(1.004), 0.895(0.898), and 1.366(1.404) nm, respectively, indicative of controllable stepwise construction of these nanosized clusters.

1.2.7. DFT Calculations. The DFT method was employed to further describe the electronic structures of $[E_2Mn_3(CO)_9]^-$ (E = S, Se) and **1─3** to rationalize their relevant reactions. All the calculations were carried out at the BP86[26,27] and B3LYP[28,29] functionals (Table S2.1). The TZVP[30] basis set was applied for all atoms in each complex for these calculations. The geometries of $[E_2Mn_3(CO)_9]^-$ (E = S, Se) and **1─3** were also fully optimized with the same level of theory. Basically similar results were obtained with the BP86 and B3LYP functionals. However, the former provided a better correlation with experimental parameters (Table S2.2) and was used for analysis of the frontier orbitals. The level of BP86 may be more reliable and work better than B3LYP for many organometallic systems.[31─33] Therefore, the present study was focused on the analysis of the geometrical results provided by BP86/TZVP calculations. In addition, the Wiberg bond indices[34] and natural population analyses (NPA)[35] for these complexes were calculated, and the results are listed in Table S2.3.

Formation of Clusters 1 and 3. The DFT calculations showed that the active sites of $[E_2Mn_3(CO)_9]^-$ (E = S, Se) for the formation of clusters **1** (**1a** and **1b**) could be related to the lowest unoccupied molecular orbitals (LUMO) and LUMO+1 of $[E_2Mn_3(CO)_9]^-$. As shown in Figure 2.4 and Table 2.2, the LUMO and LUMO+1 of the respective $[E_2Mn_3(CO)_9]^-$ (E =

S, Se) were degenerate and each had major contributions from the p orbital of the E atoms and d and p orbitals of the Mn atoms. It is reasonable to propose that the incoming chromium anions "$[HCr(CO)_5]^-$/$[Cr(CO)_5]^{2-}$"[21] could interact with the "E" site of $[E_2Mn_3(CO)_9]^-$, presumably accompanied by the hydrogen atom bridging two Mn atoms, to form new E─Cr and H─Mn bonds accompanied by one Mn─Mn bond breakage, to give rise to complexes **1a** and **1b**. Hence, the formation of complexes **1a** and **1b** was not only dominated by the frontier orbitals, but also was induced by the Mn─Mn bond breakage of $[E_2Mn_3(CO)_9]^-$ (E = S, Se), which reflected on their weaker Wiberg bond indices (0.279 and 0.285). As shown in Figure 2.4, the highest occupied molecular orbitals (HOMO) of **1a** and **1b** received major contributions from the p orbital of the E atoms (**1a**/**1b**, μ_3-E, 10.24/19.01%; μ_4-E, 4.04/0.14%) and d orbital of the Mn atoms (**1a/1b**, 62.41/59.94%). This suggests that the "μ_3-E" atoms of **1a** and **1b** were reactive sites for the secondary chromium fragment $Cr(CO)_5$ to form **3a** and **3b**, respectively, which was also supported by their space-filling models (see Figure 2.5).

The Proposed Pathway from 1a(1b) to 2a(2b). The formation of cluster **2a(2b)** is likely to occur via a nucleophilic attack of OH^- on CO of the pendant $Cr(CO)_5$ fragment of complex **1a**(**1b**), followed by loss of CO_2, forming a "$HCr(CO)_4$" fragment, followed by the Mn─Cr and E─Cr bond formation accompanied with H_2 reductive elimination. This proposed pathway was supported by that the LUMO orbital of **1a** or **1b** was mainly contributed from the $Cr(CO)_5$ fragment (59.31%, **1a**; 51.65% **1b**). Furthermore, the relative Gibb's free energies ΔG(298 K), calculated by BP86 in MeOH, for the transformation of **1a** or **1b** into **2a** or **2b** ($[HE_2Mn_3Cr(CO)_{14}]^{2-}$ (E = S, **1a**; Se, **1b**) + OH^- → $[E_2Mn_3Cr(CO)_{12}]^{3-}$ (E = S, **2a**; Se, **2b**) + CO_2 + H_2+ CO) were thermally favorable (ΔG: ─27.47 kcal/mol, E = S; ΔG: ─24.30 kcal/mol, E = Se).

Electrochemistry. In view of the effect of the $Cr(CO)_x$ fragment on the E_2Mn_3 (E = S, Se) core and structural relationships among complexes **1a**, **1b**, **2a**, **2b**, **3a**, and **3b**, their

electrochemical properties were investigated using cyclic voltammetry (CV) and differential pulse voltammetry (DPV) in MeCN under N_2, which was further compared with the related trigonal-pyramidal clusters $[E_2Mn_3(CO)_9]^-$ (E = S, Se[14e]). The CVs of these clusters were somewhat broad and could not be assigned unambiguously. Therefore, DPV studies were carried out to explore the redox behavior of these clusters. The electrochemical data for each complex studied are listed in Tables 2.3 and S2.4, and the DPVs and CVs are shown in Figures 2.6 and S2.4 and S2.5, respectively. The scan range was set between ~ +1.00 to ~ −1.00 V, due to the interference of $[PPN]^+$ and $[TMBA]^+$.

For the DPV measurements, the electron stoichiometry is determined by the measurement of the peak width at half-height ($W_{1/2}$).[36] As seen in Figures 2.6 and S2.4, the widths of the DPV peaks at half-height of $[PPN][E_2Mn_3(CO)_9]$ (E = S, Se) and clusters **1—3** (Table 2.3) were a bit greater than the value ($W_{1/2}$ = 90 mV) expected for one-electron reversible redox reactions, indicating that these DPV responses were quasi-reversible.[37] As listed in Table 2.3, mono-$Cr(CO)_5$-incorporated **1a** an **1b** each had four one-electron quasi-reversible oxidations, at +0.032 to +0.756 V and +0.127 to +0.883 V, respectively. The DFT calculations showed that the HOMO and HOMO─1 of **1a** and **1b** were mainly localized on the E_2Mn_3 moieties, suggesting that the oxidation processes of **1a** and **1b**, mainly occurred in the E_2Mn_3 core (Table 2.2 and Figure 2.4), indicative of a small effect of the attached mono-$Cr(CO)_5$ fragment. The rich quasi-reversible oxidation processes observed for the E_2Mn_3Cr-based complexes, **1a** and **1b**, were ascribed to the positive energy levels of the almost degenerate HOMO and HOMO─1 orbitals in each cluster (Figure 2.4). However, octahedral complexes, **2a** and **2b**, each exhibited two one-electron quasi-reversible oxidations at approximately +0.350 to +0.702 V and +0.370 to +0.538 V and three one-electron quasi-reversible reductions at −0.050 to −0.702 V and −0.044 to −0.684 V, respectively. The oxidative and reductive waves for **2a** and **2b** were tentatively assigned as the oxidations and

reductions occurred in the square heterometallic M_4 units, according to the HOMO and LUMO as well as LUMO+1 levels (Figure 2.4). In addition, the calculated components of Mn_3Cr in the LUMO for **2a** and **2b** (61.87 and 61.22%) were significantly greater than those for **1a** and **1b** (36.80 and 41.15%) (Table 2.2), supportive of the ease and richness of the quasi-reversible reductions of **2a** and **2b**, implying their potential use as electron sponges.[5b,8]

On the other hand, the DPV of the di-$Cr(CO)_5$-incorporatd complex **3a** revealed five one-electron quasi-reversible redox oxidations at +0.323 to +0.867 V and one quasi-reversible redox reduction at −0.160 V, whereas **3b** displayed five one-electron quasi-reversible redox oxidations at +0.325 to +0.849 V (see Figures 2.6 and S2.4). The rich quasi-reversible oxidations of **3a** and **3b** may be related to their narrow-spaced HOMO, HOMO─1, and HOMO─2 orbitals (Figure 2.4). Besides, these frontier orbitals for **3a** and **3b** mainly arose from the E_2Mn_3 metal core and di-$Cr(CO)_5$ fragment, indicating that the oxidation and reduction processes both occurred mainly in the E_2Mn_3 metal core and the di-$Cr(CO)_5$ fragments (Figure 2.4). In general, these quasi-reversible oxidation waves for complex **3a** occurred at more positive potentials than those for complex **1a**, which indicated that **3a** was difficult to be oxidized because of the two electron-withdrawing $Cr(CO)_5$ fragments (Figure 2.6). In particular, the first quasi-reversible oxidation wave of **3a** (+0.323 V) displayed a pronounced anodic shift (291 mV) compared to that of **1a** (+0.032 V), which was supported by the calculations that cluster **3a** showed a lower HOMO energy level, decreasing components of HOMO, and decreased nature charges of the $HS_2Mn_3(CO)_9$ core, as well as greater ionization energy, compared with those calculated for **1a** (**3a** *vs*. **1a**: −0.28 *vs*. 0.35 eV; 86.44 *vs*. 98.86%; −0.865 *vs*. −1.383 |e|; IE ≈ $E_{elec}(N-1) - E_{elec}(N)$, 36.59 *vs*. 19.93 kcal/mol, respectively).

2.3. Conclusions

The present study demonstrated that the chalcogen elements of the E_2Mn_3 metal core (E = S, Se) played an important role in the controlled stepwise construction of a new series of mono- or di-$Cr(CO)_5$-incorporated HE_2Mn_3-based complexes **1** and **3**, and mono-$Cr(CO)_3$-incorporated E_2M_4-based octahedral complexes **2**, under different reaction conditions, and the subsequent transformation of **1** (**1a** and **1b**) into octahedral complexes of **2** (**2a** and **2b**) was also achieved. In addition, the electrochemical properties of these resultant E─Mn─Cr complexes displayed quasi-reversible redox waves over quite a large window (+0.883 ~ −0.702 V). These results can be summarized by the following conclusions. First, the unexpected electron-sponge behavior was observed for complexes **1a** and **1b** and octahedral complexes **2a** and **2b**, which can be readily fine-tuned by the control of electronic properties exhibited by the attached mono-$Cr(CO)_x$ fragment in different metal cores (HE_2Mn_3 vs. E_2M_4). Second, in the cases of **1a** and **3a**, significant anodic shifts were observed as a higher number of $Cr(CO)_5$ groups incorporated into the HS_2Mn_3 metal core, due to the pronounced electron-withdrawing ability of the di-$Cr(CO)_5$ groups. Furthermore, the stepwise cluster-growth processes, metal skeleton transformations, electronic properties, and electrochemistry of these E─Mn─Cr carbonyl clusters were rationalized by molecular orbital calculations at the BP86 level of the DFT.

2.4. Experimental Section

All reactions were performed under an atmosphere of pure nitrogen using standard Schlenk techniques.[38] Solvents were purified, dried, and distilled under nitrogen prior to use. KOH (J. T. Baker), $Cr(CO)_6$ (Strem), PPNCl (Strem), and TMBACl (ACROS) were used as received. $[PPN][E_2Mn_3(CO)_9]$, $[TMBA][E_2Mn_3(CO)_9]$ (E = S, Se), and $[PPN][HCr(CO)_5]$ were prepared according to published methods.[14a,21e] The ^1H NMR spectra were taken on a

Bruker AV 400 at 400.13 MHz. ^{1}H chemical shifts are reported in ppm and were referenced internally with respect to the solvent resonances (^{1}H, δ = 2.49 for DMSO-d_5). Infrared spectra were recorded on a Perkin-Elmer Paragon 500 IR spectrometer as solutions in CaF_2 cells. Elemental analyses of C, H, and N were performed on a Perkin-Elmer 2400 analyzer at the NSC Regional Instrumental Center at National Taiwan University, Taipei, Taiwan. The manganese and chromium contents of complexes **1**, **2**, and **3** were determined with an inductively coupled plasma-atomic emission (ICP-AES) spectrometer (Perkin Elmer Optima 3000DV) at the NSC Regional Instrumental Center at National Tsing Hua University, Hsinchu, Taiwan.

2.4.1. Synthesis of $[PPN]_2[HS_2Mn_3Cr(CO)_{14}]$ ($[PPN]_2$[1a]). Method A: MeOH (10 mL)/MeCN (5 mL) was added to a mixture of $[PPN][S_2Mn_3(CO)_9]$ (0.66 g, 0.65 mmol), $Cr(CO)_6$ (0.14 g, 0.64 mmol), PPNCl (0.76 g, 1.32 mmol), and KOH (3.39 g, 60.4 mmol) in an ice-water bath. The mixture was stirred at room temperature for 3 h. The solid was collected by filtration, washed with deionized water and MeOH, and then extracted with CH_2Cl_2, which was recrystallized with CH_2Cl_2/MeOH/Et_2O to give a reddish-brown sample of $[PPN]_2[HS_2Mn_3Cr(CO)_{14}]$ ($[PPN]_2$[**1a**]) (0.45 g, 0.26 mmol) (yield: 41% based on $Cr(CO)_6$). IR (ν_{CO}, CH_2Cl_2): 2054 (w), 1967 (vs), 1963 (vs), 1928 (w), 1894 (m), 1869 (m) cm^{-1}. ^{1}H NMR (400 MHz, DMSO-d_6, 300 K): δ −8.94 (s, hydride) (Chemical shifts not given for $[PPN]^+$). Anal. Calcd for $[PPN]_2$[**1a**]: C, 58.98; H, 3.51; N, 1.60. Found: C, 59.14; H, 3.52; N, 1.47. Crystals of $[PPN]_2$[**1a**] suitable for X-ray diffraction were grown from CH_2Cl_2/MeOH/Et_2O. ICP-AES: Mn: Cr = 3.18: 1.

Similar procedures were applied for the preparation of $[TMBA]_2[HS_2Mn_3Cr(CO)_{14}]$ by using $[TMBA][S_2Mn_3(CO)_9]$ (0.92 g, 1.46 mmol), $Cr(CO)_6$ (0.33 g, 1.50 mmol), TMBACl (0.84 g, 4.57 mmol), and KOH (4.55 g, 81 mmol) in MeOH (15 mL)/MeCN (5 mL). The yield was 1.06 g (1.09 mmol) of ($[TMBA]_2$[**1a**]) (75% based on $[TMBA][S_2Mn_3(CO)_9]$.)

Method B: MeOH (15 mL)/MeCN (5 mL) was added to a mixture of [PPN][$S_2Mn_3(CO)_9$] (0.38 g, 0.37 mmol) and [PPN][$HCr(CO)_5$] (0.28 g, 0.38 mmol) in an ice-water bath. The mixture was stirred at room temperature for 3 h. A methanol solution of PPNCl (0.49 g, 0.85 mmol) was added dropwise into the resulting solution, precipitating the solid. The solid was worked up as above-mentioned to give a reddish-brown sample of [PPN]$_2$[**1a**] (0.38 g, 0.22 mmol) (yield: 59% based on [PPN][$S_2Mn_3(CO)_9$]).

2.4.2. Synthesis of [PPN]$_2$[$HSe_2Mn_3Cr(CO)_{14}$] ([PPN]$_2$[1b]). Method A: MeOH (15 mL)/MeCN (5 mL) was added to a mixture of [PPN][$Se_2Mn_3(CO)_9$] (0.86 g, 0.77 mmol), $Cr(CO)_6$ (0.34 g, 1.55 mmol), PPNCl (0.81 g, 1.41 mmol), and KOH (4.48 g, 80 mmol) in an ice-water bath. The mixture was stirred at room temperature for 17 h. The solid was collected by filtration, washed with deionized water and MeOH, and then extracted with CH_2Cl_2, which was recrystallized with CH_2Cl_2/MeOH/Et_2O to give a reddish-brown sample of [PPN]$_2$[$HSe_2Mn_3Cr(CO)_{14}$] ([PPN]$_2$[**1b**]) (0.63 g, 0.34 mmol) (yield: 44% based on [PPN][$Se_2Mn_3(CO)_9$]). IR (ν_{CO}, CH_2Cl_2): 2050 (w), 1964 (vs), 1958 (vs), 1930 (w), 1891 (m), 1866 (m) cm^{-1}. ^1H NMR (400 MHz, DMSO-d_6, 300 K): δ −7.78 (s, hydride) (chemical shifts not given for $[PPN]^+$). Anal. Calcd for [PPh_4]$_2$[**1b**]: C, 51.48; H, 2.86. Found: C, 51.39; H, 2.89. Crystals of [PPh_4]$_2$[**1b**] suitable for X-ray diffraction were grown from CH_2Cl_2/MeOH/Et_2O. ICP-AES: Mn: Cr = 3.06: 1.

Similar procedures were applied for the preparation of [TMBA]$_2$[$HSe_2Mn_3Cr(CO)_{14}$] by using [TMBA][$Se_2Mn_3(CO)_9$] (0.75 g, 1.04 mmol), $Cr(CO)_6$ (0.50 g, 2.27 mmol), TMBACl (0.85 g, 4.63 mmol), and KOH (4.50 g, 80 mmol) in MeOH (15 mL)/MeCN (5 mL). The yield was 0.88 g (0.83 mmol) of [TMBA]$_2$[$HSe_2Mn_3Cr(CO)_{14}$] ([TMBA]$_2$[**1b**]) (80% based on [TMBA][$Se_2Mn_3(CO)_9$].).

Method B: MeOH (15 mL)/MeCN (5 mL) was added to a mixture of [PPN][$Se_2Mn_3(CO)_9$] (0.38 g, 0.34 mmol) and [PPN][$HCr(CO)_5$] (0.50 g, 0.68 mmol) in an

ice-water bath. The mixture was stirred at room temperature for 17 h. A methanol solution of PPNCl (0.49 g, 0.85 mmol) was added dropwise to the resulting solution, precipitating the solid. The solid was worked up as above-mentioned to give a reddish-brown sample of $[PPN]_2$[**1b**] (0.19 g, 0.103 mmol) (yield: 30% based on $[PPN][Se_2Mn_3(CO)_9]$).

2.4.3. Synthesis of $[TMBA]_3[S_2Mn_3Cr(CO)_{12}]$ ($[TMBA]_3$[2a]). MeOH (20 mL) was added to a mixture of $[TMBA][S_2Mn_3(CO)_9]$ (0.88 g, 1.40 mmol), $Cr(CO)_6$ (0.31 g, 1.41 mmol), and KOH (4.51 g, 81 mmol). The mixture was stirred at 60 ^oC for 17 h. A methanol solution of TMBACl (0.91 g, 4.95 mmol) was added dropwise to the resulting solution, precipitating the solid. The solid was collected by filtration, washed with deionized water and MeOH several times, and then extracted with MeCN, which was recrystallized with $MeCN/CH_2Cl_2$ to give a purplish-black sample of $[TMBA]_3[S_2Mn_3Cr(CO)_{12}]$ ($[TMBA]_3$[**2a**]) (0.93 g, 0.88 mmol) (yield: 63% based on $[TMBA][S_2Mn_3(CO)_9]$). IR (ν_{CO}, MeCN): 1983 (w), 1937 (w), 1904 (vs), 1893 (vs, sh), 1874 (m), 1849 (m), 1790 (vw) cm^{-1}. Anal. Calcd for $[TMBA]_3$[**2a**]$\cdot CH_2Cl_2$: C, 45.04; H, 3.87; N, 3.66. Found: C, 45.12; H, 4.33; N, 3.62. Crystals of $[TMBA]_3$[**2a**]$\cdot CH_2Cl_2$ suitable for X-ray diffraction were grown from $MeCN/CH_2Cl_2$. ICP-AES: Mn: Cr = 2.89: 1.

2.4.4. Synthesis of $[TMBA]_3[Se_2Mn_3Cr(CO)_{12}]$ ($[TMBA]_3$[2b]). MeOH (20 mL) was added to a mixture of $[TMBA][Se_2Mn_3(CO)_9]$ (0.50 g, 0.69 mmol), $Cr(CO)_6$ (0.16 g, 0.73 mmol), and KOH (4.57 g, 82 mmol). The mixture was stirred at 60 ^oC for 24 h. A methanol solution of TMBACl (0.95 g, 5.17 mmol) was added dropwise to the resulting solution, precipitating the solid. The solid was collected by filtration, washed with deionized water and MeOH several times, and then extracted with MeCN, which was recrystallized with $MeCN/CH_2Cl_2$ to give a greenish-black sample of $[TMBA]_3[Se_2Mn_3Cr(CO)_{12}]$ ($[TMBA]_3$[**2b**]) (0.45 g, 0.39 mmol) (yield: 57% based on $[TMBA][Se_2Mn_3(CO)_9]$). IR (ν_{CO}, MeCN): 1978 (w), 1948 (w), 1905 (vs), 1894 (vs, sh), 1866 (m), 1850 (m), 1782 (vw) cm^{-1}.

Anal. Calcd for [TMBA]$_3$[**2b**]·0.5 CH_2Cl_2: C, 42.40; H, 4.10; N, 3.49. Found: C, 42.21; H, 3.77; N, 3.49. Crystals of [TMBA]$_3$[**2b**]·0.5 CH_2Cl_2 suitable for X-ray diffraction were grown from MeCN/CH_2Cl_2. ICP-AES: Mn: Cr = 2.95: 1.

2.4.5. Synthesis of [PPN]$_2$[$HS_2Mn_3Cr_2(CO)_{19}$] ([PPN]$_2$[3a]). CH_2Cl_2 (20 mL) was added to a mixture of [PPN]$_2$[**1a**] (0.20 g, 0.11 mmol) and $Cr(CO)_6$ (0.03 g, 0.14 mmol). The reaction mixture was heated in refluxing CH_2Cl_2 for 12 h. The resulting solution was filtered and the solvent removed under vacuum. The solid was washed with deionized water and MeOH and then extracted with CH_2Cl_2, which was recrystallized with CH_2Cl_2/MeOH/Et_2O to give a reddish-orange sample of [PPN]$_2$[$HS_2Mn_3Cr_2(CO)_{19}$] ([PPN]$_2$[**3a**]) (0.12 g, 0.06 mmol) (yield: 55% based on [PPN]$_2$[**1a**]). IR (ν_{CO}, CH_2Cl_2): 2054 (w), 1984 (vs), 1979 (vs), 1931 (m), 1905 (w), 1877 (m) cm^{-1}. ^{1}H NMR (400 MHz, DMSO-d_6, 300 K): δ −8.97 (s, hydride) (chemical shifts not given for $[PPN]^+$). Anal. Calcd for [PPN]$_2$[**3a**]: C, 56.24; H, 3.16; N, 1.44. Found: C, 56.03; H, 3.04; N, 1.52. Crystals of [PPN]$_2$[**3a**] suitable for X-ray diffraction were grown from CH_2Cl_2/MeOH/Et_2O. ICP-AES: Mn: Cr = 1.51: 1.

2.4.6. Synthesis of [PPN]$_2$[$HSe_2Mn_3Cr_2(CO)_{19}$] ([PPN]$_2$[3b]). CH_2Cl_2 (20 mL) was added to a mixture of [PPN]$_2$[**1b**] (0.20 g, 0.11 mmol) and $Cr(CO)_6$ (0.05 g, 0.23 mmol). The reaction mixture was heated in refluxing CH_2Cl_2 for 18 h. The resulting solution was filtered and the solvent removed under vacuum. The solid was washed with deionized water and MeOH, and then extracted with CH_2Cl_2, which was recrystallized with CH_2Cl_2/MeOH/Et_2O to give a reddish-orange sample of [PPN]$_2$[$HSe_2Mn_3Cr_2(CO)_{19}$] ([PPN]$_2$[**3b**]) (0.11 g, 0.05 mmol) (yield: 45% based on [PPN]$_2$[**1b**]). IR (ν_{CO}, CH_2Cl_2): 2049 (w), 1982 (vs), 1972 (vs), 1931 (m), 1902 (w), 1871 (m) cm^{-1}. ^{1}H NMR (400 MHz, DMSO-d_6, 300 K): δ −7.80 (s, hydride) (chemical shifts not given for $[PPN]^+$). Anal. Calcd for [PPN]$_2$[**3b**]·MeOH: C, 53.40; H, 3.17; N, 1.35. Found: C, 53.17; H, 3.45; N, 1.15. Crystals of [PPN]$_2$[**3b**] suitable for X-ray diffraction were grown from CH_2Cl_2/MeOH/Et_2O. ICP-AES: Mn: Cr = 1.68: 1.

2.4.7. Conversion of [TMBA]$_2$[1a] to [TMBA]$_3$[2a]. MeOH (20 mL) was added to a mixture of [TMBA]$_2$[**1a**] (1.06 g, 1.09 mmol) and KOH (2.25 g, 40 mmol). The mixture was stirred at 60 ^{o}C for 12 h. A methanol solution of TMBACl (0.82 g, 4.46 mmol) was added dropwise to the resulting solution, precipitating the solid. The solid was collected by filtration, washed with deionized water and MeOH several times, and then extracted with MeCN, which was recrystallized with MeCN/CH_2Cl_2 to give a purplish-black sample of [TMBA]$_3$[**2a**] (0.64 g, 0.60 mmol) (yield: 55% based on [TMBA]$_2$[**1a**]).

2.4.8. Conversion of [TMBA]$_2$[1b] to [TMBA]$_3$[2b]. MeOH (20 mL) was added to a mixture of [TMBA]$_2$[**1b**] (0.88 g, 0.83 mmol) and KOH (2.25 g, 40 mmol). The mixture was stirred at 60 ^{o}C for 14 h. A methanol solution of TMBACl (0.92 g, 5.01 mmol) was added dropwise to the resulting solution, precipitating the solid. The solid was collected by filtration, washed with deionized water and MeOH several times, and then extracted with MeCN, which was recrystallized with MeCN/CH_2Cl_2 to give a greenish-black sample of [TMBA]$_3$[**2b**] (0.40 g, 0.35 mmol) (yield: 42% based on [TMBA]$_2$[**1b**]).

2.4.9. X-ray Structural Characterization of [PPN]$_2$[1a], [PPh$_4$]$_2$[1b], [TMBA]$_3$[2a]·CH$_2$Cl$_2$, [TMBA]$_3$[2b]·0.5 CH$_2$Cl$_2$, [PPN]$_2$[3a], and [PPN]$_2$[3b]. Selected crystallographic data for [PPN]$_2$[**1a**], [PPh$_4$]$_2$[**1b**], [TMBA]$_3$[**2a**]·CH_2Cl_2, [TMBA]$_3$[**2b**]·0.5 CH_2Cl_2, [PPN]$_2$[**3a**], and [PPN]$_2$[**3b**] are given in Table 2.4. All crystals were mounted on glass fibers with epoxy cement. Data collection for [PPN]$_2$[**1a**], [TMBA]$_3$[**2a**]·CH_2Cl_2, [TMBA]$_3$[**2b**]·0.5 CH_2Cl_2, [PPN]$_2$[**3a**], and [PPN]$_2$[**3b**] was carried out on a Bruker Nonius Kappa CCD diffractometer using graphite-monochromated $Mo_{K\alpha}$ radiation, and an empirical absorption correction by multi-scan was applied.[39] Data collection for [PPh$_4$]$_2$[**1b**] was carried out on a Siemens Smart Apex CCD diffractometer using graphite-monochromated $Mo_{K\alpha}$ radiation employing the θ–2θ scan mode, and an empirical absorption correction by multi-scan was applied.[39] The structures of [PPN]$_2$[**1a**], [PPh$_4$]$_2$[**1b**], [TMBA]$_3$[**2a**]·CH_2Cl_2,

$[TMBA]_3$[**2b**]·0.5 CH_2Cl_2, $[PPN]_2$[**3a**], and $[PPN]_2$[**3b**] were solved by direct methods and were refined with SHELXL-97.[40] The hydride atoms of $[PPN]_2$[**1a**], $[PPh_4]_2$[**1b**], $[PPN]_2$[**3a**], and $[PPN]_2$[**3b**] were found in the bridging position across one Mn─Mn bond and were refined with isotropic temperature factors. For $[TMBA]_3$[**2a**], the Mn(1), Mn(2), Mn(3), and Mn(4) atoms and the Cr(1), Cr(2), Cr(3), and Cr(4) atoms of the M_4 square in the two independent forms were with 75 and 25% occupancy, respectively, and were refined with anisotropic temperature factors. For $[TMBA]_3$[**2b**], one independent square M_4 plane showed the disordered M(1) and M(2) atoms with Mn and Cr in 75 and 25% occupancy, and the other one showed the disordered M(3) atom with Mn and Cr present in a 50:50 ratio. All metal atoms were refined with anisotropic temperature factors. For $[PPN]_2$[**3a**], the C(3), O(3); C(4), O(4); C(5), O(5); and C(17), O(17) atoms in the four terminal COs of the di-$Cr(CO)_5$ group were disordered with 50, 55, 55, and 60% occupancy, respectively, and were refined with isotropic temperature factors. Except for the disordered C and O atoms on the di-$Cr(CO)_5$ group of $[PPN]_2$[**3a**], all of the non-hydrogen atoms for $[PPN]_2$[**1a**], $[PPh_4]_2$[**1b**], $[TMBA]_3$[**2a**]·CH_2Cl_2, $[TMBA]_3$[**2b**]·0.5 CH_2Cl_2, $[PPN]_2$[**3a**], and $[PPN]_2$[**3b**] were refined with anisotropic temperature factors. The selected distances and angles for $[PPN]_2$[**1a**], $[PPh_4]_2$[**1b**], $[TMBA]_3$[**2a**]·CH_2Cl_2, $[TMBA]_3$[**2b**]·0.5 CH_2Cl_2, $[PPN]_2$[**3a**], and $[PPN]_2$[**3b**] are listed in Table S2.5. Additional crystallographic data are available as CIF files in the Supporting Information.

2.4.10. Electrochemical Measurements. The cyclic voltammetry measurements were performed at room temperature under a nitrogen atmosphere and recorded using a BAS-100W and a CHI 621D electrochemical potentiostat. A platinum working electrode, a platinum wire auxiliary electrode, and a non-aqueous Ag/Ag^+ electrode were used in a three-electrode configuration. Tetra-*n*-butylammonium perchlorate (TBAP) was used as the supporting electrolyte, and the solute concentration was ~10^{-3} -10^{-4} M. The redox potentials

were calibrated with a ferrocenium/ferrocene (Fc^+/Fc) couple in the working solution and referenced to SCE.

2.4.11. Computational Details. All calculations reported in the present study were performed via the density functional theory (DFT) with Becke's 1988 exchange functional (B) and Perdew's 1986 gradient correlation functional (BP86)[26,27] or Becke's three-parameter (B3) exchange functional and the Lee─Yang─Parr (LYP) correlation functional (B3LYP)[28,29] with a larger basis set: TZVP[30] (triple-zeta valence with one polarization function on each atom) using the Gaussian 03 series of packages.[41] We focused our analyses on the pure DFT method (BP86) due to a better correlation with experimental structural parameters (Table S2.4). The geometries of $[E_2Mn_3(CO)_9]^-$ (E = S, Se), **1a**, **1b**, **2a**, **2b**, **3a**, and **3b** were fully optimized using the BP86/TZVP method. Wiberg bond indices[34] and natural charges[35] were evaluated with Weinhold's NBO method.[42] Graphical representations of the molecular orbitals were obtained using CS Chem3D 5.0. For orbital contributions, the molecular orbital compositions were analyzed using the AOMIX program.[43]

2.4.12. Acknowledgements. This work was supported by the National Science Council of Taiwan (NSC Grant No. 98-2113-M-003-006-MY3 to M. Shieh). We are also grateful to the National Center for High-Performance Computing, which provided the Gaussian package and computer time. Our gratitude also goes to the Academic Paper Editing Clinic, NTNU.

2.4.13. Supporting Information Available: X-ray crystallographic files in CIF format for $[PPN]_2$[**1a**], $[PPh_4]_2$[**1b**], $[TMBA]_3$[**2a**]·CH_2Cl_2, $[TMBA]_3$[**2b**]·0.5 CH_2Cl_2, $[PPN]_2$[**3a**], and $[PPN]_2$[**3b**], computational details for the optimized geometries of $[E_2Mn_3(CO)_9]^-$ (E = S, Se), **1a**, **1b**, **2a**, **2b**, **3a**, and **3b**, ORTEPs for **1a─3a**, and electrochemical data. This material is available free of charge via the Internet at http://pubs.acs.org.

References:

(1) (a) Braunstein, P., Rosé, J. In *Catalysis by Di- and Polynuclear Metal Cluster Complexes*; Adams, R. D., Cotton, F. A., Eds.; Wiley-VCH: New York, 1998; Chapter 13. pp 443─508. (b) Braunstein, P., Rosé, J. *Metal Clusters in Chemistry*; Braunstein, P., Oro, L. A., Raithby, P. R., Eds.; Wiley-VCH: Weinheim, 1999; Vol. *2*, Chapter 2.2, pp 616─677. (c) *Comprehensive Organometallic Chemistry II*; Abel, E. W., Stone, F. G. A., Wilkinson, G., Eds.; *Heteronuclear Metal─Metal Bonds*, Vol. *10*; Adams, R. D., Ed.; Elsevier: Oxford, 1995. (d) Sinfelt, J. H. *Bimetallic Catalysts. Discoveries, Concepts and Applications*; Wiley: New York, 1983. (e) *Metal Clusters in Catalysis*; Gates, B. C., Guczi, L., Knözinger, H., Eds.; *Studies in Surface Science and Catalysis Series*; Elsevier: Amsterdam, 1986; Vol. *29*. (f) Hermans, S., Khimyak, T., Raja, R., Sankar, G., Thomas, J. M., Johnson, B. F. G. in *Nanotechnology in Catalysis*; Zhou, B., Hermans, S., Somorjai, G. A., Eds.; Kluwer Academic, Plenum Publishers: New York, 2004.

(2) (a) Thomas, J. M.; Johnson, B. F. G.; Raja, R.; Sankar, G.; Midgley, P. A. *Acc. Chem. Res.* **2003**, *36*, 20─30. (b) Sivaramakrishna, A.; Clayton, H. S.; Makhubela, B. C. E.; Moss, J. R. *Coord*. *Chem*. *Rev*. **2008**, *252*, 1460─1485. (c) Adams, R. D.; Captain, B. *Acc*. *Chem*. *Res*. **2009**, *42,* 409─418. (d) Adams, R. D.; Captain, B. *Angew. Chem., Int. Ed.* **2008**, *47*, 252─257. (e) Braunschweig, H.; Cogswell, P.; Schwab, K. *Coord*. *Chem*. *Rev*. **2011**, *255*, 101─117.

(3) (a) Kahn, O. *Molecular Magnetism*; VCH: Weinheim, 1993. (b) Mathonière, C., Sutter, J.-P., Yakhmi, J. V. Bimetallic magnets: Present and perspectives. In *Magnetism: molecules to materials*; Miller, J. S., Drillon, M., Eds.; Wiley-VCH: Weinheim, 2002; Vol. *4*.

(4) (a) Robinson, I.; Zacchini, S.; Tung, L. D.; Maenosono, S.; Thanh, N. T. K. *Chem*. *Mater*. **2009**, *21*, 3021─3026. (b) Femoni, C.; Iapalucci, M. C.; Longoni, G.; Wolowska, J.;

Zacchini, S.; Zanello, P.; Fedi, S.; Riccò, M.; Pontiroli, D.; Mazzani, M. *J. Am. Chem. Soc*. **2010**, *132*, 2919─2927. (c) Riccò, M.; Shiroka, T.; Carretta, S.; Bolzoni, F.; Femoni, C.; Iapalucci, M. C.; Longoni, G. *Chem.─Eur. J.* **2005**, *11*, 2856─2861. (d) Eichhöfer, A.; Olkowska-Oetzel, J.; Fenske, D.; Fink, K.; Mereacre, V.; Powell, A. K.; Buth, G. *Inorg. Chem.* **2009**, *48*, 8977─8984. (e) Muratsugu, S.; Sodeyama, K.; Kitamura, F.; Sugimoto, M.; Tsuneyuki, S.; Miyashita, S.; Kato, T.; Nishihara, H. *J. Am. Chem. Soc*. **2009**, *131*, 1388─1389. (f) Costa, M.; Della Pergola, R.; Fumagalli, A.; Laschi, F.; Losi, S.; Macchi, P.; Sironi, A.; Zanello, P. *Inorg. Chem.* **2007**, *46*, 552─560. (g) Prinz, M.; Kuepper, K.; Taubitz, C.; Raekers, M.; Khanra, S.; Biswas, B.; Weyhermüller, T.; Uhlarz, M.; Wosnitza, J.; Schnack, J.; Postnikov, A. V.; Schröder, C.; George, S. J.; Neumann, M.; Chaudhuri, P. *Inorg. Chem.* **2010**, *49*, 2093─2102. (h) Bechlars, B.; Issac, I.; Feuerhake, R.; Clérac, R.; Fuhr, O.; Fenske, D. *Eur. J. Inorg. Chem*. **2008**, 1632─1644. (i) Shieh, M.; Chung, R.-L.; Yu, C.-H.; Hsu, M.-H.; Ho, C.-H.; Peng, S.-M.; Liu, Y.-H. *Inorg. Chem*. **2003**, *42*, 5477─5479.

(5) (a) Kong, X.-J.; Long, L.-S.; Zheng, Z.; Huang, R.-B.; Zheng, L.-S. *Acc. Chem. Res.* **2010**, *43*, 201─209. (b) Femoni, C.; Iapalucci, M. C.; Kaswalder, F.; Longoni, G.; Zacchini, S. *Coord. Chem. Rev*. **2006**, *250*, 1580─1604. (c) Welsch, S.; Gröger, C.; Sierka, M.; Scheer, M. *Angew. Chem. Int. Ed.* **2011**, *50*, 1435─1438. (d) de Silva, N.; Dahl, L. F. *Inorg. Chem.* **2006**, *45*, 8814─8816. (e) Scheer, M.; Schindler, A.; Merkle, R.; Johnson, B. P.; Linseis, M.; Winter, R.; Anson, C. E.; Virovets, A. V. *J. Am. Chem. Soc*. **2007**, *129*, 13386─13387. (f) Femoni, C.; Iapalucci, M. C.; Longoni, G.; Zacchini, S.; Zarra, S. *J. Am. Chem. Soc*. **2011**, *133*, 2406─2409.

(6) (a) Ferrando, R.; Jellinek, J.; Johnston, R. L. *Chem. Rev*. **2008**, *108*, 845─910. (b) Femoni, C.; Iapalucci, M. C.; Longoni, G.; Tiozzo, C.; Zacchini, S. *Angew. Chem. Int. Ed.* **2008**, *47*, 6666─6669. (c) Naitabdi, A.; Toulemonde, O.; Bucher, J. P.; Rosé, J.; Braunstein, P. ;

Welter, R.; Drillon, M. *Chem.─Eur. J.* **2008**, *14*, 2355─2362. (d) Schweyer-Tihay, F.; Estournès, C.; Braunstein, P.; Guille, J.; Paillaud, J.-L.; Richard-Plouet, M.; Rosé, J. *Phys. Chem. Chem. Phys.* **2006**, *8*, 4018─4028.

(7) (a) Adams, R. D. In *The Chemistry of Metal Cluster Complexes*; Shriver, D. F., Kaesz, H. D.; Adams, R. D., Eds.; VCH: New York, 1990; Chapter 3, p 121. (b) Roberts, D. A., Geoffroy, G. L. In *Comprehensive Organometallic Chemistry*; Wilkinson, G., Stone, F. G. A., Abel, E. W., Eds.; Pergamon: Oxford, 1982; Vol. *6*, Chapter 40, p 763.

(8) (a) Wadepohl, H. *Coord. Chem. Rev.* **1999**, *185─186*, 551─568. (b) Cador, O.; Cattey, H.; Halet, J.-F.; Meier, W.; Mugnier, Y.; Wachter, J.; Saillard, J.-Y.; Zouchoune, B.; Zabel, M. *Inorg. Chem.* **2007**, *46*, 501─509.

(9) (a) Whitmire, K. H. *J. Coord. Chem.* **1988**, *17*, 95─204. (b) Roof, L. C.; Kolis, J. W. *Chem. Rev.* **1993**, *93*, 1037─1080. (c) Mathur, P. *Adv. Organomet. Chem.* **1997**, *41*, 243─314. (d) Ogino, H.; Inomata, S.; Tobiya, H. *Chem. Rev.* **1988**, *98*, 2093─2021. (e) King, R. B.; Bitterwolf, T. E. *Coord. Chem. Rev.* **2000**, *206─207*, 563─579.

(10) (a) Lesch, D. A.; Rauchfuss, T. B. *Inorg. Chem.* **1981**, *20*, 3583─3585. (b) Holliday, R. L.; Roof, L. C.; Hargus, B.; Smith, D. M.; Wood, P. T.; Pennington, W. T.; Kolis, J. W. *Inorg. Chem.* **1995**, *34*, 4392─4401. (c) Drake, G. W.; Schimek, G. L.; Kolis, J. W. *Inorg. Chim. Acta* **1995**, *240*, 63─69. (d) Calderoni, F.; Demartin, F.; Iapalucci, M. C.; Laschi, F.; Longoni, G.; Zanello, P. *Inorg. Chem.* **1996**, *35*, 898─905. (e) Hecht, C.; Herdtweck, E.; Rohrmann, J.; Hermann, W. A.; Beck, W.; Fritz, P. M. *J. Organomet. Chem.* **1987**, *330*, 389─396. (f) Imhof, W.; Huttner, G.; Eber, B.; Günauer, D. *J. Organomet. Chem.* **1992**, *428*, 379─400. (g) Bachman, R. E.; Whitmire, K. H. *Organometallics* **1993**, *12*, 1988─1992. (h) Bachman, R. E.; Whitmire, K. H. *Inorg. Chem.* **1994**, *33*, 2527─2533.

(11) (a) Shieh, M. *J. Cluster Sci.* **1999**, *10*, 3─36. (b) Shieh, M.; Ho, C.-H. *C. R. Chimie* **2005**, *8*, 1838─1849. (c) Lai, Y.-W.; Cherng, J.-J.; Sheu, W.-S.; Lee, G.-A.; Shieh, M.

Organometallics **2006**, *25*, 184─190.

(12) (a) Adams, R. D.; Kwon, O.-S.; Miao, S. *Acc. Chem. Res.* **2005**, *38*, 183─190. (b) Adams, R. D.; Miao, S. *J. Organomet. Chem.* **2003**, *665*, 43─47. (c) Huang, S. D.; Lai, C. P.; Barnes, C. L. *Angew. Chem. Int. Ed. Engl.* **1997**, *36*, 1854─1856. (d) Fang, Z.-G.; Hor, T. S. A.; Mok, K. F.; Ng, S.-C.; Liu, L.-K.; Wen, Y.-S. *Organometallics* **1993**, *12*, 1009─1011. (e) Alper, H.; Sibtain, F.; Einstein, F. W. B.; Willis, A. C. *Organometallics* **1985**, *4*, 604─606. (f) Ruiz, J.; Ceroni, M.; Quinzani, O. V.; Riera, V.; Vivanco, M.; García-Granda, S.; Van der Maelen, F.; Lanfranchi, M.; Tiripicchio, A. *Chem.─Eur. J.* **2001**, *7*, 4422─4430. (g) Yao, W.-R.; Guo, D.-S.; Liu, Z.-H.; Zhang, Q.-F. *J. Mol. Struct.* **2003**, *657*, 165─175.

(13) (a) Seidel, R.; Schnautz, B.; Henkel, G. *Angew. Chem. Int. Ed. Engl.* **1996**, *35*, 1710─1712. (b) Hermann, W. A.; Hecht, C.; Ziegler, M. L.; Balbach, B. *J. Chem. Soc., Chem. Commun.* **1984**, 686─687. (c) Belletti, D.; Graiff, C.; Pattacini, R.; Predieri, G.; Tiripicchio, A. *Eur. J. Inorg. Chem.* **2004**, 3564─3569. (d) Ruiz, J.; Araúz, R.; Ceroni, M.; Vivanco, M.; Van der Maelen, F.; García-Granda, S. *Organometallics* **2010**, *29*, 3058─3061.

(14) (a) Huang, K.-C.; Tsai, Y.-C.; Lee, G.-H.; Peng, S.-M.; Shieh, M. *Inorg. Chem.* **1997**, *36*, 4421─4425. (b) Shieh, M.; Chen, H.-S.; Yang, H.-Y.; Ueng, C.-H. *Angew. Chem., Int. Ed.* **1999**, *38*, 1252─1254. (c) Shieh, M.; Chen, H.-S.; Yang, H.-Y.; Lin, S.-F.; Ueng, C.-H. *Chem.−Eur. J.* **2001**, *7*, 3152─3158. (d) Shieh, M.; Ho, C.-H.; Sheu, W.-S.; Chen, H.-W. *J. Am. Chem. Soc.* **2010**, *131*, 4032─4033. (e) Ho, C.-H.; Chu, Y.-Y.; Lin, C.-N.; Chen, H.-W.; Huang, C.-Y.; Shieh, M. *Organometallics* **2010**, *29*, 4396─4405.

(15) (a) Hoefler, M.; Tebbe, K.-F.; Veit, H.; Weiler, N. E. *J. Am. Chem. Soc.* **1983**, *105*, 6338─6339. (b) Darensbourg, D. J.; Zalewski, D. J. *Organometallics* **1984**, *3*, 1598─1600. (c) Fischer, R. A.; Kneuper, H.-J.; Herrmann, W. A. *J. Organomet. Chem.*

1987, *330*, 365─376.

(16) (a) Goh, L. Y. *Coord*. *Chem*. *Rev*. **1999**, *185─186*, 257─276. (b) Hausmann, H.; Höfler, M.; Kruck, T.; Zimmermann, H. W. *Chem*. *Ber*. **1981**, *114*, 975─981. (c) Rohrmann, J.; Herrmann, W. A.; Herdtweck, E.; Riede, J.; Ziegler, M.; Sergeson, G. *Chem*. *Ber*. **1986**, *119*, 3544─3557. (d) Blacque, O.; Brunner, H.; Kubicki, M. M.; Nuber, B.; Stubenhofer, B.; Watchter, J.; Wrackmeyer, B. *Angew*. *Chem*., *Int*. *Ed*. **1997**, *36*, 351─353. (e) Stauf, S.; Reisner, C.; Tremel, W. *Chem*. *Commun*. **1996**, 1749─1750. (f) Song, L.-C.; Cheng, H.-W.; Hu, Q.-M. *Organometallics* **2004**, *23*, 1072─1080.

(17) (a) Shieh, M.; Ho, L.-F.; Guo, Y.-W.; Lin, S.-F.; Lin, Y.-C.; Peng, S.-M.; Liu, Y.-H. *Organometallics* **2003**, *22*, 5020─5026. (b) Shieh, M.; Ho, L.-F.; Chen, P.-C.; Hsu, M.-H.; Chen, H.-L.; Guo, Y.-W.; Pan, Y.-W.; Lin, Y.-C. *Organometallics* **2007**, *26*, 6184─6196. (c) Shieh, M. Miu, C.-Y. *J*. *Chin*. *Chem*. *Soc*. **2010**, *57*, 956─966.

(18) (a) Pasynskii, A. A.; Eremenko, I. L.; Orazsakhatov, B.; Kalinnikov, V. T.; Aleksandrov, G. G.; Struchkov, Y. T. *J*. *Organomet*. *Chem*. **1981**, *216*, 211─221. (b) Pasynskii, A. A.; Eremenko, I. L.; Orazsakhatov, B.; Gasanov, G. S.; Novotortsev, V. M.; Ellert, O. G.; Seifulina, Z. M.; Shklover, V. E.; Struchkov, Y. T. *J*. *Organomet*. *Chem*. **1984**, *270*, 53─64. (c) Pasynskii, A. A.; Eremenko, I. L.; Orazsakhatov, B.; Rakitin, Y. V.; Novotortsev, V. M.; Ellert, O. G.; Kalinnikov, V. T.; Aleksandrov, G. G.; Struchkov, Y. T. *J*. *Organomet*. *Chem*. **1981**, *214*, 351─365. (d) Pasynskii, A. A.; Skabitski, I. V.; Torubaev, Y. V.; Semenova, N. I.; Novotortsev, V. M.; Ellert, O. G.; Lyssenko, K. A. *J*. *Organomet*. *Chem*. **2003**, *671*, 91─100.

(19) (a) Pasynskii, A. A.; Grigoriev, V. N.; Torubaev, Y. V.; Blokhin, A. I.; Shapovalov, S. S.; Dobrokhotova, Z. V.; Novotortsev, V. M. *Russ. Chem. Bull.* **2003**, *52*, 2689─2700. (b) Pasynskii, A. A.; Torubaev, Y. V.; Grigoriev, V. N.; Blokhin, A. I.; Herberhold, M.; Mathur, P. *J*. *Cluster Sci.* **2009**, *20*, 193─204. (c) Shieh, M.; Lin, C.-N.; Miu, C.-Y.; Hsu,

M.-H.; Pan, Y.-W.; Ho, L.-F. *Inorg. Chem.* **2010**, *49*, 8056─8066.

(20) (a) Ma, Y. Q.; Yu, L.; Hu, C. S.; Chen, X.; Li, J.; Wang, H. G.; Miguel, D. *J. Mol. Struct.* **2003**, *650*, 45─48. (b) Ma, Y.-Q.; Yin, N.; Li, J.; Xie, Q.-L.; Miguel, D. *J. Organomet. Chem.* **2004**, *689*, 1949─1955. (c) Alvarez, B.; García-Granda, S.; Jeannin, Y.; Miguel, D.; Miguel, J. A.; Riera, V. *Organometallics* **1991**, *10*, 3005─3007.

(21) (a) Behrens, H.; Weber, R. *Z. Anorg. Allg. Chem.* **1957**, *291*, 122─130. (b) Behrens, H.; Vogl, J. *Chem. Ber.* **1963**, *96*, 2220─2229. (c) Darensbourg, D. J.; Rokicki, A.; Darensbourg, M. Y. *J. Am. Chem. Soc.* **1981**, *103*, 3223─3224. (d) Darensbourg, M. Y.; Slater, S. *J. Am. Chem. Soc.* **1981**, *103*, 5914─5915. (e) Darensbourg, M. Y.; Deaton, J. C. *Inorg. Chem.* **1981**, *20*, 1644─1646. (f) Darensbourg, M. Y.; Bau, R.; Marks, M. W.; Burch, R. R.; Deaton, J. C. Jr.; Slater, S. *J. Am. Chem. Soc.* **1982**, *104*, 6961─6969.

(22) Cauzzi, D.; Graiff, C.; Pattacini, R.; Predieri, G.; Tiripicchio, A.; Kahlal, S.; Saillard, J.-Y. *Eur. J. Inorg. Chem.* **2004**, 1063─1072.

(23) (a) Vergamini, P. J.; Vahrenkamp, H.; Dahl, L. F. *J. Am. Chem. Soc.* **1971**, *93*, 6326─6327. (b) Seyferth, D.; Henderson, R. S.; Fackler, J. P. Jr.; Mazany, A. M. *J. Organomet. Chem.* **1981**, *213*, C21─C25. (c) Adams, R. D.; Captain, B.; Kwon, O.-S.; Miao, S. *Inorg. Chem.* **2003**, *42*, 3356─3365. (d) Adams, R. D.; Horváth, I. T.; Wang, S. *Inorg. Chem.* **1985**, *24*, 1728─1730. (e) Adams, R. D.; Babin, J. E.; Wang, J.-G.; Wu, W. *Inorg. Chem.* **1989**, *28*, 703─709. (f) Brunner, H.; Lucas, D.; Monzon, T.; Mugnier, Y.; Nuber, B.; Stubenhofer, B.; Stückl, A. C.; Wachter, J. Wanninger, R.; Zabel, M. *Chem.−Eur. J.* **2000**, *6*, 493─503.

(24) (a) Adams, R. D.; Wolfe, T. A.; Wu, W. *Polyhedron*, **1991**, *10*, 447─454. (b) Mathur, P.; Hossain, M. M.; Rashid, R. S. *J. Organomet. Chem.* **1994**, *467*, 245─249. (c) Fong, S.-W. A.; Vittal, J. J.; Hor, T. S. A. *Organometallics* **2000**, *19*, 918─924. (d) Belletti, D.; Graiff, C.; Pattacini, R.; Predieri, G.; Tiripicchio, A.; de Biani, F. F.; Zanello, P. *Inorg. Chim.*

Acta **2005**, *358*, 161─172.

(25) Ghosh, S.; Kabir, S. E.; Pervin, S.; Hossain, G. M. G.; Haworth, D. T.; Lindeman, S. V.; Siddiquee, T. A.; Bennett, D. W.; Roesky, H. W. *Z. Anorg. Allg. Chem*. **2009**, *635*, 76─87.

(26) Becke, A. D. *Phys. Rev. A* **1988**, *38*, 3098─3100.

(27) Perdew, J. P. *Phys. Rev. B* **1986**, *33*, 8822─8824.

(28) (a) Becke, A. D. *J. Chem. Phys.* **1993**, *98*, 5648─5652. (b) Becke, A. D. *J. Chem. Phys.* **1992**, *96*, 2155─2160. (c) Becke, A. D. *J. Chem. Phys.* **1992**, *97*, 9173─9177.

(29) Lee, C.; Yang, W.; Parr, R. G. *Phys. Rev. B* **1988**, *37*, 785─789.

(30) Schäfer, A.; Huber, C.; Ahlrichs, R. *J. Chem. Phys*. **1994**, *100*, 5829─5835.

(31) See especially: Furche, F.; Perdew, J. P. *J. Chem. Phys*. **2006**, *124*, 044103─044127.

(32) Wang, H. Y.; Xie, Y.; King, R. B.; Schaefer, H. F. *J. Am. Chem. Soc*. **2005**, *127*, 11646─11651.

(33) Wang, H. Y.; Xie, Y.; King, R. B.; Schaefer, H. F. *J. Am. Chem. Soc*. **2006**, *128*, 11376─11384.

(34) Wiberg, K. B. *Tetrahedron* **1968**, *24*, 1083─1096.

(35) (a) Reed, A. E.; Weinhold, F. *J. Chem. Phys*. **1983**, *78*, 4066─4073. (b) Reed, A. E.; Weinstock, R. B.; Weinhold, F. *J. Chem. Phys.* **1985**, *83*, 735─746.

(36) Bard, A. J., Faulkner, L. R. *Electrochemical Methods; Fundamentals and Applications,* 2nd ed.; John Wiley & Sons: New York, 2001; p 291.

(37) Nakanishi, T.; Murakami, H.; Sagara, T.; Nakashima, N. *J. Phy. Chem. B* **1999**, *103*, 304─308.

(38) Shriver, D. F., Drezdon, M. A. *The Manipulation of Air-Sensitive Compounds*; Wiley-VCH Publishers: New York, 1986.

(39) Blessing, R. H. *Acta Crystallogr. Sect. A* **1995**, *51*, 33─38.

(40) Sheldrick, G. M. *SHELXL97*, version 97-2; University of Göttingen, Germany, 1997

(41) Frisch, M. J.; Trucks, G. W.; Schlegel, H. B.; Scuseria, G. E.; Robb, M. A.; Cheeseman, J. R.; Montgomery, J. A., Jr.; Vreven, T.; Kudin, K. N.; Burant, J. C.; Millam, J. M.; Iyengar, S. S.; Tomasi, J.; Barone, V.; Mennucci, B.; Cossi, M.; Scalmani, G.; Rega, N.; Petersson, G. A.; Nakatsuji, H.; Hada, M.; Ehara, M.; Toyota, K.; Fukuda, R.; Hasegawa, J.; Ishida, M.; Nakajima, T.; Honda, Y.; Kitao, O.; Nakai, H.; Klene, M.; Li, X.; Knox, J. E.; Hratchian, H. P.; Cross, J. B.; Bakken, V.; Adamo, C.; Jaramillo, J.; Gomperts, R.; Stratmann, R. E.; Yazyev, O.; Austin, A. J.; Cammi, R.; Pomelli, C.; Ochterski, J. W.; Ayala, P. Y.; Morokuma, K.; Voth, G. A.; Salvador, P.; Dannenberg, J. J.; Zakrzewski, V. G.; Dapprich, S.; Daniels, A. D.; Strain, M. C.; Farkas, O.; Malick, D. K.; Rabuck, A. D.; Raghavachari, K.; Foresman, J. B.; Ortiz, J. V.; Cui, Q.; Baboul, A. G.; Clifford, S.; Cioslowski, J.; Stefanov, B. B.; Liu, G.; Liashenko, A.; Piskorz, P.; Komaromi, I.; Martin, R. L.; Fox, D. J.; Keith, T.; Al-Laham, M. A.; Peng, C. Y.; Nanayakkara, A.; Challacombe, M.; Gill, P. M. W.; Johnson, B.; Chen, W.; Wong, M. W.; Gonzalez, C.; Pople, J. A. *Gaussian 03*, Revision E.04; Gaussian, Inc.: Wallingford, CT, 2004

(42) Reed, A. E.; Curtiss L. A.; Weinhold F. *Chem. Rev.* **1988**, *88*, 899─926.

(43) Gorelsky, S. I. *AOMix* program, http://www.sg-chem.net/.

Table 2.1. Averaged Bond Distance (Å) for $[PPN]_2$[**1a**], $[PPh_4]_2$[**1b**], $[TMBA]_3$[**2a**]·CH_2Cl_2, $[TMBA]_3$[**2b**]·0.5 CH_2Cl_2, $[PPN]_2$[**3a**], $[PPN]_2$[**3b**], and Related Complexes

complex	E─Mn	Mn─Mn	E─Cr	H─Mn	Mn─Cr	ref
$[PPN]_2$[**1a**]	2.32(2)	2.69(2)	2.427(2)	1.7(2)		*a*
$[PPh_4]_2$[**1b**]	2.43(3)	2.78(2)	2.532(1)	1.68(2)		*a*
$[TMBA]_3$[**2a**]·CH_2Cl_2	2.40(2)	2.68(4)	2.35(6)		2.6(3)	*a*
$[TMBA]_3$[**2b**]·0.5 CH_2Cl_2	2.51(1)	2.73(4)	2.49(5)		2.73(3)	*a*
$[PPN]_2$[**3a**]	2.32(2)	2.72(2)	2.45(1)	1.6(2)		*a*
$[PPN]_2$[**3b**]	2.43(2)	2.76(1)	2.533(4)	1.7(1)		*a*
$[PPN][S_2Mn_3(CO)_9]$	2.24(1)	2.768(3)				12g
$[Et_4N][Se_2Mn_3(CO)_9]$	2.36(2)	2.83(2)				14a
$[PPh_4]_2[Se_2Mn_3(CO)_9]$	2.43(2)	2.76(6)				13a
$[PPN]_2[Se_2Mn_4(CO)_{12}]$	2.475(2)	2.705(8)				14a
$[Cp_2Cr_2(\mu\text{-}SCMe_3)(\mu_3\text{-}S)_2Mn(CO)_3]$	2.29(2)		2.30(4)		2.77(8)	18b
$[CrMn_2(CO)_8(\mu\text{-}CO)_2(\mu_3\text{-}SN_2C_4H_5)_2]$	2.320(2)		2.343(2)		2.849(1)	25
$[CpMnSe_2Cr(CO)_7]$	2.50(1)		2.503(2)			19a
$[CpMnSe_2Cr_2(CO)_{12}]$	2.53(2)		2.50(1)			19a
$[Et_4N]_2[Se_2Mn_3(CO)_{10}\{Cr(CO)_5\}_2]$	2.43(2)	2.671(2)	2.541(1)			19c

Table 2.2. Calculated Components of the Selected Frontier Molecular Orbitals for $[E_2Mn_3(CO)_9]^-$ (E = S, Se), **1a**, **1b**, **2a**, **2b**, **3a**, **3b**

complex	atoms						
	E	Mn	Cr	H	CO	$HE_2Mn_3(CO)_9$ /$E_2Mn_3(CO)_9$ (sum)	$Cr_m(CO)_n$ (sum)
$[E_2Mn_3(CO)_9]^-$ (E = S)							
LUMO+1	23.78	50.61			25.61	100	0
LUMO	23.79	50.62			25.59	100	0
HOMO	5.92	68.28			25.80	100	0
HOMO─1	6.90	65.90			27.20	100	0
$[E_2Mn_3(CO)_9]^-$ (E = Se)							
LUMO+1	26.60	49.90			23.50	100	0
LUMO	26.71	49.87			23.52	100	0
HOMO	7.97	67.10			24.93	100	0
HOMO─1	7.96	67.08			24.96	100	0
1a							
LUMO (m = 1, n = 5)	3.44	20.67	16.13	0.06	59.70	40.69	59.31
HOMO (m = 1, n = 5)	14.28	62.41	0.69	0.30	22.32	98.86	1.14
1b							
LUMO (m = 1, n = 5)	3.76	26.11	15.04	0.01	55.08	48.35	51.65
HOMO (m = 1, n = 5)	19.15	59.94	0.06	0.06	20.79	99.92	0.08
2a							
LUMO (m = 1, n = 3)	3.26	53.87	8.00		34.87	86.53	13.47
HOMO (m = 1, n = 3)	0.49	51.86	14.01		33.64	80.55	19.45
2b							
LUMO (m = 1, n = 3)	3.91	52.46	8.76		34.87	85.54	14.46
HOMO (m = 1, n = 3)	0.32	55.17	10.72		33.79	85.44	14.56
3a							
LUMO (m = 2, n = 10)	2.90	31.45	12.04	0.02	53.59	55.98	44.02
HOMO (m = 2, n = 10)	12.66	53.16	8.20	0.01	25.97	86.44	13.56
3b							
LUMO (m = 2, n = 10)	3.18	36.91	10.62	0.02	49.27	63.58	36.42
HOMO (m = 2, n = 10)	15.57	51.58	8.60	0.01	24.24	86.28	13.72

Table 2.3. Differential Pulse Voltammetry of [PPN][$S_2Mn_3(CO)_9$], [PPN][$Se_2Mn_3(CO)_9$], [PPN]$_2$[**1a**], [PPN]$_2$[**1b**], [TMBA]$_3$[**2a**], [TMBA]$_3$[**2b**], [PPN]$_2$[**3a**], [PPN]$_2$[**3b**], and $Cr(CO)_6$

complex	oxidation process		reduction process	
	Ep^{ox}/V^a ($W_{1/2}$/mV^c)	Ep^{red}/V^b ($W_{1/2}$/mV^c)	Ep^{ox}/V^a ($W_{1/2}$/mV^c)	Ep^{red}/V^b ($W_{1/2}$/mV^c)
[PPN][$S_2Mn_3(CO)_9$]	0.605 (130)	0.645 (130)		
[PPN][$Se_2Mn_3(CO)_9$][e]	0.554 (110)	0.601 (118)		
[PPN]$_2$[**1a**]	0.756 (90)	0.796 (101)		
	0.604 (130)	0.656 (135)		
	0.328 (90)	0.396 (93)		
	0.032 (130)	0.060 (150)		
[PPN]$_2$[**1b**]	0.883 (142)	0.877 (111)		
	0.551 (105)	0.561 (115)		
	0.359 (100)	0.337 (99)		
	0.127 (100)	0.121 (115)		
[TMBA]$_3$[**2a**]	0.702 (138)	0.666 (132)	−0.046 (106)	−0.050 (100)
	0.542 (130)		−0.270 (111)	−0.258 (115)
	∼0.350 ([d]) (br)	0.366 (98)	−0.690 (115)	−0.702 (108)
[TMBA]$_3$[**2b**]	0.702 (138)		−0.050 (110)	−0.044 (104)
	0.538 (136)	0.544 (96)	−0.274 (112)	−0.234 (101)
	∼0.370 ([d]) (br)	0.368 (100)	−0.694 (115)	−0.684 (108)
[PPN]$_2$[**3a**]	0.867 (128)	0.872 (129)	−0.137 (210) (br)	−0.160 (212) (br)
	0.755 (99)	([d]) (br)		
	0.675 (95)	∼0.688 ([d]) (br)		
	0.595 (91)	([d]) (br)		
	0.323 (92)	0.324 (110)		
[PPN]$_2$[**3b**]	0.849 (133)	0.853 (105)		−0.182 (150) (br)
	0.693 (115)	([d]) (br)		
	0.561 (173)	([d]) (br)		
	0.325 (80)	0.345 (84)		
	0.069 (91)			
$Cr(CO)_6$			−0.063 (493) (br)	−0.233 (415) (br)

[a] Ep^{ox} = oxidative peak potential. [b] Ep^{red} = reductive peak potential. [c] $W_{1/2}$ = width at half-height. [d] Difficult to determine. [e] ref 14e.

Table 2.4. Crystallographic Data for $[PPN]_2[HS_2Mn_3Cr(CO)_{14}]$ ($[PPN]_2$[**1a**]), $[PPh_4]_2[HSe_2Mn_3Cr(CO)_{14}]$ ($[PPh_4]_2$[**1b**]), $[TMBA]_3[S_2Mn_3Cr(CO)_{19}]\cdot CH_2Cl_2$ ($[TMBA]_3$[**2a**]$\cdot CH_2Cl_2$), $[TMBA]_3[Se_2Mn_3Cr(CO)_{19}]\cdot 0.5\ CH_2Cl_2$ ($[TMBA]_3$[**2b**]$\cdot 0.5\ CH_2Cl_2$), $[PPN]_2[HS_2Mn_3Cr_2(CO)_{19}]$ ($[PPN]_2$[**3a**]), and $[PPN]_2[HSe_2Mn_3Cr_2(CO)_{19}]$ ($[PPN]_2$[**3b**])

	$[PPN]_2$[**1a**]	$[PPh_4]_2$[**1b**]	$[TMBA]_3$[**2a**]$\cdot CH_2Cl_2$
empirical formula	$C_{86}H_{61}CrMn_3N_2O_{14}P_4S_2$[a]	$C_{62}H_{41}CrMn_3O_{14}P_2Se_2$	$C_{43}H_{44}Cl_2CrMn_3N_3O_{12}S_2$
fw	1751.19	1446.63	1146.65
cryst syst	Triclinic	Orthorhombic	Triclinic
space group	$P\bar{1}$	*Pbca*	$P\bar{1}$
cryst dimensions (mm)	0.38 × 0.34 × 0.08	0.50 × 0.15 × 0.02	0.34 × 0.14 × 0.04
a (Å)	13.6111(6)	19.3174(3)	12.2105(4)
b (Å)	14.6217(7)	24.2509(4)	13.2732(4)
c (Å)	21.674(1)	26.8237(1)	16.8203(6)
α (deg)	88.358(2)		68.679(2)
β (deg)	87.626(2)		85.157(2)
γ (deg)	82.321(2)		88.312(1)
V (Å^3)	4269.9(3)	12565.9(3)	2530.5(1)
Z	2	8	2
D_{calcd} (g cm^{-3})	1.362	1.529	1.505
μ ($Mo_{K\alpha}$) (mm^{-1})	0.743	2.029	1.188
diffractometer	Nonius (Kappa CCD)	Siemens Smart (Apex CCD)	Nonius (Kappa CCD)
radiation (λ) (Å)	0.71073	0.71073	0.71073
temp (K)	298	298	200
θ range for data collecn (deg)	1.92─24.98	1.52─25.00	1.65─25.02
T_{min}/T_{max}	0.77/0.94	0.55/0.72	0.69/0.95
no. of indep reflns	7898 ($I > 2\ \sigma(I)$)	6562 ($I > 2\ \sigma(I)$)	4983 ($I > 2\ \sigma(I)$)
no. of parameters	1003	761	607
R1[b]/wR2[b] ($I > 2\ \sigma(I)$)	0.0571/0.1329	0.0554/0.0807	0.0666/0.1562
R1[b]/wR2[b] (all data)	0.1334/0.1843	0.1178/0.0989	0.1198/0.1922

[a] Water molecule, H_2O, is excluded in the formula, formula weight, calculated density, μ, F(000), and R1/wR2 according to the Platon Squeeze procedure. [b] The functions minimized during least-squares cycles were $R1 = \Sigma||F_o| - |F_c||/\Sigma|F_o|$ and $wR2 = [\Sigma[w(F_o^2 - F_c^2)^2]/\Sigma[w(F_o^2)^2]]^{1/2}$.

	[TMBA]$_3$[**2b**]·0.5 CH_2Cl_2	[PPN]$_2$[**3a**]	[PPN]$_2$[**3b**]
empirical formula	$C_{85}H_{98}Cl_2Cr_2Mn_6N_6O_{24}Se_4$	$C_{91}H_{61}Cr_2Mn_3N_2O_{19}P_4S_2$	$C_{91}H_{61}Cr_2Mn_3N_2O_{19}P_4Se_2$
fw	2408.07	1943.24	2037.04
cryst syst	Orthorhombic	Triclinic	Triclinic
space group	*Pcan*	*P*$\bar{1}$	*P*$\bar{1}$
cryst dimensions (mm)	0.43 × 0.4 × 0.2	0.40 × 0.34 × 0.16	0.19 × 0.09 × 0.04
a (Å)	13.2857(1)	14.506(2)	14.344(1)
b (Å)	20.3204(2)	15.018(2)	14.846(1)
c (Å)	35.3790(4)	23.780(3)	23.494(2)
α (deg)		79.726(8)	79.085(4)
β (deg)		83.814(7)	83.113(4)
γ (deg)		64.256(6)	64.752(3)
V (Å^3)	9551.3(2)	4588.6(9)	4438.9(6)
Z	4	2	2
D_{calcd} (g cm^{-3})	1.675	1.406	1.524
μ ($Mo_{K\alpha}$) (mm^{-1})	2.639	0.814	1.614
diffractometer	Nonius (Kappa CCD)	Nonius (Kappa CCD)	Nonius (Kappa CCD)
radiation (λ) (Å)	0.71073	0.71073	0.71073
temp (K)	200	298	100
θ range for data collecn (deg)	2.16─25.68	1.64─25.01	1.57─25.03
T_{min}/T_{max}	0.34/0.46	0.74/0.88	0.75/0.94
no. of indep reflns	8819 ($I > 2\ \sigma(I)$)	5514 ($I > 2\ \sigma(I)$)	9147
no. of parameters	6940	1099	1096
R1[b]/wR2[b] ($I > 2\ \sigma(I)$)	0.0402/0.1013	0.1211/0.2948	0.0651/0.1119
R1[b]/wR2[b] (all data)	0.0595/0.1127	0.2791/0.3845	0.1367/0.1346

[b] The functions minimized during least-squares cycles were $R1 = \Sigma||F_o| - |F_c||/\Sigma|F_o|$ and $wR2 = [\Sigma[w(F_o^2 - F_c^2)^2]/\Sigma[w(F_o^2)^2]]^{1/2}$.

.

Figure Captions

Figure 2.1. ORTEP diagram (30% thermal ellipsoids) showing the structure and atom labeling for **1b**.

Figure 2.2. ORTEP diagram (30% thermal ellipsoids) showing the structure and atom labeling for **2b**. CH_2Cl_2 molecules were omitted for clarity.

Figure 2.3. ORTEP diagram (30% thermal ellipsoids) showing the structure and atom labeling for **3b**.

Figure 2.4. The spatial graphs (isovalue = 0.04) of the selected frontier molecular orbitals and their associated calculated energies of $[S_2Mn_3(CO)_9]^-$, $[Se_2Mn_3(CO)_9]^-$, **1a**, **1b**, **2a**, **2b**, **3a**, and **3b**.

Figure 2.5. Space filling structures of **1a** and **1b** (yellow: S atoms; Orange: Se atoms; blue: H atom; red: O atoms; white: C atoms).

Figure 2.6. DPVs in MeCN for $[PPN][S_2Mn_3(CO)_9]$ (black), $[PPN]_2$[**1a**] (red), $[TMBA]_3$[**2a**] (green), and $[PPN]_2$[**3a**] (blue). Conditions: electrolyte, 0.1 M Bu_4NClO_4; working electrode, platinum; scan rate, 100 mV s^{-1}. Potentials are vs SCE.

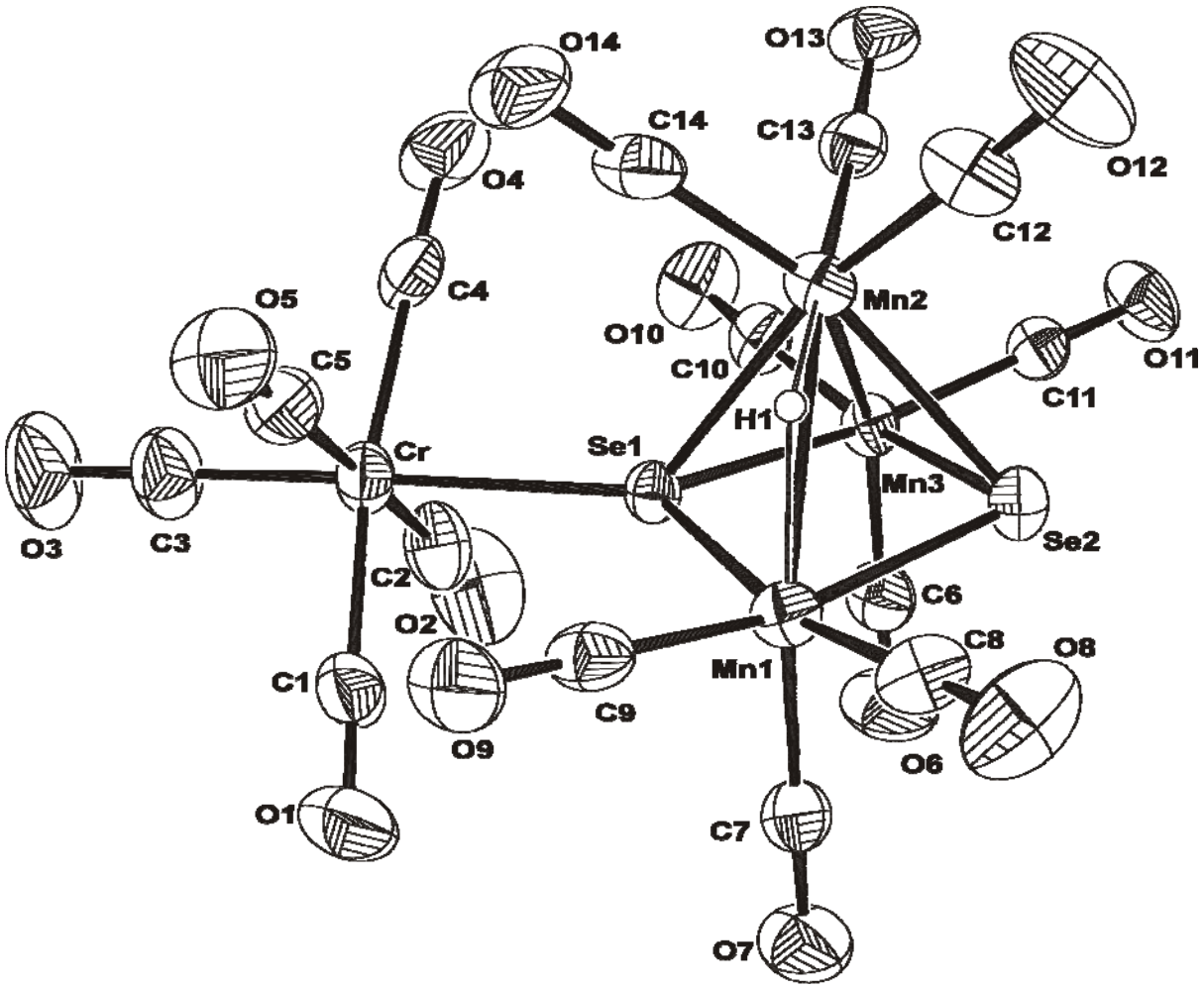
O14
O13
C14
C13
O12
O4
C12
C4
O5
Mn2
O10
C5
C10
O11
C11
H1
Cr
Se1
Mn3
O3
C3
Se2
C2
C6
O2
C8
O8
C1
Mn1
C9
O9
O6
O1
C7
O7

Figure 2.1.

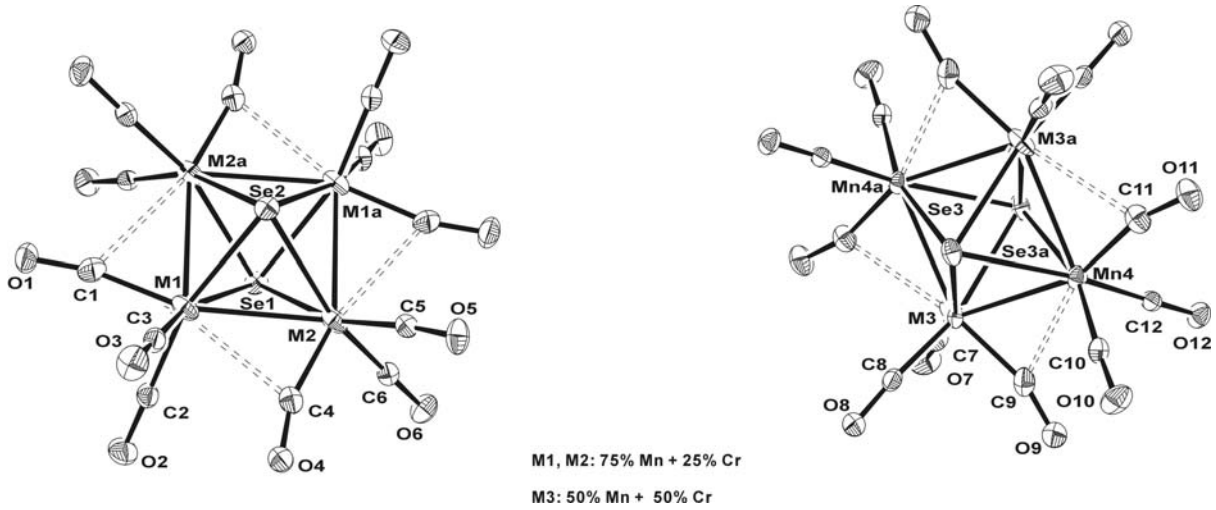
M2a
Se2
M1a
O1
C1
M1
Se1
C3
O3
C5
O5
M2
C2
C4
C6
O6
O2
O4
M1, M2: 75% Mn + 25% Cr
M3: 50% Mn + 50% Cr
M3a
O11
Mn4a
C11
Se3
Se3a
Mn4
M3
C12
O12
C8
C7
C10
O7
O8
C9
O10
O9

Figure 2.2.

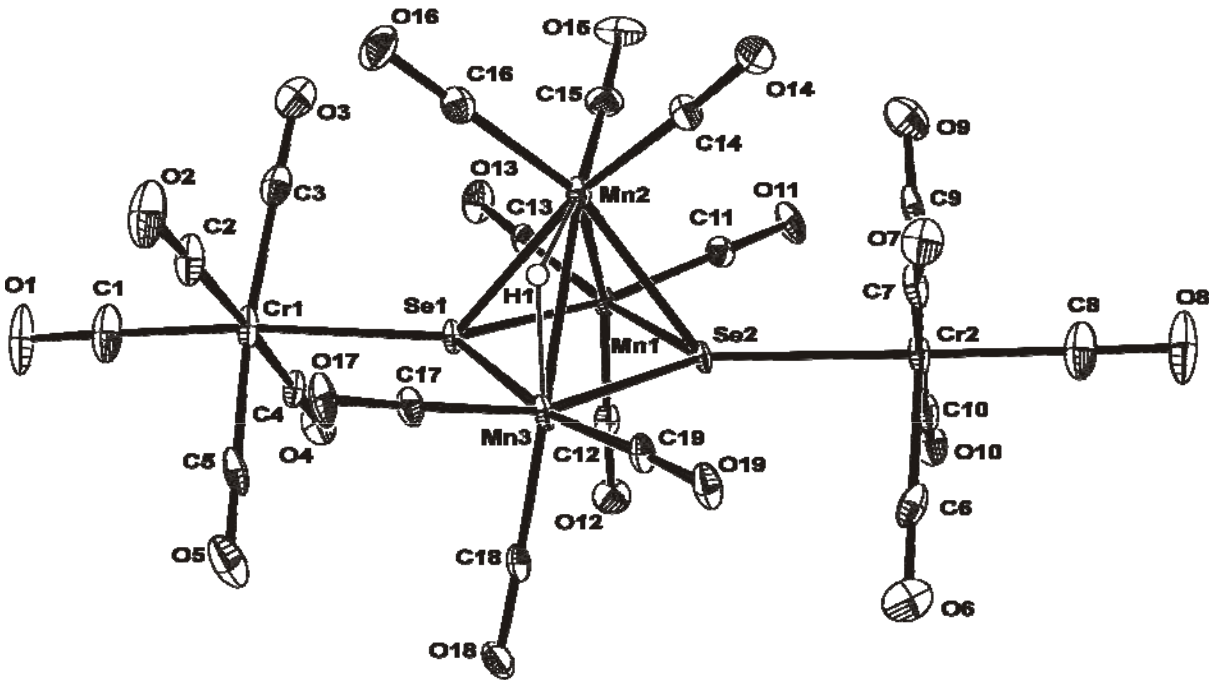
O16
O15
C16
C15
O14
O3
C14
O9
O13
Mn2
O11
O2
C3
C13
C9
C2
C11
O7
O1
C1
Cr1
Se1
H1
C7
C8
O8
Mn1
Se2
Cr2
O17
C17
C4
C10
Mn3
C19
O10
O4
C12
O19
C5
C6
O12
O5
C18
O6
O18

Figure 2.3.

$[S_2Mn_3(CO)_9]^-$	$[Se_2Mn_3(CO)_9]^-$	**1a**	**1b**
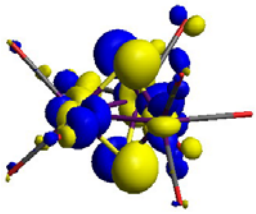	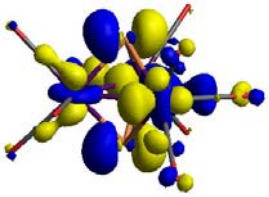	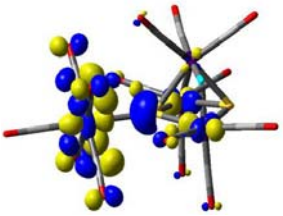	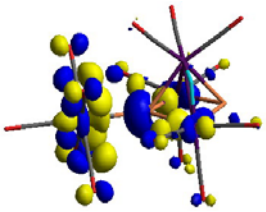
LUMO+1, −0.58 eV	LUMO+1, −0.62 eV	LUMO, 2.31 eV	LUMO, 2.18 eV
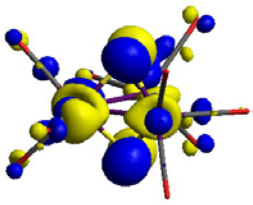	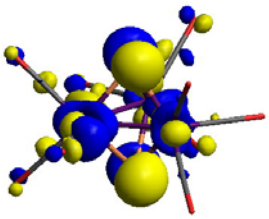	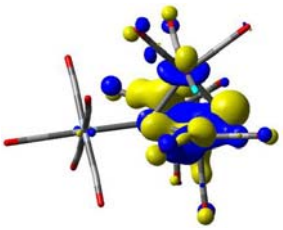	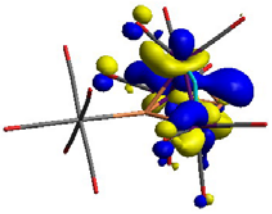
LUMO, −0.58 eV	LUMO, −0.62 eV	HOMO, 0.35 eV	HOMO, 0.29 eV
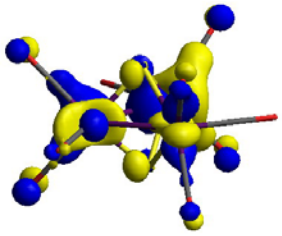	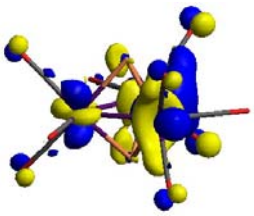	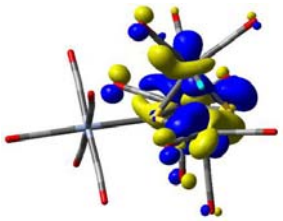	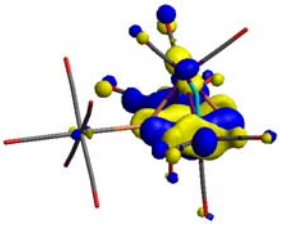
HOMO, −2.74 eV	HOMO, −2.72 eV	HOMO−1, 0.33 eV	HOMO−1, 0.25 eV
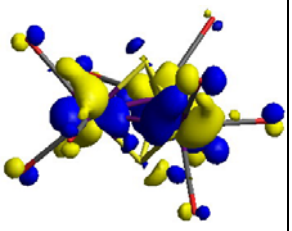	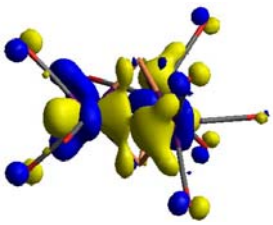		
HOMO−1, −2.75 eV	HOMO−1, −2.72 eV		

Figure 2.4.

2a	2b	3a	3b
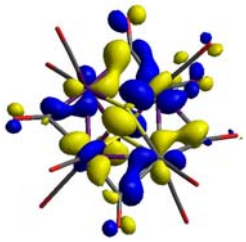 LUMO+1, 6.17 eV	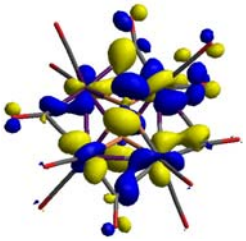 LUMO+1, 6.02 eV	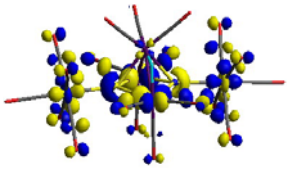 LUMO, 1.71 eV	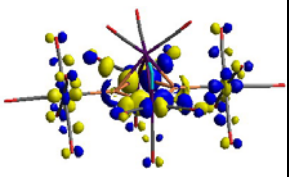 LUMO, 1.57 eV
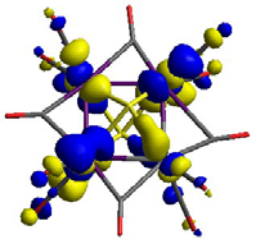 LUMO, 5.91 eV	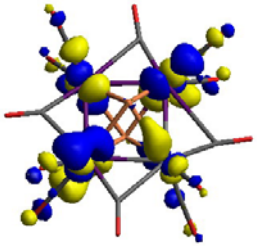 LUMO, 5.74 eV	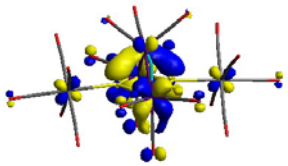 HOMO, −0.28 eV	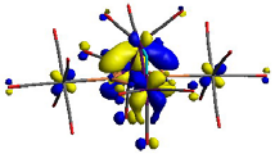 HOMO, −0.34 eV
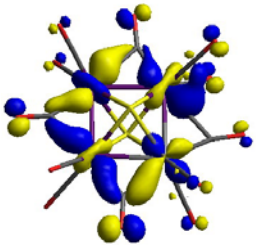 HOMO, 4.24 eV	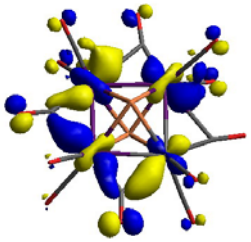 HOMO, 4.20 eV	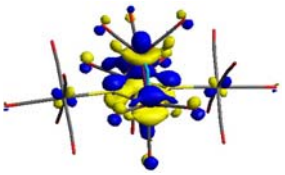 HOMO−1, −0.32 eV	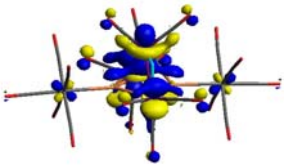 HOMO−1, −0.38 eV
		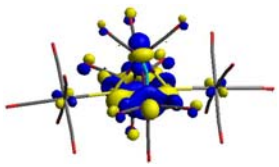 HOMO−2, −0.34 eV	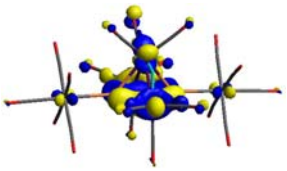 HOMO−2, −0.44 eV

Figure 2.4. (continued)

$[HE_2Mn_3Cr(CO)_{14}]^{2-}$	
E = S, **1a**	E = Se, **1b**
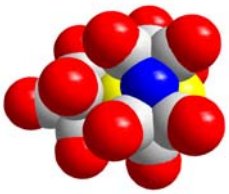	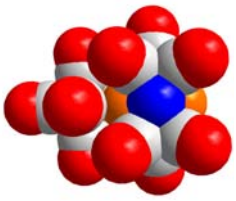

Figure 2.5.

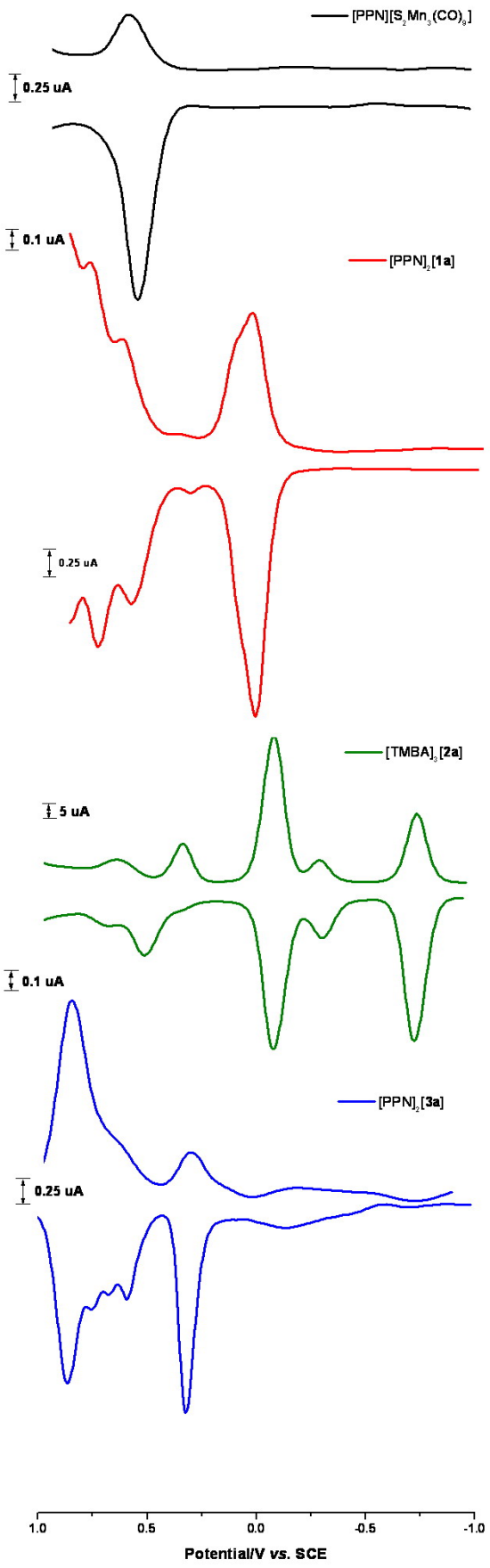
[PPN][S2Mn3(CO)9]
0.25 uA
0.1 uA
[PPN]2[1a]
0.25 uA
[TMBA]2[2a]
5 uA
0.1 uA
[PPN]2[3a]
0.25 uA
1.0
0.5
0.0
-0.5
-1.0
Potential/V vs. SCE

Figure 2.6.

Supporting Information for

Stepwise Construction of Manganese─Chromium Carbonyl Chalcogenide Complexes: Synthesis, Electrochemical Properties, and Computational Studies

Minghuey Shieh,* Chia-Yeh Miu, Kuo-Chih Huang, Chung-Feng Lee, and Bo-Gaun Chen
Department of Chemistry, National Taiwan Normal University, Taipei 116, Taiwan, Republic of China

Figure S2.1. ORTEP diagram (30% thermal ellipsoids) showing the structure and atom labeling for **1a**.

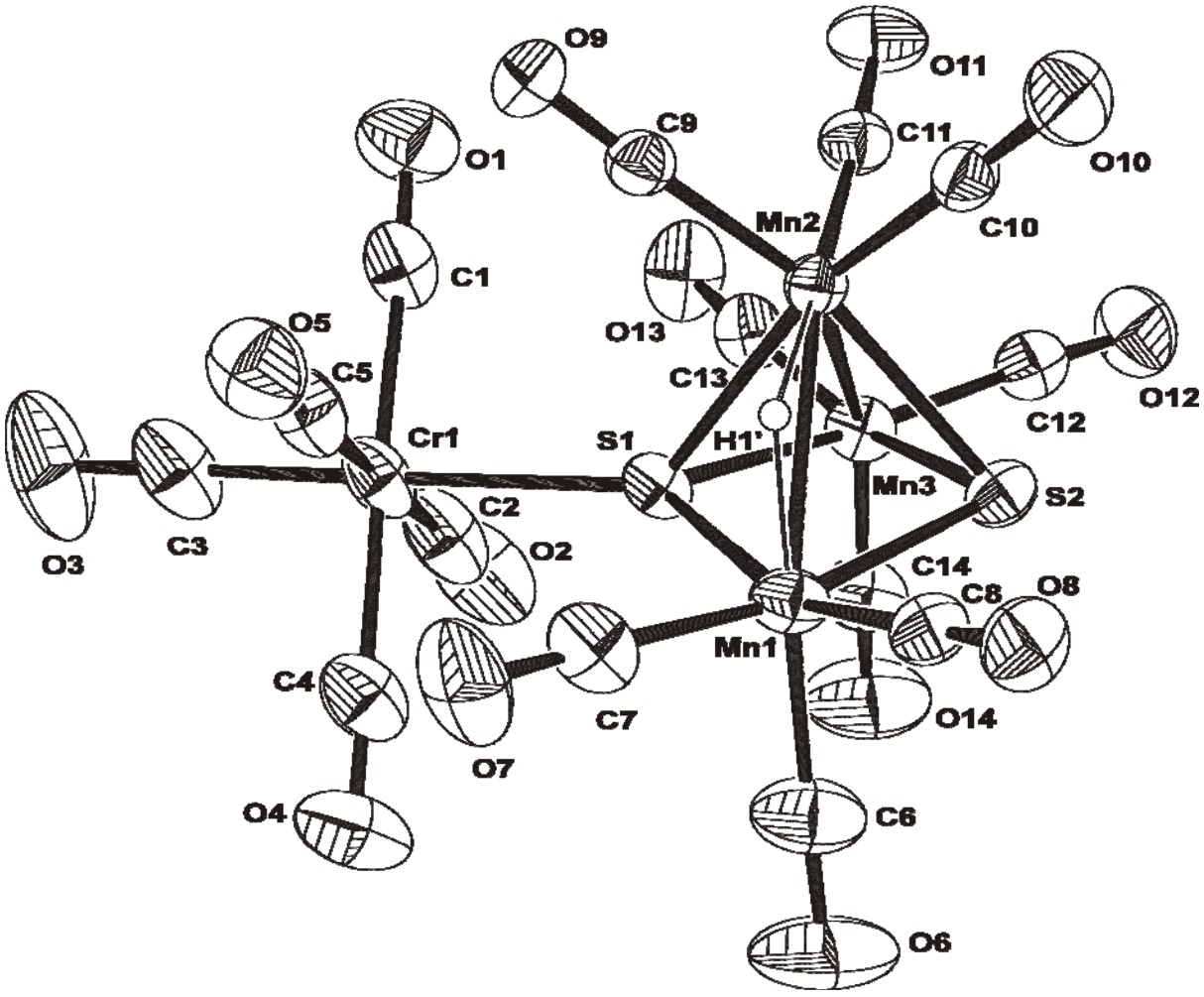

Figure S2.2. ORTEP diagram (30% thermal ellipsoids) showing the structure and atom labeling for **2a**. CH_2Cl_2 molecules were omitted for clarity.

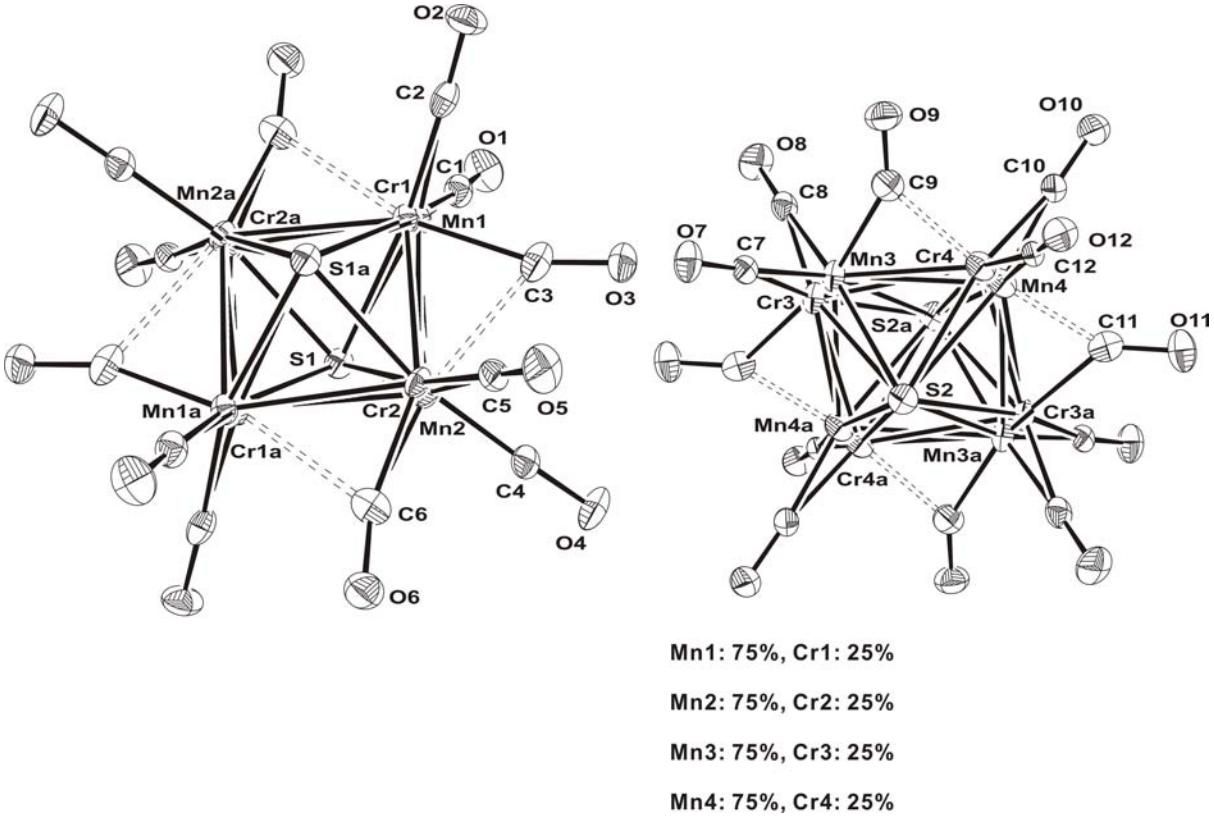

Figure S2.3. ORTEP diagram (30% thermal ellipsoids) showing the structure and atom labeling for **3a**.

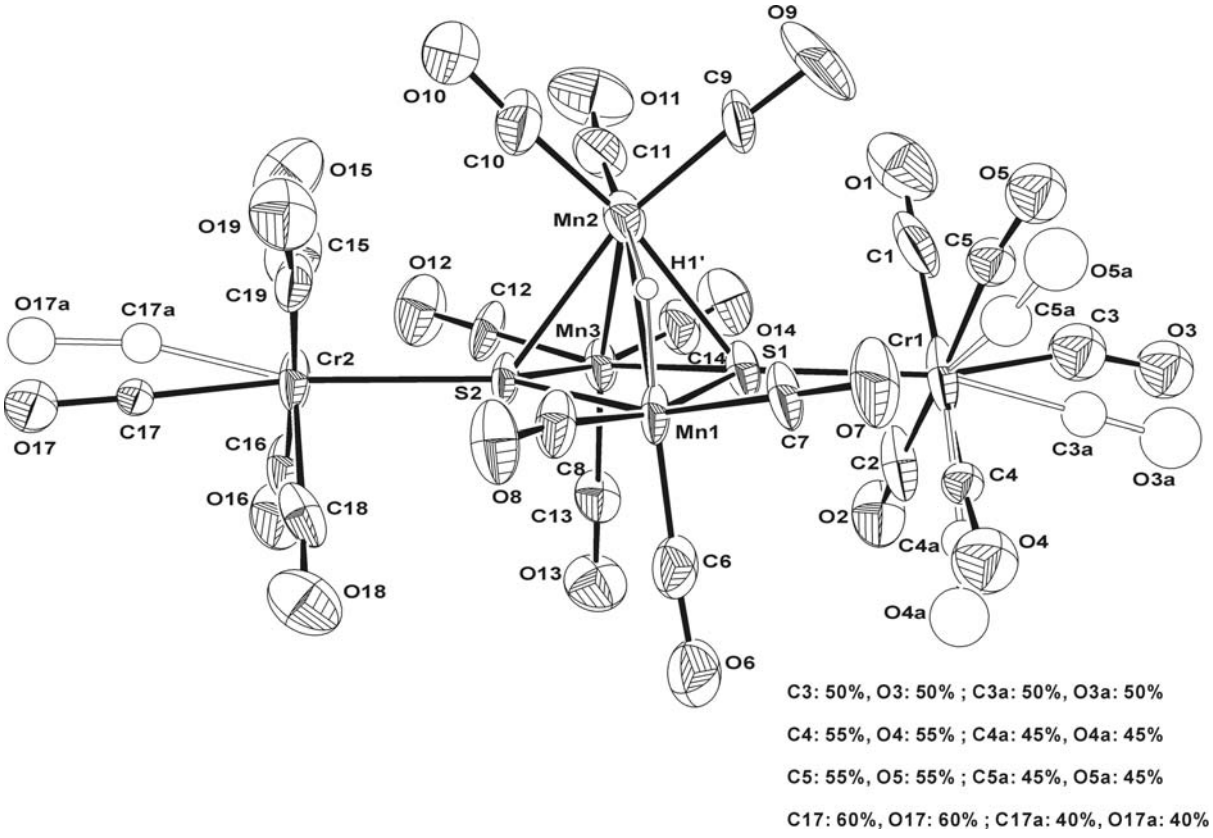

Figure S2.4. DPVs in MeCN for $[PPN][Se_2Mn_3(CO)_9]$ (black), $[PPN]_2$[**1b**] (red), $[TMBA]_3$[**2b**] (green), and $[PPN]_2$[**3b**] (blue). Insert: the quasi-reversible reduction peaks of $[PPN]_2$[**3b**] (blue) in a higher concentration in the oxidation process (+1.0 ~ +0.4 V). Conditions: electrolyte, 0.1 M Bu_4NClO_4; working electrode, platinum; scan rate, 100 mV s^{-1}. Potentials are vs. SCE.

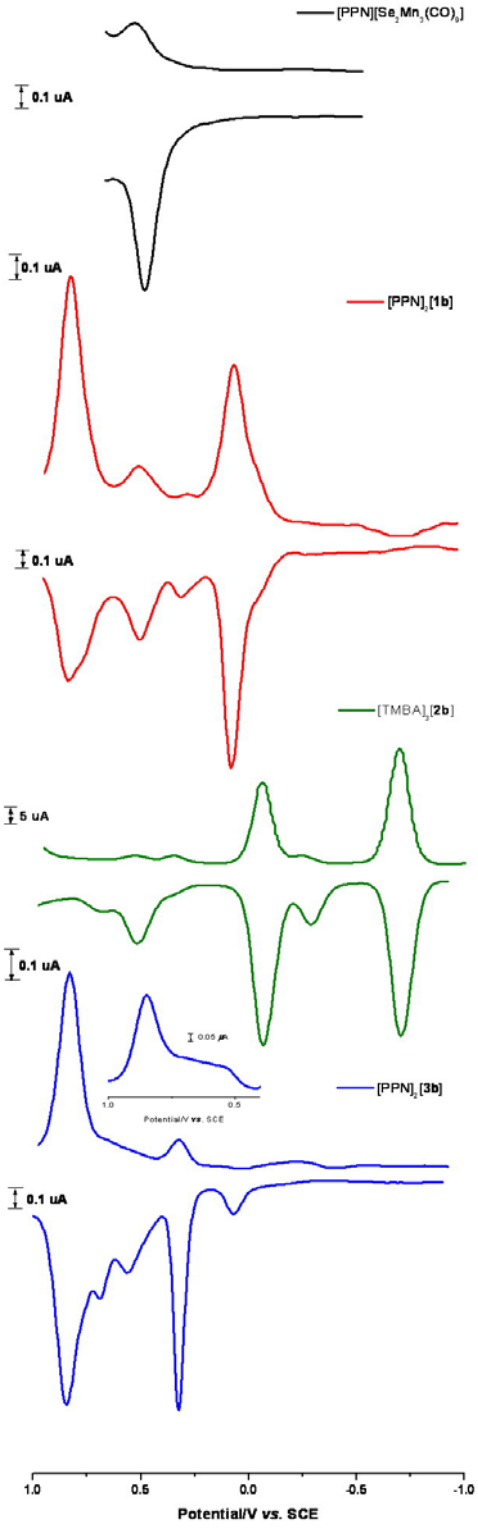

Figure S2.5. (a) CVs in MeCN for $[PPN][S_2Mn_3(CO)_9]$ (black), $[PPN]_2$[**1a**] (red), $[TMBA]_3$[**2a**] (green), and $[PPN]_2$[**3a**] (blue). (b) CVs in MeCN for $[PPN][Se_2Mn_3(CO)_9]$ (black), $[PPN]_2$[**1b**] (red), $[TMBA]_3$[**2b**] (green), and $[PPN]_2$[**3b**] (blue). Conditions: electrolyte, 0.1 M Bu_4NClO_4; working electrode, platinum; scan rate, 100 mV s^{-1}. Potentials are vs. SCE.

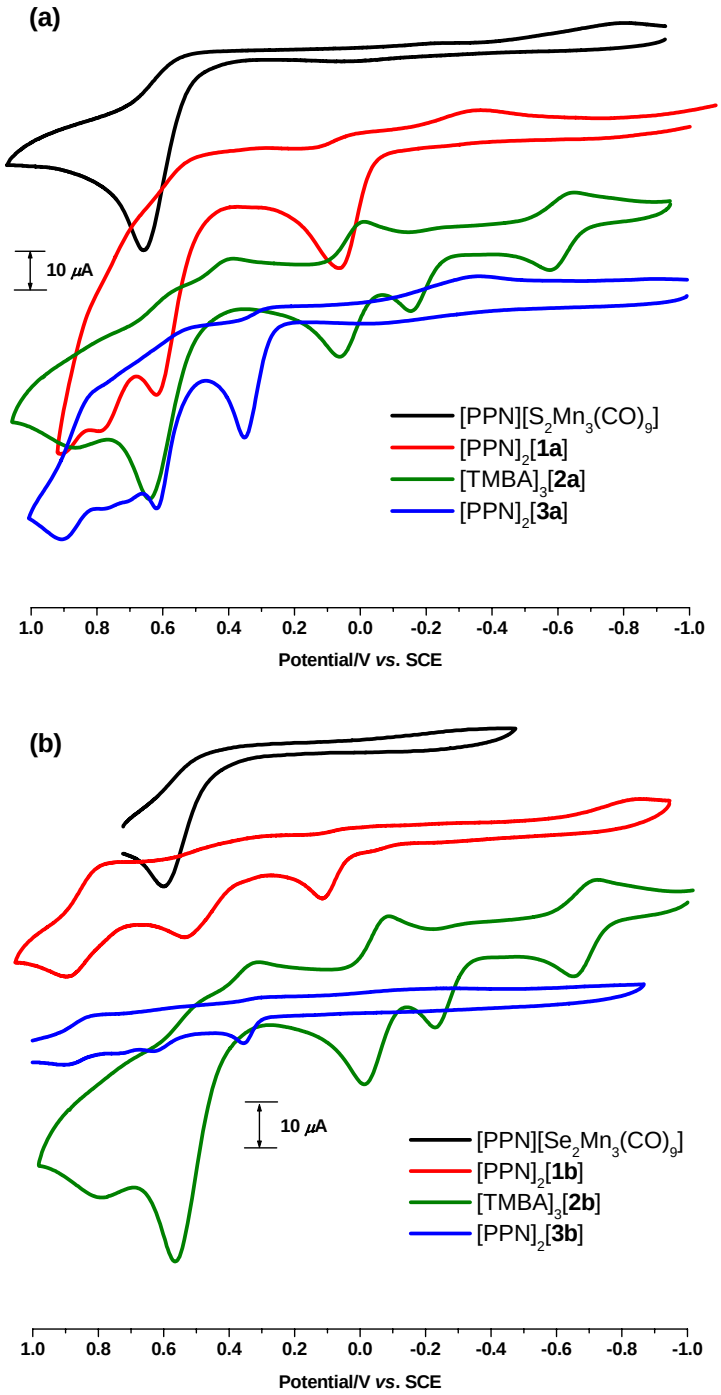

Computational details (Part I and Part II):

Part I

Table S2.1. All calculations reported in this study were performed via the density functional theory (DFT) with the Becke's 1988 exchange functional (B) and the Perdew's 1986 gradient correlation functional (BP86) or the Becke's three-parameter (B3) exchange functional and the Lee─Yang─Parr (LYP) correlation functional (B3LYP) with a larger basis set: TZVP using the Gaussian 03 series of packages. The geometries of complexes $[E_2Mn_3(CO)_9]^-$ (E = S, Se), **1a**, **1b**, **2a**, **2b**, **3a**, and **3b** were fully optimized using the BP86/TZVP and B3LYP/TZVP methods.

$[S_2Mn_3(CO)_9]^-$ (BP86/TZVP)
G = -5270.984640 a.u.

	x	y	z
Mn	0.246600	1.608461	0.000692
Mn	-1.518248	-0.590832	0.000714
Mn	1.269995	-1.018567	0.000646
S	-0.000383	-0.000913	1.597156
S	-0.000413	-0.001040	-1.597163
C	-0.185826	2.791719	1.295481
C	-0.210081	2.794991	-1.282816
C	1.942469	2.129066	-0.013779
C	-2.816507	0.617632	-0.009966
C	-2.317414	-1.576731	-1.284805
C	-2.324378	-1.559726	1.294693
C	2.515041	-1.228298	1.292640
C	0.875616	-2.748202	-0.006853
C	2.522762	-1.218176	-1.285534
O	-0.456634	3.572683	2.118285
O	-0.497217	3.577976	-2.097998
O	3.056797	2.485723	-0.023465
O	-3.682665	1.404260	-0.017108
O	-2.851548	-2.214818	-2.101881
O	-2.863452	-2.186525	2.117350
O	3.329507	-1.379547	2.113597
O	0.628566	-3.891871	-0.011762
O	3.342139	-1.362748	-2.102711

$[S_2Mn_3(CO)_9]^-$ (B3LYP/TZVP)
G = -5270.240465 a.u.

	x	y	z
Mn	-0.303853	1.665679	0.000006
Mn	-1.291386	-1.096321	-0.000100
Mn	1.596371	-0.570358	-0.000036
S	0.000982	-0.001002	1.569588
S	0.000988	-0.000959	-1.569686
C	-1.101357	2.623004	1.321631
C	-1.102802	2.623132	-1.320673
C	1.138716	2.720338	-0.000905

C	-2.924916	-0.371796	0.000030
C	-1.724130	-2.265399	-1.321225
C	-1.723817	-2.265304	1.321205
C	2.824031	-0.357455	1.321495
C	1.788319	-2.346829	0.000153
C	2.824056	-0.357754	-1.321602
O	-1.612931	3.229325	2.154804
O	-1.615407	3.229536	-2.153148
O	2.077705	3.390771	-0.001593
O	-3.974479	0.107386	0.000131
O	-1.994952	-3.011404	-2.154072
O	-1.994446	-3.011211	2.154204
O	3.604541	-0.216524	2.154832
O	1.899319	-3.495245	0.000303
O	3.604599	-0.217043	-2.154942

$[Se_2Mn_3(CO)_9]^-$ (BP86/TZVP)
G = -9278.174006 a.u.

	x	y	z
Se	-0.000514	0.000010	-1.722469
Mn	0.466779	1.601248	0.000625
Mn	-1.620912	-0.396510	0.000190
Mn	1.154046	-1.205447	-0.000129
Se	-0.000723	-0.000764	1.722838
C	-0.855009	2.784031	0.000870
C	1.377600	2.482690	-1.280668
C	1.378341	2.483823	1.280551
C	-2.840405	-0.041967	-1.278640
C	-2.839224	-0.055007	1.283649
C	-1.984779	-2.132476	-0.007498
C	1.466710	-2.431609	-1.283405
C	1.460092	-2.437258	1.279357
C	2.838748	-0.650689	0.004956
O	-1.715116	3.577166	0.001017
O	1.969352	3.086586	-2.085595
O	1.970569	3.088811	2.084308
O	-3.659750	0.172652	-2.081968
O	-3.658014	0.150785	2.089893
O	-2.241985	-3.273840	-0.012736
O	1.697419	-3.243594	-2.089807
O	1.686157	-3.252980	2.083259
O	3.955342	-0.301320	0.008541

$[Se_2Mn_3(CO)_9]^-$ (B3LYP/TZVP)
G = -9276.999148 a.u.

	x	y	z
Se	0.003064	-0.002882	-1.686106
Mn	-1.233329	-1.242392	0.002070

Mn	1.695382	-0.445173	0.003627
Mn	-0.460743	1.687045	0.001987
Se	0.002287	-0.001853	1.689383
C	-0.637866	-2.927244	-0.013513
C	-2.442707	-1.565993	-1.307059
C	-2.427792	-1.583891	1.320382
C	2.580499	-1.339294	-1.299784
C	2.600263	-1.290304	1.325905
C	2.847644	0.920106	-0.031204
C	-0.143085	2.897690	-1.307581
C	-0.167809	2.895584	1.319206
C	-2.219771	2.001725	-0.014986
O	-0.242509	-4.010900	-0.023786
O	-3.224623	-1.777873	-2.125100
O	-3.200696	-1.808095	2.143789
O	3.154989	-1.916508	-2.113552
O	3.189405	-1.835493	2.151372
O	3.582991	1.808597	-0.054272
O	0.059608	3.682352	-2.125329
O	0.019140	3.679547	2.141485
O	-3.357173	2.193841	-0.026069

$[HS_2Mn_3Cr(CO)_{14}]^{2-}$ (**1a**) (BP86/TZVP)
G = -6883.221145 a.u.

	x	y	z
Cr	2.794791	-0.057324	0.131142
Mn	-1.067728	1.947286	-0.593384
Mn	-1.493655	0.038667	1.309229
Mn	-1.151695	-1.707742	-0.792388
C	2.518421	-1.364330	1.484098
C	2.917519	-1.400708	-1.203077
C	4.616504	-0.156705	0.353775
C	2.995343	1.258808	-1.220307
C	2.748653	1.307962	1.455515
C	-0.790045	2.183839	-2.345186
C	0.108679	3.211501	-0.100578
C	-2.403368	3.133917	-0.551662
C	-0.491444	0.362673	2.760315
C	-3.044475	0.446950	2.103115
C	-1.676549	-1.684533	1.834262
C	-2.555840	-2.819376	-0.881494
C	-0.057981	-3.080786	-0.383933
C	-0.847590	-1.844180	-2.531026
O	2.413647	-2.154526	2.328589
O	3.084945	-2.205070	-2.026198
O	5.783135	-0.222568	0.496491
O	3.184901	2.051366	-2.050032
O	2.835167	2.131108	2.270776

O	-0.637378	2.375633	-3.491488
O	0.832172	4.086774	0.195238
O	-3.269189	3.927278	-0.533522
O	0.108064	0.574080	3.743966
O	-4.048017	0.718972	2.643110
O	-1.854715	-2.691702	2.414855
O	-3.463591	-3.557102	-0.978517
O	0.608152	-4.020532	-0.164280
O	-0.668748	-1.945216	-3.686356
S	0.296063	0.039396	-0.234688
S	-2.568942	0.135980	-0.784420
H	-1.377288	1.736348	1.127943

$[HS_2Mn_3Cr(CO)_{14}]^{2-}$ (**1a**) (B3LYP/TZVP)
G = -6882.263900 a.u.

	x	y	z
Cr	2.851479	-0.013357	0.127548
Mn	-1.135786	1.907969	-0.648275
Mn	-1.499434	0.068498	1.371275
Mn	-1.133638	-1.759133	-0.777246
C	2.594661	-1.287094	1.532652
C	2.963409	-1.405913	-1.173003
C	4.681917	-0.061519	0.335382
C	2.981762	1.269303	-1.281248
C	2.754313	1.407887	1.409073
C	-0.868644	2.008419	-2.429580
C	0.048417	3.204130	-0.230232
C	-2.510424	3.068460	-0.658916
C	-0.467896	0.496303	2.785032
C	-3.059065	0.504709	2.155851
C	-1.641323	-1.638603	1.964548
C	-2.539376	-2.894418	-0.830738
C	0.020091	-3.085243	-0.327798
C	-0.825029	-1.908652	-2.525182
O	2.483498	-2.041623	2.389933
O	3.100362	-2.225364	-1.966667
O	5.837999	-0.095373	0.466721
O	3.106909	2.030553	-2.132264
O	2.792253	2.255762	2.181024
O	-0.721655	2.088414	-3.573111
O	0.774855	4.068333	0.025384
O	-3.393094	3.818387	-0.665793
O	0.156152	0.778408	3.715628
O	-4.053506	0.802409	2.663918
O	-1.784120	-2.638469	2.536180
O	-3.438516	-3.619269	-0.890619
O	0.721001	-3.965129	-0.063026
O	-0.641827	-1.988798	-3.664396

S	0.301317	0.019679	-0.217352
S	-2.621274	0.038201	-0.739327
H	-1.414115	1.748628	1.063514

$[HSe_2Mn_3Cr(CO)_{14}]^{2-}$ (**1b**) (BP86/TZVP)
G = -10890.415995 a.u.

	x	y	z
Se	0.441509	0.040898	-0.281414
Se	-2.628892	0.075161	-0.707260
Cr	3.058439	-0.018979	0.066530
Mn	-1.064330	1.999062	-0.515502
Mn	-1.364300	0.021866	1.418595
Mn	-1.083239	-1.824823	-0.691562
C	3.209818	1.281979	-1.303411
C	3.153948	-1.382953	-1.246925
C	4.883405	-0.091400	0.261771
C	2.810274	-1.307957	1.441290
C	2.988899	1.364669	1.368882
C	-0.878292	-2.022207	-2.437353
C	-0.882377	2.270986	-2.273534
C	-2.420834	3.150110	-0.369455
C	0.113454	3.269901	-0.052895
C	0.071060	-3.145277	-0.289753
C	-2.465246	-2.962514	-0.646175
C	-2.873178	0.423598	2.288844
C	-1.488958	-1.692561	1.983691
C	-0.281610	0.385751	2.797075
O	3.362340	2.070530	-2.145587
O	3.290715	-2.203520	-2.060286
O	6.052527	-0.139907	0.386509
O	2.719684	-2.088016	2.297005
O	3.048106	2.204692	2.169149
O	-0.762454	-2.167002	-3.596500
O	-0.788465	2.484089	-3.422817
O	-3.298864	3.925734	-0.284412
O	0.841173	4.148719	0.220293
O	0.784427	-4.051066	-0.077100
O	-3.357682	-3.725182	-0.657791
O	-3.843202	0.690005	2.890256
O	-1.618032	-2.691947	2.589707
O	0.371193	0.622012	3.740318
H	-1.288709	1.720972	1.207640

$[HSe_2Mn_3Cr(CO)_{14}]^{2-}$ (**1b**) (B3LYP/TZVP)
G = -10889.028356 a.u.

	x	y	z
Se	0.448697	0.023973	-0.269093
Se	-2.680178	-0.019212	-0.663152

Cr	3.113454	0.018219	0.064409
Mn	-1.129539	1.966903	-0.588222
Mn	-1.367047	0.079183	1.479106
Mn	-1.062787	-1.874724	-0.675884
C	3.212275	1.265822	-1.375180
C	3.199015	-1.409522	-1.197396
C	4.945514	-0.011078	0.251393
C	2.876580	-1.220924	1.502920
C	2.997550	1.470542	1.307201
C	-0.855002	-2.103946	-2.429293
C	-0.958907	2.099280	-2.378778
C	-2.520838	3.100664	-0.496843
C	0.057367	3.269337	-0.207577
C	0.151984	-3.141240	-0.226792
C	-2.442237	-3.035646	-0.583598
C	-2.880435	0.524072	2.340551
C	-1.459029	-1.614041	2.118140
C	-0.257842	0.551389	2.814511
O	3.315221	2.009717	-2.245367
O	3.308966	-2.254053	-1.969201
O	6.102900	-0.032497	0.368901
O	2.776660	-1.956566	2.378039
O	3.012082	2.341172	2.054228
O	-0.736164	-2.239525	-3.572064
O	-0.870827	2.201251	-3.526948
O	-3.411004	3.839487	-0.439101
O	0.788637	4.136803	0.020190
O	0.900123	-3.981774	0.035181
O	-3.320657	-3.787412	-0.551858
O	-3.839671	0.826841	2.910338
O	-1.560620	-2.603957	2.714531
O	0.416193	0.862312	3.699935
H	-1.318944	1.754164	1.125545

$[S_2Mn_3Cr(CO)_{12}]^{3-}$ (**2a**) (BP86/TZVP)
G = -6655.741567 a.u.

	x	y	z
C	-3.152357	-0.190518	1.269271
O	-4.002483	-0.191367	2.093380
Mn	-1.913167	-0.229342	-0.000058
C	-3.151894	-0.189825	-1.269805
C	-1.961661	-2.110163	-0.000584
C	-2.121245	2.075100	0.001204
Mn	0.179838	-1.837801	-0.000012
Mn	-0.299271	1.882350	0.000019
S	-0.052576	0.046892	1.508274
S	-0.052459	0.047055	-1.508338
O	-4.001664	-0.190213	-2.094285

O	-2.639122	-3.098597	-0.001127
O	-3.130224	2.714099	0.002446
C	0.193604	-3.070732	1.277781
C	0.194731	-3.070739	-1.277808
C	2.127796	-1.923482	0.001350
Cr	1.904070	0.209243	-0.000038
C	2.337192	2.016509	-0.002060
C	-0.131652	3.119300	-1.266414
C	-0.129690	3.119076	1.266409
O	0.214490	-3.913208	2.107386
O	0.216371	-3.913194	-2.107420
O	3.032759	-2.706415	0.002534
C	3.152644	0.092718	-1.324821
C	3.152262	0.095573	1.325332
O	2.914113	3.055524	-0.003401
O	-0.058251	3.971589	-2.084883
O	-0.054928	3.971242	2.084879
O	3.988563	0.042746	-2.165965
O	3.987810	0.047539	2.166967

$[S_2Mn_3Cr(CO)_{12}]^{3-}$ (**2a**) (B3LYP/TZVP)
G = -6654.760906 a.u.

	x	y	z
C	3.162872	0.287627	-1.282524
O	3.963023	0.480166	-2.111763
Mn	1.972460	-0.044306	0.000675
C	3.161448	0.287277	1.285252
C	2.369113	-1.817918	0.000612
C	1.792504	2.541773	0.000748
Mn	0.024778	-1.867491	-0.000656
Mn	0.108132	1.939015	0.000538
S	0.064334	0.060168	-1.502889
S	0.063297	0.059185	1.502870
O	3.960600	0.479625	2.115509
O	3.096136	-2.749798	0.000971
O	2.736087	3.241254	0.000763
C	0.274114	-3.069974	-1.295119
C	0.271339	-3.069778	1.294500
C	-1.805933	-2.276990	-0.001483
Cr	-1.949087	0.002974	-0.000886
C	-2.729951	1.663715	-0.000422
C	-0.369374	3.074752	1.295676
C	-0.366703	3.075280	-1.295007
O	0.428502	-3.873468	-2.126380
O	0.418500	-3.872047	2.128264
O	-2.640802	-3.111873	-0.002053
C	-3.136300	-0.374099	1.337834
C	-3.136205	-0.373729	-1.339947

O	-3.415045	2.618309	-0.000952
O	-0.661925	3.835866	2.129014
O	-0.650342	3.835030	-2.132701
O	-3.917613	-0.587744	2.185337
O	-3.919594	-0.588956	-2.185141

$[Se_2Mn_3Cr(CO)_{12}]^{3-}$ (**2b**) (BP86/TZVP)
G = -10662.933741 a.u.

	x	y	z
Se	-0.057022	0.060985	1.611918
Mn	-1.958900	-0.300720	0.000037
Cr	1.959795	0.236260	-0.000160
Mn	-0.358751	1.940190	0.000138
Mn	0.229925	-1.880895	0.000013
Se	-0.057252	0.061078	-1.612081
C	3.196606	0.057726	-1.327956
C	3.199916	0.047952	1.323293
C	2.484525	2.000944	0.006241
C	2.125340	-1.996469	-0.006825
C	-3.198661	-0.194796	1.263476
C	-3.196660	-0.201796	-1.265919
C	-2.040392	-2.138530	0.005085
C	-2.136377	2.222020	-0.006164
C	-0.106769	3.156363	1.272646
C	-0.096677	3.158525	-1.268286
C	0.186447	-3.117359	-1.271856
C	0.196532	-3.112976	1.276358
O	4.028348	-0.023730	-2.170873
O	4.034226	-0.039788	2.163019
O	3.047089	3.046582	0.011258
O	3.065404	-2.734751	-0.012314
O	-4.054336	-0.163752	2.082201
O	-4.050792	-0.175412	-2.086410
O	-2.656810	-3.163397	0.009879
O	-3.179594	2.793842	-0.011590
O	0.018543	3.998619	2.094527
O	0.035415	4.002458	-2.087339
O	0.182690	-3.966453	-2.095394
O	0.199868	-3.958515	2.103552

$[Se_2Mn_3Cr(CO)_{12}]^{3-}$ (**2b**) (B3LYP/TZVP)
G = -10661.526562 a.u.

	x	y	z
Se	-0.048814	-0.040345	-1.603069
Mn	-2.028056	0.029706	0.001092
Cr	2.034715	0.022650	-0.000140
Mn	-0.077511	-1.993766	-0.000977
Mn	-0.043542	1.942135	-0.000060

Se	-0.047058	-0.041095	1.602563
C	3.191074	0.532863	1.317733
C	3.190092	0.516741	-1.325129
C	2.931864	-1.562686	0.012666
C	1.684663	2.519525	-0.009445
C	-3.157871	-0.458198	-1.288310
C	-3.154124	-0.476105	1.286696
C	-2.636242	1.709265	0.012447
C	-1.680490	-2.757777	-0.018839
C	0.533529	-3.066565	-1.291631
C	0.505836	-3.069415	1.300354
C	-0.453985	3.102352	1.292615
C	-0.467734	3.101347	-1.289034
O	3.965609	0.827424	2.149003
O	3.963458	0.801458	-2.160929
O	3.641731	-2.500261	0.024571
O	2.548466	3.315307	-0.017617
O	-3.923341	-0.746071	-2.121400
O	-3.917199	-0.775786	2.117861
O	-3.351920	2.642044	0.021789
O	-2.611359	-3.469450	-0.031843
O	0.901817	-3.790813	-2.126922
O	0.857123	-3.794821	2.141988
O	-0.698599	3.885319	2.122080
O	-0.721467	3.883825	-2.116274

$[HS_2Mn_3Cr_2(CO)_{19}]^{2-}$ (**3a**) (BP86/TZVP)
G = -8494.877093 a.u.

	x	y	z
Cr	-3.972441	0.042280	-0.330058
Cr	3.972437	0.042272	-0.330062
Mn	0.000009	1.916351	-0.209502
Mn	-0.000003	-0.060315	1.682647
Mn	-0.000003	-1.762898	-0.487547
C	-4.057049	-1.311067	1.005074
C	-3.872660	-1.254629	-1.714042
C	-5.803820	0.010804	-0.494720
O	-6.974142	-0.011737	-0.599690
C	-3.864211	1.409064	-1.644086
O	-3.870582	2.234771	-2.461560
C	-4.177445	1.362194	1.026421
O	-4.427783	2.156636	1.835236
C	0.000049	2.224347	-1.976339
C	-1.255809	3.153198	0.109906
C	1.255813	3.153196	0.109961
C	-1.304184	0.263390	2.868821
C	1.304179	0.263380	2.868823
C	0.000012	-1.802313	2.187565

C	1.257103	-3.037199	-0.323639
C	-0.000014	-1.875322	-2.258348
C	-1.257110	-3.037196	-0.323620
C	4.057042	-1.311098	1.005047
C	3.872644	-1.254608	-1.714073
C	5.803815	0.010792	-0.494732
O	6.974136	-0.011751	-0.599708
C	3.864208	1.409091	-1.644053
C	4.177446	1.362162	1.026440
O	-4.184744	-2.120560	1.826906
O	-3.903517	-2.024301	-2.584007
O	0.000053	2.455193	-3.122098
O	-2.031909	4.007805	0.305727
O	2.031906	4.007799	0.305831
O	-2.114441	0.471015	3.684976
O	2.114438	0.471000	3.684977
O	0.000027	-2.824014	2.765308
O	2.030475	-3.912544	-0.253580
O	-0.000029	-1.955455	-3.425583
O	-2.030483	-3.912539	-0.253547
O	4.184736	-2.120602	1.826867
O	3.903494	-2.024264	-2.584052
O	3.870578	2.234826	-2.461499
O	4.427785	2.156591	1.835267
S	-1.448443	0.042041	-0.183051
S	1.448441	0.042034	-0.183052
H	0.000021	1.645016	1.531994

$[HS_2Mn_3Cr_2(CO)_{19}]^{2-}$ (**3a**) (B3LYP/TZVP)
G = -8493.716849 a.u.

	x	y	z
Cr	-4.049994	0.019529	-0.320606
Cr	4.049996	0.019527	-0.320609
Mn	0.000000	1.915716	-0.287821
Mn	0.000002	0.023547	1.729845
Mn	-0.000001	-1.788638	-0.471473
C	-4.106527	-1.286342	1.079427
C	-3.929709	-1.341952	-1.655569
C	-5.887891	-0.007781	-0.480453
O	-7.045373	-0.028491	-0.581166
C	-3.903380	1.338429	-1.696913
O	-3.864983	2.121794	-2.534772
C	-4.215601	1.408425	0.991203
O	-4.419961	2.233011	1.761225
C	0.000000	2.072630	-2.090829
C	-1.280619	3.162257	-0.040835
C	1.280622	3.162256	-0.040836
C	-1.320427	0.425233	2.890130

C	1.320433	0.425234	2.890128
C	0.000000	-1.700508	2.306383
C	1.285241	-3.049770	-0.258273
C	-0.000004	-1.933402	-2.252940
C	-1.285243	-3.049768	-0.258271
C	4.106529	-1.286346	1.079422
C	3.929709	-1.341952	-1.655574
C	5.887892	-0.007784	-0.480458
O	7.045375	-0.028494	-0.581172
C	3.903380	1.338430	-1.696913
C	4.215606	1.408421	0.991202
O	-4.190632	-2.054833	1.926455
O	-3.926751	-2.139675	-2.481306
O	-0.000007	2.179862	-3.238150
O	-2.070053	3.990848	0.113430
O	2.070057	3.990845	0.113427
O	-2.139610	0.691216	3.656341
O	2.139618	0.691219	3.656337
O	-0.000003	-2.707857	2.877428
O	2.070747	-3.885184	-0.138617
O	-0.000024	-2.004347	-3.403749
O	-2.070751	-3.885181	-0.138614
O	4.190634	-2.054837	1.926449
O	3.926750	-2.139675	-2.481311
O	3.864980	2.121798	-2.534770
O	4.419967	2.233005	1.761226
S	-1.472419	0.017949	-0.170926
S	1.472420	0.017949	-0.170927
H	-0.000001	1.708204	1.445375

$[HSe_2Mn_3Cr_2(CO)_{19}]^{2-}$ (**3b**) (BP86/TZVP)
G = -12502.072730 a.u.

	x	y	z
Cr	-4.165241	0.018418	-0.325075
Cr	4.165266	0.018430	-0.325061
Mn	-0.000031	2.001277	-0.232541
Mn	0.000052	-0.008670	1.701929
Mn	0.000021	-1.855574	-0.436490
C	-4.184981	-1.282917	1.062560
C	-4.068654	-1.334937	-1.652387
C	-5.998880	-0.036307	-0.442116
O	-7.170662	-0.073481	-0.517279
C	-4.089266	1.338083	-1.686417
O	-4.105803	2.138962	-2.528886
C	-4.328610	1.386178	0.987743
O	-4.541519	2.210908	1.776504
C	-0.000066	2.325606	-1.995141
C	-1.263015	3.223192	0.104297

C	1.262919	3.223245	0.104233
C	-1.311524	0.361065	2.863511
C	1.311707	0.360851	2.863488
C	-0.000299	-1.729586	2.269264
C	1.265684	-3.105005	-0.193463
C	0.000039	-2.070097	-2.196139
C	-1.265638	-3.105018	-0.193494
C	4.185013	-1.282884	1.062593
C	4.068703	-1.334954	-1.652344
C	5.998907	-0.036277	-0.442073
O	7.170691	-0.073441	-0.517217
C	4.089306	1.338063	-1.686435
C	4.328586	1.386218	0.987736
O	-4.265342	-2.063592	1.917514
O	-4.090075	-2.146827	-2.483786
O	-0.000086	2.568110	-3.138913
O	-2.050385	4.065550	0.306885
O	2.050259	4.065643	0.306772
O	-2.127029	0.601176	3.665736
O	2.127270	0.600809	3.665702
O	-0.000515	-2.731546	2.880390
O	2.052978	-3.962357	-0.074863
O	0.000055	-2.219913	-3.356934
O	-2.052925	-3.962380	-0.074925
O	4.265387	-2.063553	1.917552
O	4.090138	-2.146863	-2.483725
O	4.105856	2.138919	-2.528926
O	4.541457	2.210968	1.776486
H	-0.000026	1.693551	1.500409
Se	1.530567	0.044013	-0.246720
Se	-1.530543	0.043999	-0.246715

$[HSe_2Mn_3Cr_2(CO)_{19}]^{2-}$ (**3b**) (B3LYP/TZVP)
G = -12500.481645 a.u.

	x	y	z
Cr	-4.244710	-0.011569	-0.301373
Cr	4.244709	-0.011571	-0.301374
Mn	0.000001	2.003550	-0.340260
Mn	0.000000	0.101455	1.742520
Mn	-0.000003	-1.881812	-0.427053
C	-4.231286	-1.248501	1.160455
C	-4.135753	-1.440548	-1.563175
C	-6.085637	-0.063830	-0.399057
O	-7.244981	-0.099934	-0.461270
C	-4.149343	1.241928	-1.739502
O	-4.136911	1.989357	-2.611150
C	-4.361320	1.437930	0.947492
O	-4.524224	2.300133	1.685420

C	0.000011	2.166329	-2.142285
C	-1.288381	3.238358	-0.084946
C	1.288382	3.238355	-0.084929
C	-1.324117	0.558191	2.874688
C	1.324108	0.558223	2.874684
C	0.000020	-1.595438	2.390659
C	1.295658	-3.111298	-0.127697
C	-0.000008	-2.144253	-2.193984
C	-1.295666	-3.111293	-0.127687
C	4.231301	-1.248564	1.160404
C	4.135749	-1.440502	-1.563231
C	6.085635	-0.063821	-0.399067
O	7.244980	-0.099918	-0.461286
C	4.149338	1.241980	-1.739456
C	4.361312	1.437879	0.947548
O	-4.270047	-1.978744	2.043877
O	-4.130668	-2.285495	-2.340888
O	0.000019	2.281376	-3.289204
O	-2.088343	4.056184	0.070439
O	2.088344	4.056178	0.070472
O	-2.145233	0.861043	3.625363
O	2.145220	0.861103	3.625353
O	0.000037	-2.583012	2.994685
O	2.096036	-3.922893	0.044067
O	-0.000022	-2.294360	-3.337508
O	-2.096046	-3.922884	0.044085
O	4.270076	-1.978845	2.043793
O	4.130661	-2.285419	-2.340976
O	4.136906	1.989442	-2.611076
O	4.524205	2.300050	1.685514
H	-0.000010	1.775540	1.384342
Se	1.556191	0.019798	-0.239436
Se	-1.556191	0.019800	-0.239438

Part II.

Table S2.2. Comparison of selected structural parameters of the optimized geometries for **1a**, **1b**, **2a**, **2b**, **3a**, and **3b** with the experimental structural parameters shown in parentheses, calculated at the BP86 and B3LYP levels with different basis sets. (the mixed basis sets, LanL2DZ for S(Se), Mn, and Cr atoms and 6-31+G* for C, O, and H atoms; the mixed basis sets, TZVP for S(Se), Mn, and Cr atoms and 6-31+G* for C, O, and H atoms)

bond distance	level/basis set					
	B3LYP				BP86	
	LanL2DZ	LanL2DZ/ 6-31+G*	TZVP/ 6-31+G*	TZVP	LanL2DZ/ 6-31+G*	TZVP
1a						
S(33)─Mn(2)	2.439(2.320)	2.449	2.412	2.412	2.419	2.372
S(33)─Mn(3)	2.433(2.326)	2.440	2.403	2.402	2.411	2.364
S(33)─Mn(4)	2.387(2.283)	2.392	2.353	2.353	2.382	2.337
S(34)─Mn(2)	2.424(2.337)	2.425	2.389	2.390	2.403	2.360
S(34)─Mn(3)	2.428(2.328)	2.426	2.391	2.390	2.399	2.356
S(34)─Mn(4)	2.372(2.296)	2.370	2.333	2.333	2.367	2.326
H(35)─Mn(2)	1.747(1.593)	1.739	1.742	1.742	1.754	1.762
H(35)─Mn(3)	1.707(1.836)	1.699	1.710	1.710	1.700	1.711
Mn(2)─Mn(3)	2.750(2.675)	2.746	2.757	2.756	2.724	2.728
Mn(3)─Mn(4)	2.825(2.706)	2.822	2.844	2.844	2.748	2.754
S(33)─Cr(1)	2.591(2.427)	2.604	2.573	2.574	2.569	2.527
1b						
Se(1)─Mn(4)	2.534(2.426)	2.546	2.523	2.523	2.513	2.481
Se(1)─Mn(5)	2.535(2.438)	2.544	2.521	2.521	2.512	2.480
Se(1)─Mn(6)	2.481(2.392)	2.487	2.461	2.461	2.475	2.444
Se(2)─Mn(4)	2.539(2.468)	2.541	2.520	2.521	2.516	2.487
Se(2)─Mn(5)	2.535(2.454)	2.536	2.515	2.515	2.504	2.474
Se(2)─Mn(6)	2.486(2.425)	2.485	2.461	2.462	2.478	2.449
H(35)─Mn(4)	1.744(1.692)	1.735	1.738	1.737	1.752	1.760
H(35)─Mn(5)	1.712(1.656)	1.702	1.712	1.713	1.704	1.714
Mn(4)─Mn(5)	2.799(2.761)	2.793	2.811	2.810	2.770	2.782
Mn(5)─Mn(6)	2.888(2.791)	2.883	2.923	2.925	2.801	2.818
Se(1)─Cr(3)	2.696(2.532)	2.704	2.685	2.686	2.667	2.641
2a						
S(9)─Mn(3)	(2.399)			2.432		2.411
S(9)─Mn(7)	(2.416)			2.444		2.425
S(9)─Mn(8)	(2.440)			2.407		2.388
S(10)─Mn(3)	(2.426)			2.432		2.411
S(10)─Mn(7)	(2.440)			2.444		2.425
S(10)─Mn(8)	(2.416)			2.407		2.388
S(9)─Cr(17)	(2.258)			2.513		2.476
S(10)─Cr(17)	(2.362)			2.513		2.476
Mn(3)─Mn(7)	(2.702)			2.668		2.640
Mn(3)─Mn(8)	(2.721)			2.722		2.658
Cr(17)─Mn(7)	(2.557)			2.719		2.676
Cr(17)─Mn(8)	(2.684)			2.825		2.767
2b						

Se(1)─Mn(2)	(2.497)			2.549		2.519
Se(1)─Mn(4)	(2.511)			2.527		2.494
Se(1)─Mn(5)	(2.522)			2.549		2.540
Se(6)─Mn(2)	(2.487)			2.548		2.519
Se(6)─Mn(4)	(2.522)			2.527		2.494
Se(6)─Mn(5)	(2.511)			2.550		2.540
Se(1)─Cr(3)	(2.484)			2.630		2.588
Se(6)─Cr(3)	(2.472)			2.628		2.588
Mn(2)─Mn(4)	(2.783)			2.811		2.754
Mn(2)─Mn(5)	(2.682)			2.756		2.700
Cr(3)─Mn(4)	(2.733)			2.920		2.877
Cr(3)─Mn(5)	(2.708)			2.829		2.734
3a						
S(44)─Mn(3)	2.432(2.299)	2.439	2.405	2.405	2.413	2.369
S(44)─Mn(4)	2.436(2.323)	2.440	2.406	2.404	2.409	2.364
S(44)─Mn(5)	2.383(2.300)	2.385	2.350	2.350	2.376	2.334
S(45)─Mn(3)	2.432(2.336)	2.439	2.405	2.405	2.413	2.369
S(45)─Mn(4)	2.436(2.339)	2.440	2.406	2.404	2.409	2.364
S(45)─Mn(5)	2.383(2.302)	2.385	2.350	2.350	2.376	2.334
Mn(3)─Mn(4)	2.762(2.702)	2.757	2.769	2.766	2.734	2.736
Mn(4)─Mn(5)	2.844(2.729)	2.837	2.857	2.851	2.757	2.758
Cr(1)─S(44)	2.599(2.461)	2.613	2.582	2.582	2.572	2.528
Cr(2)─S(45)	2.600(2.445)	2.613	2.582	2.582	2.572	2.528
H(46)─Mn(3)	1.751(1.401)	1.742	1.745	1.746	1.755	1.763
H(46)─Mn(4)	1.707(1.745)	1.699	1.709	1.709	1.701	1.712
3b						
Se(46)─Mn(3)	2.536(2.450)	2.545	2.523	2.523	2.515	2.485
Se(46)─Mn(4)	2.536(2.446)	2.542	2.522	2.521	2.509	2.478
Se(46)─Mn(5)	2.485(2.408)	2.489	2.464	2.464	2.477	2.447
Se(45)─Mn(3)	2.537(2.424)	2.545	2.523	2.523	2.515	2.485
Se(45)─Mn(4)	2.536(2.441)	2.542	2.522	2.521	2.509	2.478
Se(45)─Mn(5)	2.485(2.407)	2.489	2.464	2.464	2.477	2.447
Mn(3)─Mn(4)	2.811(2.750)	2.804	2.824	2.821	2.778	2.790
Mn(4)─Mn(5)	2.909(2.770)	2.901	2.944	2.939	2.808	2.830
Cr(1)─Se(46)	2.699(2.536)	2.709	2.689	2.689	2.664	2.636
Cr(2)─Se(45)	2.699(2.530)	2.709	2.689	2.689	2.664	2.636
H(44)─Mn(3)	1.746(1.572)	1.737	1.739	1.740	1.752	1.760
H(44)─Mn(4)	1.712(1.745)	1.702	1.712	1.712	1.703	1.714

Table S2.3. Results of Natural Bond Order and Natural Population Analyses of $[E_2Mn_3(CO)_9]^-$ (E = S, Se), **1a**, **1b**, **2a**, **2b**, **3a**, and **3b**

complex	Wiberg bond index					Natural charge					
	E─Mn	Mn─Mn	E─Cr	H─Mn	Mn─Cr	E	Mn	Cr	H	$HE_2Mn_3(CO)_9$ /$E_2Mn_3(CO)_9$ (sum)	$Cr_m(CO)_n$ (sum)
$[E_2Mn_3(CO)_9]^-$ (E = S)	0.806	0.279				0.408	−1.692			−1	0
$[E_2Mn_3(CO)_9]^-$ (E = Se)	0.807	0.285				0.517	−1.735			−1	0
1a (m = 1; n = 5)	0.732	0.284	0.613	0.355		0.389	−1.826	−2.847	0.246	−1.383	−0.617
1b (m = 1; n = 5)	0.736	0.285	0.605	0.356		0.498	−1.867	−2.890	0.243	−1.329	−0.671
2a (m = 1; n = 3)	0.613	0.279	0.610		0.257	0.336	−1.595	−2.235		−1.719	−1.281
2b (m = 1; n = 3)	0.618	0.283	0.617		0.261	0.432	−1.613	−2.238		−1.686	−1.314
3a (m = 2; n = 10)	0.699	0.277	0.610	0.355		0.493	−1.786	−2.821	0.246	−0.865	−1.135
3b (m = 2; n = 10)	0.702	0.278	0.608	0.356		0.630	−1.839	−2.861	0.242	−0.768	−1.232

Table S2.4. Cyclic Voltammetry (CV) of [PPN][$S_2Mn_3(CO)_9$], [PPN][$Se_2Mn_3(CO)_9$], [PPN]$_2$[**1a**], [PPN]$_2$[**1b**], [TMBA]$_3$[**2a**], [TMBA]$_3$[**2b**], [PPN]$_2$[**3a**], [PPN]$_2$[**3b**], and $Cr(CO)_6$

	oxidation process				reduction process			
complex	Ep^{ox}/V[a]	Ep^{red}/V[b]	$E_{1/2}$/V	ΔE/mV	Ep^{ox}/V[a]	Ep^{red}/V[b]	$E_{1/2}$/V	ΔE/mV
[PPN][$S_2Mn_3(CO)_9$]	0.660	-[c]						
[PPN][$Se_2Mn_3(CO)_9$][d]	0.603	-[c]						
[PPN]$_2$[**1a**]	0.795	-[c]				−0.366		
	0.620	-[c]						
	0.065	-[c]						
[PPN]$_2$[**1b**]	0.901	-[c]						
	0.538	-[c]						
	0.116	-[c]						
[TMBA]$_3$[**2a**]	0.867	-[c]			−0.154	-[c]		
	0.641				−0.576	−0.648	−0.612	72
	-[c]	0.384						
	0.062	−0.013	0.025	75				
[TMBA]$_3$[**2b**]	0.791				−0.012	−0.088	−0.050	76
	0.565	-[c]			−0.230	-[c]		
	-[c]	0.308			−0.652	−0.726	−0.689	74
[PPN]$_2$[**3a**]	0.908	-[c]						
	~ 0.774	-[c]			-[c]	−0.361		
	~ 0.701	-[c]						
	0.619	-[c]						
	0.353	-[c]						
[PPN]$_2$[**3b**]	0.905	-[c]						
	0.744	-[c]						
	0.636	-[c]						
	0.356	-[c]						
$Cr(CO)_6$						−0.350		

[2a] Ep^{ox} = oxidative peak potential. [b] Ep^{red} = reductive peak potential. [c] Difficult to determine. [d] ref 14e

Table S2.5. Selected bond distances (Å) and bond angles (deg) for $[PPN]_2[HS_2Mn_3Cr(CO)_{14}]$ ($[PPN]_2$[**1a**]), $[PPh_4]_2[HSe_2Mn_3Cr(CO)_{14}]$ ($[PPh_4]_2$[**1b**]), $[TMBA]_3[S_2Mn_3Cr(CO)_{12}]\cdot CH_2Cl_2$ ($[TMBA]_3$[**2a**]$\cdot CH_2Cl_2$), $[TMBA]_3[Se_2Mn_3Cr(CO)_{12}]\cdot 0.5\ CH_2Cl_2$ ($[TMBA]_3$[**2b**]$\cdot 0.5\ CH_2Cl_2$), $[PPN]_2[HS_2Mn_3Cr_2(CO)_{19}]$ ($[PPN]_2$[**3a**]), and $[PPN]_2[HSe_2Mn_3Cr_2(CO)_{19}]$ ($[PPN]_2$[**3b**])

$[PPN]_2$[**1a**]

S(1)─Mn(1)	2.320(2)	S(1)─Mn(2)	2.326(2)
S(1)─Mn(3)	2.284(2)	S(2)─Mn(1)	2.337(2)
S(2)─Mn(2)	2.328(2)	S(2)─Mn(3)	2.296(2)
S(1)─Cr(1)	2.427(2)	Mn(1)─Mn(2)	2.676(1)
Mn(2)─Mn(3)	2.706(1)	H(1)─Mn(1)	1.5929(9)
H(1)─Mn(2)	1.8362(8)		
S(1)─Mn(1)─S(2)	76.59(5)	S(1)─Mn(3)─S(2)	78.12(6)
S(1)─Mn(2)─S(2)	76.63(6)	Mn(3)─S(1)─Mn(1)	102.38(6)
Mn(3)─S(2)─Mn(1)	101.49(6)	S(1)─Mn(2)─Mn(1)	54.72(4)
S(2)─Mn(2)─Mn(1)	55.15(5)	S(1)─Mn(2)─Mn(3)	53.33(4)
S(2)─Mn(2)─Mn(3)	53.63(4)	H(1)─Mn(1)─Mn(2)	42.11(3)
H(1)─Mn(2)─Mn(1)	35.57(2)	Cr(1)─S(1)─Mn(1)	128.40(7)
Cr(1)─S(1)─Mn(2)	128.03(7)	Cr(1)─S(1)─Mn(3)	128.56(6)

$[PPh_4]_2$[**1b**]

Se(1)─Mn(1)	2.4265(9)	Se(1)─Mn(2)	2.4380(9)
Se(1)─Mn(3)	2.3924(9)	Se(2)─Mn(1)	2.4681(9)
Se(2)─Mn(2)	2.454(1)	Se(2)─Mn(3)	2.4246(9)
Se(1)─Cr(1)	2.532(1)	Mn(1)─Mn(2)	2.761(1)
Mn(2)─Mn(3)	2.791(1)	H(1)─Mn(1)	1.69(4)
H(1)─Mn(2)	1.66(4)		
Se(1)─Mn(1)─Se(2)	77.83(3)	Se(1)─Mn(3)─Se(2)	79.33(3)
Se(1)─Mn(2)─Se(2)	77.87(3)	Mn(3)─Se(1)─Mn(1)	102.05(3)
Mn(3)─Se(2)─Mn(1)	99.94(3)	Se(1)─Mn(2)─Mn(1)	55.22(3)
Se(2)─Mn(2)─Mn(1)	56.12(3)	Se(1)─Mn(2)─Mn(3)	53.94(2)
Se(2)─Mn(2)─Mn(3)	54.61(2)	H(1)─Mn(1)─Mn(2)	34.0(14)
H(1)─Mn(2)─Mn(1)	34.9(14)	Cr(1)─Se(1)─Mn(1)	129.68(3)
Cr(1)─Se(1)─Mn(2)	128.17(4)	Cr(1)─Se(1)─Mn(3)	127.92(3)

$[TMBA]_3$[**2a**]$\cdot CH_2Cl_2$

S(1)─Mn(1)	2.40(2)	S(1)─Mn(1a)	2.43(2)
S(1)─Mn(2)	2.42(2)	S(1)─Mn(2a)	2.44(1)
S(1)─Cr(1)	2.36(6)	S(1)─Cr(1a)	2.26(5)
S(1)─Cr(2)	2.38(6)	S(1)─Cr(2a)	2.25(4)
Mn(1)─Mn(2)	2.70(2)	Mn(1)─Mn(2a)	2.72(2)
Mn(1)─Cr(2)	2.60(6)	Mn(1a)─Cr(2)	2.63(7)
Mn(2)─Cr(1)	2.68(7)	Mn(2a)─Cr(1)	2.56(5)
Mn(1)─Mn(2)─Mn(1a)	89.4(6)	Mn(2)─Mn(1)─Mn(2a)	90.6(6)
Mn(1a)─Mn(2)─Cr(1)	85.9(12)	Mn(1a)─Mn(2a)─Cr(1)	88.8(17)
Mn(2a)─Mn(1)─Cr(2)	88.4(15)	Mn(2a)─Mn(1a)─Cr(2)	88.1(14)
Mn(1)─Cr(2)─Mn(1a)	94.0(20)	Mn(2)─Cr(1)─Mn(2a)	94.7(19)
S(1)─Cr(1)─S(1a)	79.4(17)	S(1)─Cr(2)─S(1a)	79.4(15)

S(1)─Mn(1)─S(1a)	75.5(5)	S(1)─Mn(2)─S(1a)	74.9(4)
S(2)─Mn(3)	2.385(3)	S(2)─Mn(3a)	2.379(3)
S(2)─Mn(4)	2.392(5)	S(2)─Mn(4a)	2.389(5)
S(2)─Cr(3)	2.390(8)	S(2)─Cr(3a)	2.404(9)
S(2)─Cr(4)	2.41(2)	S(2)─Cr(4a)	2.37(2)
Mn(3)─Mn(4)	2.626(3)	Mn(3)─Mn(4a)	2.658(4)
Mn(3)─Cr(4)	2.32(1)	Mn(3)─Cr(4a)	2.94(1)
Mn(4)─Cr(3)	2.978(7)	Mn(4)─Cr(3a)	2.289(8)
Mn(3)─Mn(4)─Mn(3a)	89.7(1)	Mn(4)─Mn(3)─Mn(4a)	90.3(1)
Mn(3)─Mn(4)─Cr(3a)	97.8(2)	Mn(3)─Mn(4a)─Cr(3a)	82.1(2)
Mn(4)─Mn(3)─Cr(4a)	83.9(3)	Mn(4)─Mn(3a)─Cr(4a)	96.8(4)
Mn(3)─Cr(4)─Mn(3a)	89.7(5)	Mn(4)─Cr(3)─Mn(4a)	89.7(2)
S(2)─Cr(3)─S(2a)	76.5(2)	S(2)─Cr(4)─S(2a)	76.8(5)
S(2)─Mn(3)─S(2a)	77.09(9)	S(2)─Mn(4)─S(2a)	76.8(1)

[TMBA]$_3$[**2b**]·0.5 CH_2Cl_2

Se(3)─Mn(4a)	2.5221(7)	Se(3)─Mn(4)	2.5113(7)
Se(3)─Mn(3a)	2.50(1)	Se(3)─Mn(3)	2.49(1)
Se(3)─Cr(3)	2.49(1)	Se(3)─Cr(3a)	2.47(1)
Mn(3)─Mn(4)	2.681(8)	Mn(3)─Mn(4a)	2.782(8)
Cr(3)─Mn(4)	2.733(9)	Cr(3)─Mn(4a)	2.708(9)
Mn(4)─Mn(3)─Mn(4a)	91.0(3)	Mn(3)─Mn(4)─Cr(3a)	90.1(2)
Mn(3a)─Mn(4)─Cr(3)	87.5(2)	Mn(4)─Cr(3)─Mn(4a)	91.5(3)
Se(3)─Cr(3)─Se(3a)	80.0(3)	Se(3)─Mn(3)─Se(3a)	79.5(3)
Se(3)─Mn(4)─Se(3a)	78.53(2)		
Se(1)─Cr(2)	2.53(2)	Se(1)─Cr(1)	2.53(2)
Se(2)─Cr(2)	2.52(1)	Se(2)─Cr(1)	2.41(3)
Se(1)─Mn(2)	2.482(4)	Se(1)─Mn(1)	2.509(7)
Se(2)─Mn(2)	2.504(4)	Se(2)─Mn(1)	2.519(8)
Mn(1)─Mn(2)	2.740(7)	Mn(1a)─Mn(2)	2.726(7)
Mn(1)─Cr(2)	2.74(2)	Mn(1a)─Cr(2)	2.78(2)
Mn(2)─Cr(1)	2.68(2)	Mn(2a)─Cr(1)	2.71(2)
Mn(2)─Mn(1)─Mn(2a)	89.2(2)	Mn(1)─Mn(2)─Mn(1a)	90.8(2)
Cr(1)─Mn(2)─Mn(1a)	90.0(4)	Cr(1)─Mn(2a)─Mn(1a)	89.7(4)
Cr(2)─Mn(1)─Mn(2a)	90.1(4)	Cr(2)─Mn(1a)─Mn(2a)	89.5(4)
Mn(2)─Cr(1)─Mn(2a)	90.9(7)	Mn(1)─Cr(2)─Mn(1a)	89.6(4)
Se(1)─Cr(1)─Se(2)	80.3(7)	Se(1)─Cr(2)─Se(2)	78.2(4)
Se(1)─Mn(1)─Se(2)	78.6(2)	Se(1)─Mn(2)─Se(2)	79.36(9)

[PPN]$_2$[**3a**]

S(1)─Mn(1)	2.298(5)	S(1)─Mn(2)	2.324(5)
S(1)─Mn(3)	2.301(4)	S(2)─Mn(1)	2.336(4)
S(2)─Mn(2)	2.339(5)	S(2)─Mn(3)	2.302(5)

S(1)─Cr(1)	2.461(5)	S(2)─Cr(2)	2.445(4)
Mn(1)─Mn(2)	2.702(4)	Mn(2)─Mn(3)	2.728(3)
H(1)─Mn(1)	1.401(3)	H(1)─Mn(2)	1.745(3)
S(1)─Mn(1)─S(2)	75.3(2)	S(1)─Mn(3)─S(2)	75.9(2)
S(1)─Mn(2)─S(2)	74.7(2)	Mn(3)─S(1)─Mn(1)	104.5(2)
Mn(3)─S(2)─Mn(1)	103.2(2)	S(1)─Mn(2)─Mn(1)	54.6(1)
S(2)─Mn(2)─Mn(1)	53.8(1)	S(1)─Mn(2)─Mn(3)	53.5(1)
S(2)─Mn(2)─Mn(3)	53.4(1)	H(1)─Mn(1)─Mn(2)	34.8(1)
H(1)─Mn(2)─Mn(1)	27.24(8)	Cr(1)─S(1)─Mn(1)	127.9(2)
Cr(1)─S(1)─Mn(2)	131.1(2)	Cr(1)─S(1)─Mn(3)	126.1(2)
Cr(2)─S(2)─Mn(1)	128.5(2)	Cr(2)─S(2)─Mn(2)	125.7(2)
Cr(2)─S(2)─Mn(3)	128.0(2)		

$[PPN]_2$[**3b**]

Se(1)─Mn(1)	2.407(1)	Se(1)─Mn(2)	2.442(1)
Se(1)─Mn(3)	2.424(1)	Se(2)─Mn(1)	2.408(1)
Se(2)─Mn(2)	2.446(1)	Se(2)─Mn(3)	2.450(1)
Se(1)─Cr(1)	2.530(1)	Se(2)─Cr(2)	2.536(1)
Mn(1)─Mn(2)	2.770(1)	Mn(2)─Mn(3)	2.750(2)
H(2)─Mn(2)	1.745(1)	H(2)─Mn(3)	1.572(1)
Se(1)─Mn(1)─Se(2)	77.35(4)	Se(1)─Mn(3)─Se(2)	76.22(4)
Se(1)─Mn(2)─Se(2)	75.98(4)	Mn(3)─Se(1)─Mn(1)	103.50(4)
Mn(3)─Se(2)─Mn(1)	102.68(4)	Se(1)─Mn(2)─Mn(1)	54.57(3)
Se(2)─Mn(2)─Mn(1)	54.56(3)	Se(1)─Mn(2)─Mn(3)	55.29(4)
Se(2)─Mn(2)─Mn(3)	55.91(3)	H(2)─Mn(2)─Mn(3)	32.02(3)
H(2)─Mn(3)─Mn(2)	36.06(4)	Cr(1)─Se(1)─Mn(1)	128.54(4)
Cr(1)─Se(1)─Mn(2)	130.08(5)	Cr(1)─Se(1)─Mn(3)	127.59(5)
Cr(2)─Se(2)─Mn(1)	127.67(4)	Cr(2)─Se(2)─Mn(2)	122.67(5)
Cr(2)─Se(2)─Mn(3)	129.57(4)		

Chapter 3

Insight to Mixed-Metal Chemistry of Mn─Ru Carbonyl Chalcogenide Clusters and Comparison of Their Corrosponding Homo- or Hetero-nuclear Octahedral Clusters: Synthesis, Electrochemistry, Optical Properties, and Computational Studies

Abstract

Heating trinuclear E_2Mn_3-trigonal-bipyramidal clusters, $[E_2Mn_3(CO)_9]^-$ (E = S, Se) with $Ru_3(CO)_{12}$ in a molar ratio of 1: 1 in MeCN/MeOH solutions afforded two tetranuclear products, E_2Ru_4-octahedral clusters $[HE_2Ru_4(CO)_{10}]^-$ (E = S, **3a**; Se, **3b**) and mixed-metal $E_2Mn_2Ru_2$-octahedral clusters $[E_2Mn_2Ru_2(CO)_{11}]^{2-}$ (E = S, **4a**; Se, **4b**). Clusters **3a** and **3b** were isomorphous and each displayed an E_2Ru_4 octahedral core with one Ru─Ru bond bridged by one hydrogen atom and two Ru─Ru bonds each bridged by one carbonyl group. Clusters **4a** and **4b** were isomorphous and consisted of an $E_2Mn_2Ru_2$ octahedral core with one Ru─Ru bond bridged by one carbonyl group and two Mn─Ru bonds each semibridged by one carbonyl group. In addition, **4a** and **4b** exhibited intense electronic communication through the M_4 square during oxidation of $Mn_2(CO)_6$ fragment, which were compared to the analogous homonuclear group 7 clusters, $[E_2Mn_4(CO)_{12}]^{2-}$ (E = S, **1a**; Se, **1b**) and the heteronuclear mixed-group 6/7 clusters, $[E_2Mn_3Cr(CO)_{12}]^{3-}$ (E = S, **2a**; Se, **2b**). The electronic absorptions of $[E_2Mn_3(CO)_9]^-$ and **1** were assigned as the MLCT (Mn→E or COs) transitions while those of **2** and **4** were attributed to the MLCT (Mn→E or COs) and MMCT (Mn→Cr or Ru) transitions. Moreover, these clusters also showed optical transitions with band gaps of 1.25 to 1.80 eV. Furthermore, the formation and electronic properties as well as

electrochemical and optical properties of these E_2M_4-octahedral carbonyl sulfides and selenides were studied and elucidated with the aid of molecular calculations at the BP86 level of the density functional theory.

Chapter 4

Reactivity of $[TeRu_5(CO)_{14}]^{2-}$ Toward Copper Salts: Synthesis, Transformations, Electrochemistry, Optical Properties, and Computational Studies

Abstract

When $[PPh_4]_2[TeRu_5(CO)_{14}]$ was treated with 1 equiv. of $[Cu(MeCN)_4][BF_4]$ in dichloromethane (CH_2Cl_2) at low temperature, the Cu_3Cl-incorporated di-$TeRu_5$ carbonyl cluster $[PPh_4]_2[\{TeRu_5(CO)_{14}\}_2Cu_3Cl]$ ($[PPh_4]_2$[**1**]) was formed. X-ray analysis showed that complex **1** exhibited two $TeRu_5$ cores that are linked by a Cu_3Cl moiety. When $[PPh_4]_2[TeRu_5(CO)_{14}]$ reacted with 2 equiv. of $[Cu(MeCN)_4][BF_4]$ in CH_2Cl_2 at low temperature, both Cu_4Cl_2-incorporated di-$TeRu_5$ carbonyl clusters $[PPh_4]_2[\{TeRu_5(CO)_{14}\}_2Cu_4Cl_2]\cdot CH_2Cl_2$ ($[PPh_4]_2$[**2**]$\cdot CH_2Cl_2$) and $[TeRu_5(\mu\text{-}CO)_2(CO)_{12}Cu_2(MeCN)_2]$ (**3a**) were obtained. However, similar reaction of $[PPh_4]_2[TeRu_5(CO)_{14}]$ with 2 equiv. of $[Cu(MeCN)_4][BF_4]$ in CH_2Cl_2 at room temperature produced complex **2** and $[TeRu_5(\mu\text{-}CO)_3(CO)_{11}Cu_2(MeCN)_2]$ (**3b**). The formation of **1** and **2** involved the abstraction of chloride from dichloromethane while the formation of isomers **3a** and **3b** was governed by the reaction temperature. Cluster **3a** was structurally characterized by X-ray analysis to display a $TeRu_5$ core with two adjacent Ru_3 triangles each capped by a μ_3-Cu(MeCN) fragment and two Ru─Ru bonds each bridged by a CO ligand. Cluster **3b** consists of a $TeRu_5$ core with one Ru_3 triangle further capped by a $Cu_2(MeCN)_2$ fragment with the two Cu bonded and three Ru─Ru bonds each bridged by a CO ligand. The nature, stepwise cluster transformation, electrochemical and optical properties of these CuX (X = MeCN or Cl)-incorporated mono- or di-$TeRu_5$-based clusters were discussed in terms of the

effects of copper, tellurium, temperature, and the size of the metal skeleton, which was elucidated in detail by DFT calculations at the MPW1PW91 level of the density function theory.

Chapter 5

Semiconducting Te─Fe─Cu─Dipyridyl Carbonyl Polymers: Controlled Synthesis, Optical Properties, and Computational Studies

Abstract

Four new mixed-metal cluster-based organometallic-organic hybrid polymers **1─4**, were synthesized from the reactions of the neutral heterometallic cluster $[TeFe_3(CO)_9\{Cu(MeCN)\}_2]$ with various ditopic organic linkers such as 1,2-bis(4-pyridine)ethene (bpe), 1,2-bis(4-pyridine)ethane (H_2bpe), and 4,4′-trimethylene-dipyridine (tmdpy) in the stoichiometric molar ratios in THF. Besides, the corresponding anionic clusters in **3** and **4**, $[\{TeFe_3(CO)_9Cu\}_2L]^{2-}$ (L = H_2bpe, **5**; tmdpy, **6**), could be isolated from a one-pot reaction of $[TeFe_3(CO)_9]^{2-}$, $[Cu(MeCN)_4][BF_4]$, and H_2bpe or tmdpy. Moreover, the diffuse-reflectance spectra revealed that parent cluster $[TeFe_3(CO)_9]^{2-}$ and complexes **1─6** with low band gaps, which exhibited the semiconducting behaviors. The ternary Te─Fe─Cu─dipyridyl complexes **1─6** were characterized spectroscopically and their nature, formation, and semiconducting properties were discussed systematically in terms of the nature of N-donor dipyridyl linkers, the dimensionalities, and the intermolecular hydrogen interactions with the aid of molecular calculations at the B3LYP level of the density functional theory.

Appendix A

Other Reactions

Experimental Section

All reactions were performed under an atmosphere of pure nitrogen using standard Schlenk techniques.[1] Solvents were purified, dried, and distilled under nitrogen prior to use. $BiCl_3$ (Strem), AgCl, 4,4′-trimethylene-dipyridine (tmdpy) (Aldrich), $Cr(CO)_6$ (Strem) were used as received. $[Cu(MeCN)_4][BF_4]$ was prepared according to the published method.[2] Infrared spectra were recorded on a Perkin-Elmer Paragon 500 IR spectrometer. Elemental analyses of C, H, and N were performed on a Perkin-Elmer 2400 analyzer at the NSC Regional Instrumental Center at National Taiwan University, Taipei, Taiwan. ESI-mass spectra were obtained on a Thermo Finnigan LCQ Advantage mass spectrometer.

X-ray Structural Characterization. Selected crystallographical data for $[Et_4N][SeFe_3(CO)_9Bi]$, $[Et_4N]_2[Se_4Fe_5(CO)_{12}]$, and $[PPN]_2[S_2Mn_3Cr(CO)_{20}]$ are given in Table A.1. All crystals were mounted on glass fibers with epoxy cement. Data collection for $[Et_4N][SeFe_3(CO)_9Bi]$ and $[Et_4N]_2[Se_4Fe_5(CO)_{12}]$ was carried out on a Bruker-Nonius Kappa CCD diffractometer and for $[PPN]_2[S_2Mn_3Cr(CO)_{20}]$ was carried out on a Bruker Apex II CCD diffractometer using graphite-monochromated Mo Kα radiation. An empirical absorption correction by multiscans was applied.[5] The structures were solved by direct methods and refined with SHELXL-97.[6]

References

(1) Shriver, D. F., Drezdon, M. A. *The Manipulation of Air-Sensitive Compounds*; Wiley-VCH Publishers: New York, 1986.

(2) (a) Kubas, G. J. *Inorg*. *Synth*. **1979**, *19*, 90─92. (b) Simmons, M. G.; Merrill, C. L.; Wilson, L. J.; Bottomley, L. A.; Kadish, K. M. *J*. *Chem*. *Soc*., *Dalton Trans*. **1980**, 1827─1837.

(3) Shieh, M.; Kung, C.-H. Unpublished results.

(4) Shieh, M.; Miu, C.-Y.; Huang, K.-H.; Lee, C.-F.; Chen, B.-G. *Inorg*. *Chem*. **2011**, *50*, 7735─7748.

(5) Blessing, R. H. *Acta Crystallogr*. *Sect*. *A* **1995**, *51*, 33─38.

(6) (a) Sheldrick, G. M. *SHELXL97*, version 97-2; University of Göttingen, Germany, 1997. (b) Sheldrick, G. M. *Acta Crystallogr*. *Sect*. *A* **2008**, *64*, 112─122.

Appendix B

Publications

1. M.-H. Hsu, C.-Y. Miu, Y.-C. Lin and M. Shieh,* "Selenium-Capped Trimolybdenum and Tritungsten Carbonyl Clusters $[Se_2M_3(CO)_{10}]^{2-}$ (M = Mo, W)," *J. Organomet. Chem.* **2006**, *691*, 966─974.
2. M. Shieh,* M.-H. Hsu, W.-S. Sheu, L.-F. Jang, S.-F. Lin, Y.-Y. Chu, C.-Y. Miu, Y.-W. Lai, H.-L. Liu and J.-L. Her, "A New Series of Copper Halide-Bridged Ruthenium Telluride Carbonyl Complexes: Discovery of a Unique Semiconducting Cluster Chain Polymer $[\{PPh_4\}_2\{Te_2Ru_4(CO)_{10}Cu_4Br_2Cl_2\}\cdot THF]_\infty$," *Chem.─Eur. J.* **2007**, *13*, 6605─6616.
3. M. Shieh,* C.-Y. Miu, C.-J. Lee, W.-C. Chen, Y.-Y. Chu and H.-L. Chen, "Construction of Copper Halide-Triiron Selenide Carbonyl Complexes: Synthetic, Electrochemical, and Theoretical Studies," *Inorg. Chem*. **2008**, *47*, 11018─11031.
4. M. Shieh,* C.-H. Ho, W.-S. Sheu,* B.-G. Chen, Y.-Y. Chu, C.-Y. Miu, H.-L. Liu and C.-C. Shen, "Semiconducting Tellurium─Iron─Copper Carbonyl Polymers," *J. Am. Chem. Soc.* **2008**, *130*, 14114─14116.
5. M. Shieh,* Y.-Y. Chu, C.-Y. Miu, P.-F. Wu and T.-M. Zeng, "Bimetallic Ru─Cu Tellurido Complexes: Controlled Synthesis and Electrochemical Studies of Copper Halide-$TeRu_5$ and Te_2Ru_4 Clusters," *Dalton Trans*. **2010**, *39*, 1492─1503. (Selected as a Hot Article)
6. M. Shieh* and C.-Y. Miu, "Carbonylchromium Chalcogenide Complexes: Synthesis, Reactivity and Properties," *J. Chin. Chem. Soc.* **2010**, *57*, 956─966. (Dedicated to Professor H.-S. Wei on the Occasion of his 70th Birthday)
7. M. Shieh,* C.-N. Lin, C.-Y. Miu, M.-H. Hsu, Y.-W. Pan and L.-F. Ho, "Chromium─Manganese Selenide Carbonyl Complexes: Paramagnetic Clusters and

Relevance to C=O Activation of Acetone," *Inorg. Chem*. **2010**, *49*, 8056─8066.

8. C.-Y. Miu, H.-H. Chi, S.-W. Chen, J.-J. Cherng, M.-H. Hsu, Y.-X. Huang and M. Shieh,* "Reactions of the μ_3-Sulfido Triiron Cluster $[SFe_3(CO)_9]^{2-}$ with Functionalized Organic Halides and Mercury Salts: Selective Reactivity, Electrochemistry, and Theoretical Calculations," *New J. Chem*. **2011**, *35*, 2442─2455.
9. M. Shieh,* C.-Y. Miu, K.-C. Huang, C.-F. Lee and B.-G. Chen, "Stepwise Construction of Manganese─Chromium Carbonyl Chalcogenide Complexes: Synthesis, Electrochemical Properties, and Computational Studies," *Inorg. Chem*. **2011**, *50*, 7735─7748.
10. M. Shieh,* C.-Y. Miu, Y.-Y. Chu and C.-N. Lin, "Recent Progress in the Chemistry of Anionic Groups 6─8 Carbonyl Chalcogenide Clusters," *Coord. Chem. Rev*. **2012**, *256*, 637─694.